Development of an Intelligent Sprayer to Optimize Pesticide Applications in Nurseries and Orchards

DISSERTATION

Presented in Partial Fulfillment of the Requirements for the Degree Doctor of Philosophy in the Graduate School of The Ohio State University

By

Yu Chen

Graduate Program in Food, Agricultural and Biological Engineering

The Ohio State University

2010

Dissertation Committee:

Dr. H. Erdal Ozkan, Adviser

Dr. Heping Zhu, Co-Adviser

Dr. Richard C. Derksen

Dr. Peter P. Ling

Abstract

Variable rate spray applications using intelligent control systems can greatly reduce pesticide use and off-target contamination of environment in nursery and orchard productions. The current equipment with variable rate functions for tree crops is limited to ultrasonic sensor based control systems that only detect tree occurrence to switch nozzles on or off and measure tree width in low accuracy to change spray application rates. However, the size and foliage density of canopies can vary greatly with trees even in the same orchard or nursery. The goal of this study was to develop an intelligently functioned sprayer prototype with utilization of a high precision laser scanner controlled system to deliver variable-rate spray outputs that match the canopy sectional structures in real time, in an effort to improve pesticide spray efficiency without reducing the level of crop protection expected from pesticides.

A high speed laser scanner was used to acquire data on the geometry, density characteristics and occurrence of the canopy on-the-go. A fast algorithm was developed to calculate tree canopy characteristic parameters using the data from the laser sensor. The algorithm also performed automatic detection of the ground surface, the tree row centerline, and tree width, height, volume and foliage density. A flow rate control unit was designed with Pulse Width Modulation (PWM) signals to adjust the flow rate from each individual nozzle in accordance with the detected tree sectional canopy size and density in real time. A back pressure bypass device was assembled into the spraying

system to minimize the pressure fluctuations caused by operating solenoid valves at 10Hz frequency. A mathematic model was developed to calculate the optimal spray rate for each of 20 individual nozzles on one side of the sprayer based on the concept that the spray volume equals the effective canopy volume multiplied by a recommended spray constant.

A commercially available vineyard sprayer base was used for the development of the intelligent sprayer prototype. The laser sensor and flow rate controller circuits for sensing trees and controlling variable rate were implemented into the automatic control system for the sprayer prototype development. Four five-port air assisted nozzles with one 8002 XR flat fan nozzle in each port were constructed and mounted on each side of the intelligent sprayer prototype. System response time was determined with a high speed camera system.

Field tests were conducted in an apple orchard to spray trees at three growth stages for comparison of spray performances of three sprayers: the intelligent sprayer with automatic control, the intelligent sprayer without automatic control, and a conventional air blast sprayer.

Both laboratory and field tests verified that the algorithm developed for the intelligent sprayer was able to detect a wide variety of foliage canopy density changes, and the electro-mechanical controllers were fast enough to activate the sprayer to achieve desired coverage uniformity regardless of foliage canopy variations.

Field spray deposition tests in the orchard also illustrated that compared to the intelligent sprayer without automatic control and the conventional air blast sprayer, the

intelligent sprayer with automatic control did not produce excessive sprays inside tree canopies. Also, the intelligent sprayer with automatic control provided relatively uniform spray coverage and deposition inside canopies with different foliage densities at different growth stages. In addition, compared to the other two sprayers, the intelligent sprayer with automatic control reduced spray volume by 47% to 73% with much less off-target loss on the ground, through tree gaps and in the air.

By automatically spraying the optimal amount of spray mixtures into tree canopies and stopping spraying beyond target areas, the intelligent sprayer with automatic control can significantly reduce the amount and cost of pesticides for growers, reduce the risk of environmental pollution by pesticides, and provide safer and healthier working conditions for workers.

Dedication

This document is dedicated to my parents.

Acknowledgments

I want to thank my co-advisors, Dr. Erdal Ozkan and Dr. Heping Zhu, who provided me with numerous guidance throughout my Ph.D. study. I am grateful to Dr. Ozkan for inspiring me from the first day I started my Ph.D. program. His strong support, patience and trust in me are invaluable to this research and will never be forgotten. I am also fortunate to have Dr. Heping Zhu as my co-adviser, who spent countless hours with me providing strong technical and intellectual support for the progress and development of this research program and myself.

I would also like to thank Dr. Richard Derksen and Dr. Peter Ling for serving as my research committee members, offering great insights and suggestions and helping me make this work more complete.

I want to express my appreciation to Dr. Robert Fox for reviewing my dissertation and giving important comments. Special thanks are extended to Adam Clark, Keith Williams and Barry Nudd for their valuable technical assistance during the course of this work. I want to thank USDA-ARS Application Technology Research Unit for providing facilities and support required for this study, and Dr. Harold Keener for coordinating additional lab space for my indoor experiments. I am also grateful to the technical support from Mike Klingman, Mike Sciarini, Chris Gecik, Carl Cooper and Bryon Hand.

I wish to thank Dr. Reza Ehsani from University of Florida and Bradley Farnsworth from Case Western Reserve University for answering my technical questions about the Laser scanning sensor at the beginning of this research. I am thankful to Jeff Grimm of Capstan Ag System for allowing me the opportunity to spend a few days in their shop, providing us some equipment used in my research, and giving me technical support. I would also like to acknowledge Hongyoung Jeon, Andy Doklovic, Leslie Morris, Leona Horst, Mike Sward, Jiabing Gu, Dan Troyer, Alex Sigler, Marcelo Gimenes, Rone Oliveira and Colwyn Headley for helping me with the field tests; and Peggy Christman, Candy McBride, Carol Moody, Lori Bowman, Kay Elliott, Kevin Davison, Carolyn Heydon and Janeen Polen for helping me with all the paperwork and procedures which allowed me more time to focus on my work.

I would like to thank all my friends at The Ohio state University for their friendship, help, support and love, which made my stay in Columbus and Wooster filled with many good memories.

Finally, I would like to express my gratitude to my parents and my brother for their constant love, trust and support which keeps me moving forward.

Vita

June 20, 1983	Born – Anhui, P.R. China
2004	B.S. Engineering, China Agricultural University, P.R. China
2006	M.S. Engineering, China Agricultural University, P.R. China
2006 to 2008	Graduate Teaching Associate, Department of Food, Agricultural and Biological Engineering, The Ohio State University
2008 to present	Graduate Research Associate, Department of Food, Agricultural and Biological Engineering, The Ohio State University

Fields of Study

Major Field: Food, Agricultural and Biological Engineering

Table of Contents

List of Tables

List of Figures

Chapter 1: Introduction

1.1 Background of research

Spray applications are an important tool in the agricultural industry for the protection of crops. They have helped produce an abundance of fruit crops which are equally important as field crops to feed and clothe the world's growing population. They have also helped produce an abundance of flowers and nursery shrubs and trees to beautify our environment and improve our lifestyle. Applications of pesticides have ensured high quality products from the fruit and nursery industries to meet stringent market requirements. Pesticides include insecticides, fungicides, herbicides and various other substances. Although there are concerns about potential risks to human health and the environment from pesticides use, the practice of pesticide-free crop production is not practical with present technologies (Oerke et al., 1994; Oerke, 2006). Also, the reports indicate that anticipated maximum yield for a variety of crops would be reduced by 20 to 40 percent if pesticides are not used during production.

The fruit and ornamental nursery industries are major enterprises in U.S. agriculture. The contribution that fruits and tree nuts production add to the U.S. economy has exceeded $17.2 billion each year from 2005 to 2009 (Harris et al., 2009). Total floral and nursery sales reached $16.9 billion at wholesale prices in 2006, a $52 million increase from 2005, producing over 10% of all income from agricultural products, ranking third in gates receipts behind corn and soybean field crops (Jerardo, 2007). In

nurseries and orchard production, no alternative methods can be found for the spray technology to effectively protect trees from pests and thus preventing production loss due to pest infection and infestation. However, existing spray systems are not efficient. The level of inefficiency and inaccuracy is even higher in orchard and nursery applications than field crop sprayers. When using conventional spray equipment and flow rate estimation, most nursery crops are over sprayed. Less than 30% of pesticide sprayed actually reaches nursery canopies while the rest are lost (Zhu et al., 2006). Typically, nurseries spend approximately $500 to $1000 on pesticides per acre per year (H. Zhu, personal communication, August, 2010). Lack of proper spray equipment and technology is blamed as the reason for this high chemical input. In contrast to other field crops, orchard and nursery crops have great diversity in their form, size, canopy structure and density and can vary greatly with production circumstances. There is no universal delivery equipment or method that can address all these complex diversities. Most of the pesticides applied using current sprayers is being wasted in the form of off target losses such as airborne drift, sedimental drift, runoff, and evaporation. It is common to see a mix of different sizes of trees in an orchard or a nursery, such as shown in Figures 1.1 and 1.2. Often, there are huge gaps between these young trees. When treating these orchards and nurseries using the conventional sprayers, much of the pesticide will be wasted because it is impractical for applicators to manually adjust sprayer settings to match target tree canopy size and shape after application starts, due to the demands of pest pressure and labor costs. The spray output of a conventional sprayer cannot be adjusted once the sprayer is turned on; a constant amount of liquid is sprayed regardless

whether there is a target or not, or whether the target tree is tall or short (Figure 1.3), narrow or wide. In an orchard or a nursery, with growing different species of tree crops, canopy size, shape and density vary. Therefore, significant amount of pesticide is wasted between trees and into open areas above short trees or around trunks below canopies. Consequently, the excessive use of pesticides not only wastes the grower's money, but also increases the potential for contamination of the environment and poses health risks to the people who work or live nearby.

Figure 1.1. An apple orchard with different sizes of tree canopies

Figure 1.2. A typical nursery production plot with different canopy sizes and shapes

Figure 1.3. Overspray of a nursery sprayer when using the same setting to treat different size crops in the same production line

With the rising cost of pesticides and growing public concerns about the potential contamination of the environment caused by excessive use of pesticides, new pesticide application equipment and strategies have been consistently demanded to reduce the consumption of pesticides.

Turning off sprayers when there is no target, or adjusting application rates based on canopy size and density have been considered by researchers and sprayer manufacturers in the past. Since 1970s this concept has been seriously considered by researchers and sprayer manufacturers because of the significant advances in sensor and control technologies (Reichard and Ladd, 1981). Precision spraying technology was first introduced in boom sprayers by manufacturers in late 1980's (Bode, 2008). Variable rate technology using GPS and GIS technologies has been integrated into several boom sprayers and became commercially available (e.g. John Deere 30-series sprayers). Ultrasonic sensors were integrated into orchard sprayers to detect the presence and absence of a tree and to switch nozzles on or off as necessary (SmartSpray, Durand-Wayland, LaGrange, GA). Although it was a major step towards reducing applied pesticide, this technology can be further improved by developing a control system based on a variable rate function that incorporates information about the tree canopy height, shape and foliage density.

Therefore, to fully meet the requirements for effective and efficient treatments of fruit and nursery crops, it is necessary to develop sensor-controlled intelligent or semi-intelligent spraying systems that deliver pesticides more economically, accurately, timely

and in an environmentally sustainable manner with minimum human involvement before, during and after applications.

1.2 Literature review

1.2.1 Importance of pesticide applications in nurseries and orchards

To insure yield and the quality of production, growers rely heavily on application of pesticides. Without crop protection, the potential loss can range from 43-50% in food crops, and 53-68% in cash crops (Oerke and Dehne, 2004). Fruit production requires repeated pesticide applications while nursery crops are often associated with even higher pesticide use than any other crops because consumers' quality standards for ornamentals are higher (Oerke, and Dehne, 2004).

The use of synthetic pesticides is often unavoidable. Recently, some pesticides have even been classified as irreplaceable by the US National Research Council (Anonymous, 2000). Pesticide-free production often results in a reduction in yield and quality of field crops produced. These problems are even more apparent in fruit production (Knutson et al., 1997), because (1) genetic resistance is often overcomed by animal pests and pathogens, (2) the efficacy and reliability of biocontrol agents is limited, and (3) today manual weed control cannot be expected from most growers. However, an increase in the efficacy of pest control does not depend on an increase in the amount of pesticide used, but primarily on the targeted application of suitable products when needed.

The goal of pesticide application is to deliver effective and uniform dose of chemicals to the target areas in a safe and timely manner. Conventional spray equipment used in nurseries and orchards has some problems with spray efficiency and safety. For example, usually high percentage of chemicals is wasted in the form of drift of droplets,

over spraying, run-off, and off-target deposition. This misdirected pesticide not only reduces the effectiveness of the application and waste growers' money, it also increases the potential of environmental contamination (Deveau, 2009).

1.2.2 Sprayer used for orchard and nursery applications

Air-blast sprayers are commonly used in orchards and nurseries. They include conventional axial-fan air-blast sprayers (Figure 1.4), tower sprayers (Figure 1.5), cannon sprayer (Figure 1.6), tunnel sprayers (Figure 1.7), and custom-designed or modified air-blast sprayers (Figure 1.8 (a) to (e)). Tower sprayers are the air-assisted sprayers that discharge sprays horizontally by directing the airflow from a fan into horizontal ducts on a vertical plane. Tower sprayers are used in nurseries and orchards where horizontal spray trajectory is preferred for the trees with consistent heights.

Air-assisted cannon sprayers consist of cylindrical outlets that create high air velocity jets that break spray mixtures into fine droplets and carries them long distance downwind. The cylindrical spray outlet can be tilted downward, upward, forward or backward to aim the spray at the canopy. The cannon sprayers can cover very wide spray swaths and are often used in nursery fields where conventional air-blast sprayers are not feasible to deliver sprays to the crops. Because of high air velocity, the sprayers can penetrate canopies and create turbulence that disturb plants and increase spray deposition on both leaf surfaces. Compared with air-blast sprayers, the cannon sprayer is generally small in size, easily transported and stored, and only requires a small path for spray application. However, cannon sprayer performances are greatly influenced by wind

conditions and may not produce uniform spray deposition and coverage along the wide spray swath.

Figure 1.4. Conventional air-blast sprayer

Tunnel sprayers (Figure 1.7) became more popular in small fruit tree production during the past decade. The fabric frames of tunnel sprayers are used to enclose target trees to minimize spray drift. Some tunnel sprayers consist of recirculation devices that recycle sprays not deposited on targets back to the spray tank. The limitations of tunnel

sprayers are their large size, complicated structural configuration, frequent maintenance requirement, and difficult transportation (Doruchowski, 2000).

Figure 1.5. Tower sprayer

Figure 1.6. Cannon sprayer (www.jacto.com)

Figure 1.7. Tunnel sprayer (www.lipco.com)

Sensor-controlled variable rate application technology for air-assisted orchard sprayers also has been reported. Giles et al. (1987; 1988; 1989) developed a microcomputer-based sprayer control system with ultrasonic transducers to detect foliage volume, resulting in a commercially available sensor-controlled air-assisted orchard sprayer (i.e. SmartSpray, Durand-Wayland, LaGrange, GA). The sprayer system detects the presence or absence of a tree and switches the nozzles on or off, but it cannot detect the canopy size and foliage density. Because of limited sensor resolution or response speed of the spray-control system, none of the sensor-controlled sprayers has fully achieved variable rates to match tree-canopy shape and density (Fox et al., 2008).

(a)

(b)

(c)

(d)

(continued)

Figure 1.8. Custom – designed or modified air-blast sprayers

(Figure 1.8 continued)

(e)

1.2.3 Variable rate sprayer development for nursery and orchard applications

Variable Rate Technology (VRT) is a concept of the best practice in precision farming. It is a technology that allows variable rates of fertilizer application, seeding, chemical application and tillage within one application. There are normally two kinds of VRT: map based and sensor based. In the map based system, the applied rate is changed according to a prescription map generated with previous survey. In the sensor based system, applied rate is adjusted through information gathered in real time by sensors. GPS, GIS and machine-vision based variable rate application technologies for boom sprayers have been investigated extensively for use in production of row crops (Al-Gaadi and Ayers, 1999; Brown and Steckler, 1995; Han et al., 2001; Hanks and Beck, 1998; Paiceet al., 1995; Thorp and Tian, 2004; Tian et al., 1999; Tian, 2002). However, these technologies are not widely accepted by growers and are limited mostly to weed control.

Because the crop characteristics of nurseries and orchards change considerably during a growing season and the crop life cycle, prescription maps for variable application rates need to be updated frequently, thus making map based VRT very expensive (Mooney et al., 2009). With sensor based VRT, sensors mounted on the application equipment detect crop structure information that controllers process and use to control spray outputs as needed, in real time. Thus sensor based VRT is better suited in nurseries and orchard chemical applications than map based VRT.

There are two major steps in variable rate sprayer development. The first step is to utilize different types of sensors such as ultrasonic sensor and laser sensor to detect target crops or tree characteristics. This step includes data acquisition and data processing to obtain target characteristic information. The second step is to develop variable rate delivery equipment by modifying commercially available sprayers by implementing sensors and controllers.

As mentioned above, with the advancement of sensor and control technologies it is possible to develop variable rate sprayers for the nursery and orchard applications. Researchers have designed several variable rate sprayers using ultrasonic sensors.

Giles et al. (1987, 1988 and 1989) retrofitted a conventional air-blast orchard sprayer by integrating ultrasonic sensor technology into a sprayer control system to measure foliage volume and then control the spray output. Spray savings ranging from 28% to 35% and 36% to 52% were reported in peaches and apples, respectively. In addition, compared with a standard sprayer, the sensor-controlled sprayer had a significant reduction in off-target loss.

Escola et al. (2003) reported research on modifying a sprayer for adjusting spray rate proportional to tree volume. Later an experimental electronic control system was developed and was able to change application rate based on tree canopy width (Solanelles et al., 2006). Ultrasonic sensors were used to measure the distance between the sensor and the outside edge of the canopy and the canopy width at the same height as the ultrasonic sensors. With known values of tree row spacing, sensor position on the tractor and travel speed, the optimal spray volume was calculated and was used to trigger electro-valves for control of the nozzle flow rate. Liquid savings of 70%, 28% and 39% were reported in the olive, pear and apple orchards respectively from the variable rate sprayer compared to a conventional application. Lower spray deposition on the canopy but a higher ratio between the total spray deposit and the liquid spray output (i.e. better application efficiency) were also reported.

Following the work of Escola et al. (2003), Gil et al. (2007) modified a multi-nozzle air-blast sprayer with three ultrasonic sensors and three electro-valves. The nozzle flow rate was modulated in real time as a function of crop width in a vineyard, as measured with the ultrasonic sensors. The canopy in vineyard was divided into three height sections, each covered by one ultrasonic sensor and one electro-valve controlled nozzle. A saving of 58% percent was reported compared with conventional constant rate application while deposition quality on leaves, uniformity of liquid distribution and capability to reach the inner parts of the crop remained similar.

Using the same sprayer tested by Gil et al. (2007), Llorens et al. (2010) compared conventional spray application and variable rate application in three vine varieties at different crop growing stages. The variable rate application was reported to have an average of 58% savings in application volume with similar or even better leaf deposition.

1.2.4 Sensors used for tree crop structure detection

So far, only ultrasonic sensors have been extensively used for developing variable rate sprayers or orchard, nurseries and vineyards. However, there is a growing number of investigation on using ultrasonic sensors and other types of sensor to measure tree crop canopy structure and characteristics, which is a very important step in developing variable rate sprayer for tree crops.

Giles et al. (1988) used a commercially available ultrasonic sensor to detect apple trees. Field tests reported that the sensor was relatively precise in measuring tree width (with less than 10% average error). Tests at ground speeds of 2, 4 and 6 km/h found no significant effect of the ground speed on the sensor detection accuracy. However, it tended to overestimate the tree width due to the conical shape of the ultrasonic pattern.

A crop adapted application system has been proposed, as a result of ISAFRUIT (Increasing fruit consumption through a trans disciplinary approach leading to high quality produce from environmentally safe, sustainable methods) project launched in 2006 in Europe, to improve the efficiency and safety of spray application in orchards based on the actual needs and respect to the environment (Van de Zande et al., 2007). The system will consist of three components: crop identification system (Balsari et al.,

2007), environmentally dependent application system (Doruchowski, 2007) and crop health detection system (Van de Zande et al., 2007).The crop identification system uses ultrasonic sensors to assess canopy width and vegetation density (defined as the number of leaf layers). The environmentally dependent application system identifies environmental circumstances (such as wind velocity and direction, orchard boundary and other sensitive areas from GIS) and adjusts application parameters accordingly. The crop health detection system measures spectral wavelength distribution of picked leaves and identify the water stress, nutrient stress, cultivar and disease stress of the fruit trees.

Wei and Salyani (2004 and 2005) used a laser scanner with an offline processing algorithm to scan the citrus canopy. Based on the scanning data they calculated the canopy characteristics such as tree height, width, canopy volume, foliage density and tree boundary profile. An artificial target was tested and the results showed an accuracy of 97% for the length measurement. The density estimation was found to have good correlation with the visual assessments.

Palacin et al. (2007 and 2008) used a laser scanner to measure canopy volume and to estimate tree foliage area in real time. The validation tests with pear trees concluded there was a linear relationship between canopy volume and the foliage surface area with a coefficient of correlation (R) of 0.81. However, they also reported that the accuracy of the estimation was closely related to tree species and tree truck size could influence the estimation result.

Lee and Ehsani (2008) used a laser scanner to scan citrus trees and designed a program using the saved data to estimate the tree canopy height, width and volume. The

height estimation was compared with manual measurement and the error was found to be less than 1 cm. The width estimation was found to have an error of about 15 cm and its accuracy was believed to be dependent on the accuracy of the tractor speed measurement. The error of the volume estimation varied with the definition of the profile polygon in the algorithm. A minimum error of 0.09% was found for the volume estimation.

Rosell et al. (2009a and 2009b) used a laser scanner mounted on a tractor to scan selected trees of a vineyard and a pear orchard several times before and after defoliation. The scanned data was then used to build 3D images to determine geometrical and structural parameters of the vegetation such as volume and leaf area of trees. These geometrical and structural parameters were compared with crop leaf surface values obtained by manual measurements in which leaves were picked and one-sided projected area of the leaves was measured via shadowgraph measurement techniques. Results have shown a good linear correlation between the canopy volume calculated from the laser measurement and the total foliage area from the manual measurement.

As evident from this review of literature, the sensors most commonly used to measure tree canopy characteristics are one of two types: ultrasonic sensors or laser scanners. Ultrasonic sensors have the advantage of being simple to use and low cost; however, due to the divergence angle of sound waves, its error increases with the increases in distance measured. Also, their accuracy can be affected by the ambient temperature, humidity and even the tractor ground speed. Laser scanning is relatively more expensive but has advantages such as higher accuracy, scanning mode rather than the single point measurement as is the case when using ultrasonic sensors. With laser

scanners, more target information can be gathered in a short period of time, and they are not influenced as much by weather and field environment as the ultrasonic sensors.

Based on previous studies by other researchers, it can be concluded that a laser scanner can characterize more crop structure information with higher accuracy than an ultrasonic sensor. Because the laser sensor can offer acceptable precision and reliability to measure tree structures regardless of weather or lighting conditions, they have greater potentials to be used for the variable-rate sprayer development for orchard and nursery applications than other types of sensors.

1.3 Objectives of research

The overall goals of this study are to develop an intelligent sprayer prototype with automatic control that can match spray outputs to the canopy sectional structures and improve pesticide spray efficiency without reducing the level of crop protection expected from pesticides when compared to the performance of conventional sprayers.

Specific objectives are:

1) Develop an automatic controller to enable the variable spray outputs without changing the spray pressure at the nozzle, and consequently the droplet size.
2) Modify a conventional sprayer to improve spray penetration capability and spray deposition uniformity by newly designed five-port air assisted nozzles.
3) Develop a set of algorithms to calculate tree canopy parameters (such as tree width, height, canopy volume and foliage density) employing a fast speed laser scanning sensor and controller.
4) Develop a spray model for the newly developed variable-rate sprayer to optimize its flow rate based on the sensor data.
5) Conduct field experiments to evaluate performances of the newly developed variable-rate sprayer.

1.4 Description of contents

This study is focused on the development of a variable-rate air-assisted sprayer which integrates a high speed laser scanning system, a custom-designed sensor-data analyzer and variable-rate controller and a multi-channel air-assisted delivery system. The sprayer will have the capability to achieve variable spray rates for different canopy volumes and densities with nozzles of one size. Different flow rates will be obtained with one nozzle size instead of requiring a change of nozzles to change flow rate. A laser scanner (SICK LMS291, SICK Inc., Germany) was chosen as the detecting sensor because of its many advantages over other types of sensors, as explained in detail in the following chapter. A computational algorithm is designed to process signals from the laser and to calculate tree canopy characteristics such as tree height, width, and canopy volume and density. A spray model specifically designed for this sprayer is used to determine the optimal flow rate needed. The model output is sent to the controller circuit boards that convert these control decisions to hardware signals for activating solenoid valves and then modulating nozzle discharge rates. A series of field experiments were conducted to compare spray deposition and coverage inside tree canopies between conventional and the sprayer prototype.

Chapter 2: Research Methods and Design

The ultimate goal of the intelligent sprayer is to reduce pesticide consumption by turning the sprayer off when there is no target to spray (by detecting the gaps between trees) and by applying the optimum level of spray mixture in accordance with the characteristics of the target tree (size, shape and foliage density). Several tasks are required to achieve this goal:

1) Collect data representing the characteristics of tree canopies in a reliable and real-time manner as the sprayer moves along the tree rows. This data-acquisition mechanism should be very robust since the sprayers work in uneven terrain and harsh outdoor environmental conditions in orchards or nurseries. The data transfer rate should be sufficient to satisfy different sprayer travel speeds.
2) While data are being collected by the data-acquisition system, an on-line algorithm performs computation on the stream of real-time data to calculate the parameters that characterize the tree canopy. Based on the computed parameters, an optimal sprayer flow rate is derived to be used by the mechanical control mechanism. This on-line algorithm works on the real-time data stream collected by the data-acquisition system, therefore it must be highly efficient to produce real-time control signals, and very robust to manage a wide spectrum of data input in an outdoor field environment.
3) Given the spray flow-rate decision, a dedicated control mechanism is needed to convert the digital signals (possibly in TTL (transistor–transistor logic) level

voltages) into electrical control signals required to power the solenoid controlled valves that modulate the flow rate from the sprayer nozzles. This control mechanism should respond to the variable rate output of the online algorithm very quickly to change to state of the solenoid valves. Since it is working with very strong current to control the solenoid valves, the control mechanism must be able to tolerate the electrical interference caused by frequent switching. It also must be able to handle the dramatic change of hydraulic pressure while it is changing the state of solenoid valves.

The control system consists of three major components, as shown in Figure 2.1:

1) Sensing component. A fast response laser scanning sensor is used to scan the target tree canopy and collect data representing tree canopy characteristics. The original data produced by the sensor is accumulated in a buffer and transferred to next stage for data processing.
2) Data Processing component. An intelligent algorithm is designed to calculate the tree canopy characteristics using data input from the sensor component. Based on the computed canopy characteristics, an optimal spray flow rate is calculated for the control action.
3) Control Component. This component converts the optimal flow-rate decision into actual Pulse Width Modulation (PWM) signals that was used to activate sprayer nozzles in order to spray the optimal flow rate.

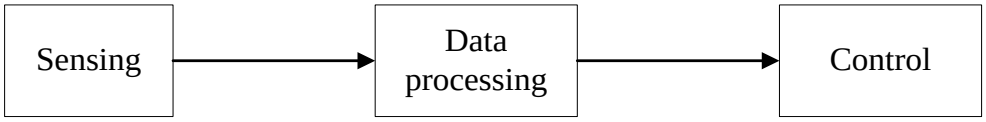

Figure 2.1. Intelligent sprayer control system - overview

Within this research, the procedure as shown in Figure 2.2 was followed. A data-acquisition system using a laser scanner to scan a target and acquire data representing the characteristics of the target was designed (section 2.1). Then an intelligent algorithm was designed to calculate tree shape and density (section 2.2). In the meantime, the performance of the solenoid valves and the nozzles to be used in the intelligent sprayer system were evaluated and calibrated using a specially designed experiment station. An electronic circuit was designed to drive the electronic valves (section 2.3). To use the data generated by the sensor to adjust the controller for varying spray output, a spray model was established (section 2.4). The output from the spray model was used to match the variable flow-rate control of the sprayer to the spray target. A mechanical prototype of the intelligent sprayer was also developed (modified from a commercially available sprayer) to be used for field tests and to demonstrate the effectiveness of our approach (section 2.5). Comprehensive field tests (section 2.6) and an outdoor test on container trees (section 2.7) were conducted to evaluate the performance of the intelligent sprayer prototype in terms of spray uniformity, spray loss off the target, downwind drift and

liquid consumption(section 2.8) comparing to intelligent sprayer without automatic control and a conventional air-blast sprayer.

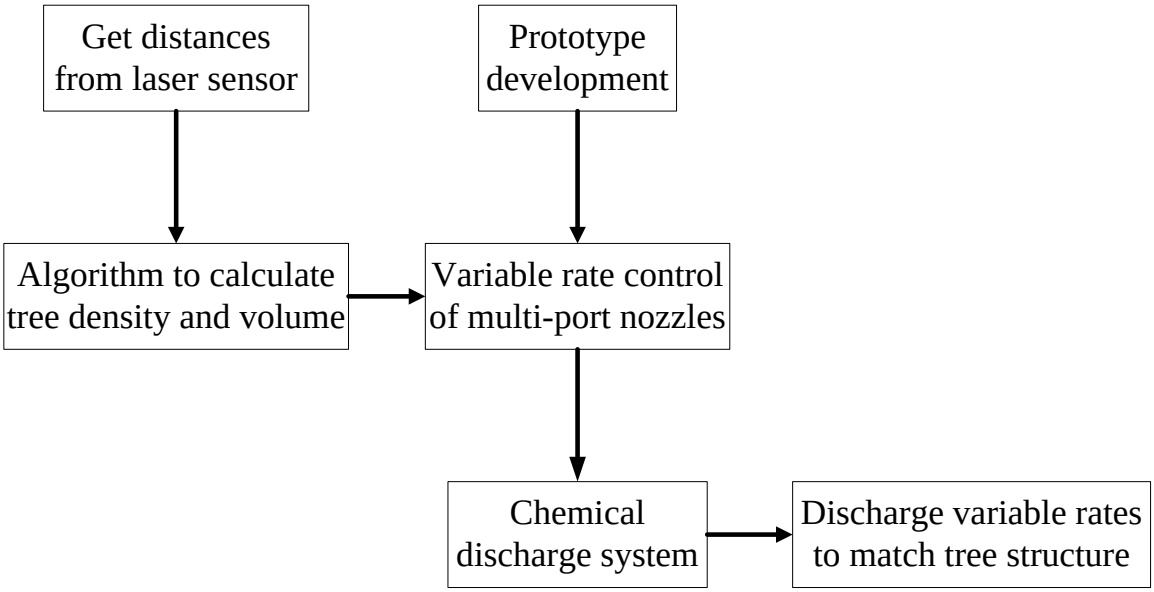

Figure 2.2. Intelligent sprayer control system – detail

2.1 Data Acquisition System

A high speed laser scanning sensor was used to acquire the data needed to characterize tree canopy. The canopy information was compiled into a data stream that was then transferred to a laptop computer using a fast baud rate gateway. Software functions included: initializing the laser sensor, establishing communication with specified mode settings, and manipulating the ranged data stream.

2.1.1 Hardware components

As described in Figure 2.3, the hardware used for scanning and acquiring data includes a laser scanner (LMS291, SICK Inc., Germany) as shown in Figure 2.4 (a), a 12VDC to 24VDC converter VHK100W-Q24-S24 (CUI Inc., Tualatin, OR) to power the laser scanner with tractor battery, a high speed serial (RS422)-to-Ethernet communication gateway DeviceMaster 500 (shown in Figure 2.4 (b), Comtrol Co., New Brighton, MN) and a laptop computer.

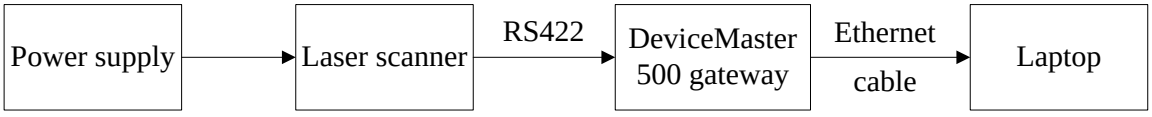

Figure 2.3. Flow chart of hardware for laser communication

(a) LMS 291 (b) DeviceMaster 500 1 port unit

Figure 2.4. (a) Laser scanner and (b) fast baud rate gateway DeviceMaster 500

2.1.1.1 Laser scanner

As shown in Figure 2.5, the laser scanner operates based on the Time-of-Flight (ToF) principle. A pulsed laser beam is emitted from a diode inside the laser scanner and then after hitting an object, part of the beam is reflected back via the same path along which it was sent and is received by a receiving diode. A counter starts to count time as soon as the light pulse is transmitted and stops when the reflected signal is received. Range measurement is calculated by multiplying the speed of light with the time difference between transmitting and receiving of the pulsed laser signal. With a rotating mirror and an encoder, a sequence of range measurements can be made on a 2-D plane (with the maximum range of 180° for Model LMS291).

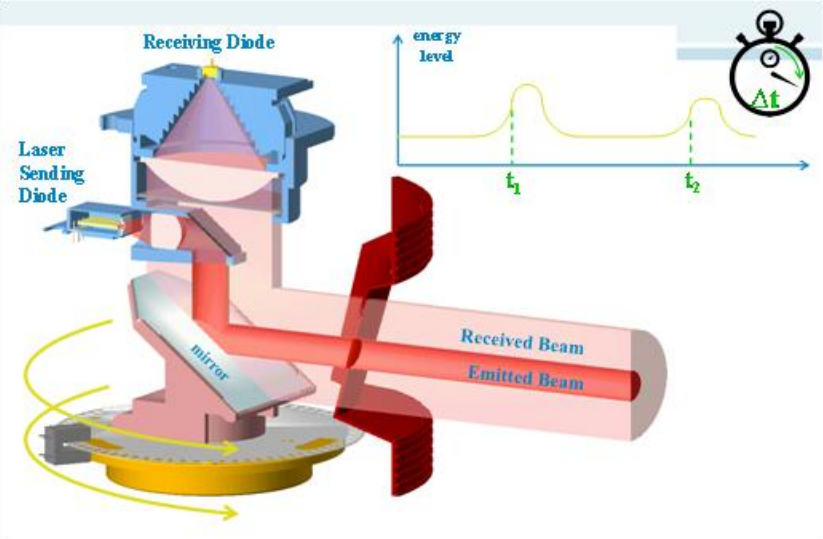

Figure 2.5. Time-of-Flight measurement with SICK LMS2XX series (source: SICK Inc.)

As shown in Table 2.1, the laser scanner LMS291 has several scanning modes and ranges. It can scan any angular range smaller than or equal to 180°.The angular resolution can be chosen from 0.25° (for less than 100°scanning ranges only), 0.5° and 1°. Vertical resolution is affected by the angular resolution, the distance from the scanner to the object and the shape of the scanned object. For example, when using 0.5° angular resolution, if the center of the laser scanner is 1.62 m away from the tree trunk center, the vertical resolution at the tree center line is: $1.62\,m \times \tan(0.5°) = 0.014\,m = 1.4$ cm, and the vertical resolution for the tree surface measurement on the half of the tree which is closer to laser, is less than 1.4 cm. Horizontal resolution depends on the time the laser takes for one scan and the travel speed. For example, if the laser is configured to scan from 0° to 180° with 0.5° angular resolution, it takes 26 ms to finish one full scan, and if

the laser is mounted on a tractor with a forward speed of 3.22 km/h, the horizontal resolution then is: $26\,ms \times 3.22\,km/h = 0.023\,m = 2.3\,cm$. In all the tests done for this study, the laser was configured with 0° to 180° scanning range and 0.5° angular resolution.

Features	Specifications
Scanning angle (field of vision)	180° Maximum
Angular resolution	0.25°/0.5°/1° (selectable)
Response time	53 ms/26 ms/13 ms
Range	80 m Maximum
Measurement resolution	10 mm
Statistical error standard deviation	± 5 mm
Laser diode (wavelength)	Infra-red (λ = 905 nm)
Laser class of device	Class 1 (eye-safe)
Data interface	RS232/RS422 (configurable)
Transfer rate	9.6/19.2/38.4/500 kbps
Data format	1 start bit, 8 data bits, 1 stop bit, no parity
Supply voltage	24 VDC ± 15%
Power consumption	Approximately 20 W (without load)

Table 2.1. Specifications of LMS291 laser scanning sensor
(Source: LMS291 user manual)

2.1.1.2 Fast baud rate gateway

The laser scanner and a portable computer were connected with the DeviceMaster 500 (as shown in Figure 2.4 (b)) and Ethernet cable. Data interface for the laser scanner was configured with a 4-wire RS422 connector. The default transfer rate for the data interface was 9.6 kbps which was used at the start–up point, but it was switched to 500 kbps after initialization for the real time measurement.

2.1.2 Software design

The flow chart for programming the laser scanner is shown in Figure 2.6 (details as shown in Appendix A). The software design included three major functions: initialization of the laser scanner with a proper scanning mode, starting and stopping the streaming of measurement data and transmitting data to laptop computer. In each step, telegram command(s) in the form of hexadecimal strings were sent to the laser, for configuring the operating mode of the laser and for controlling the laser scanner to perform certain actions. A response telegram was received and compared with an expected value after each command was sent and before the next action was taken. For example, in the initialization step, several telegram commands were sent to the laser to configure its scanning range, angular resolution, range unit, and transmission baud rate. After response telegrams were received and each configuration was confirmed to be successful, another telegram was sent to the laser scanner to start streaming the scanned data.

At a baud rate of 500 kbps, all the scanned data was transferred from the scanner to a portable computer serial port buffer. In this operation, the header of each data string was first identified, and then expected length of the string was parsed. After that, a frame of range measurements was read. At the end of each telegram, a checksum (CRC) was attached. With the structure of the checksums provided in the product manual, CRC was checked after the data string was received and a correct data transfer was made.

In addition, error handlers were created and were used throughout every step. If the program ran into exceptions, actions such as stop data streaming were taken and the operator notified.

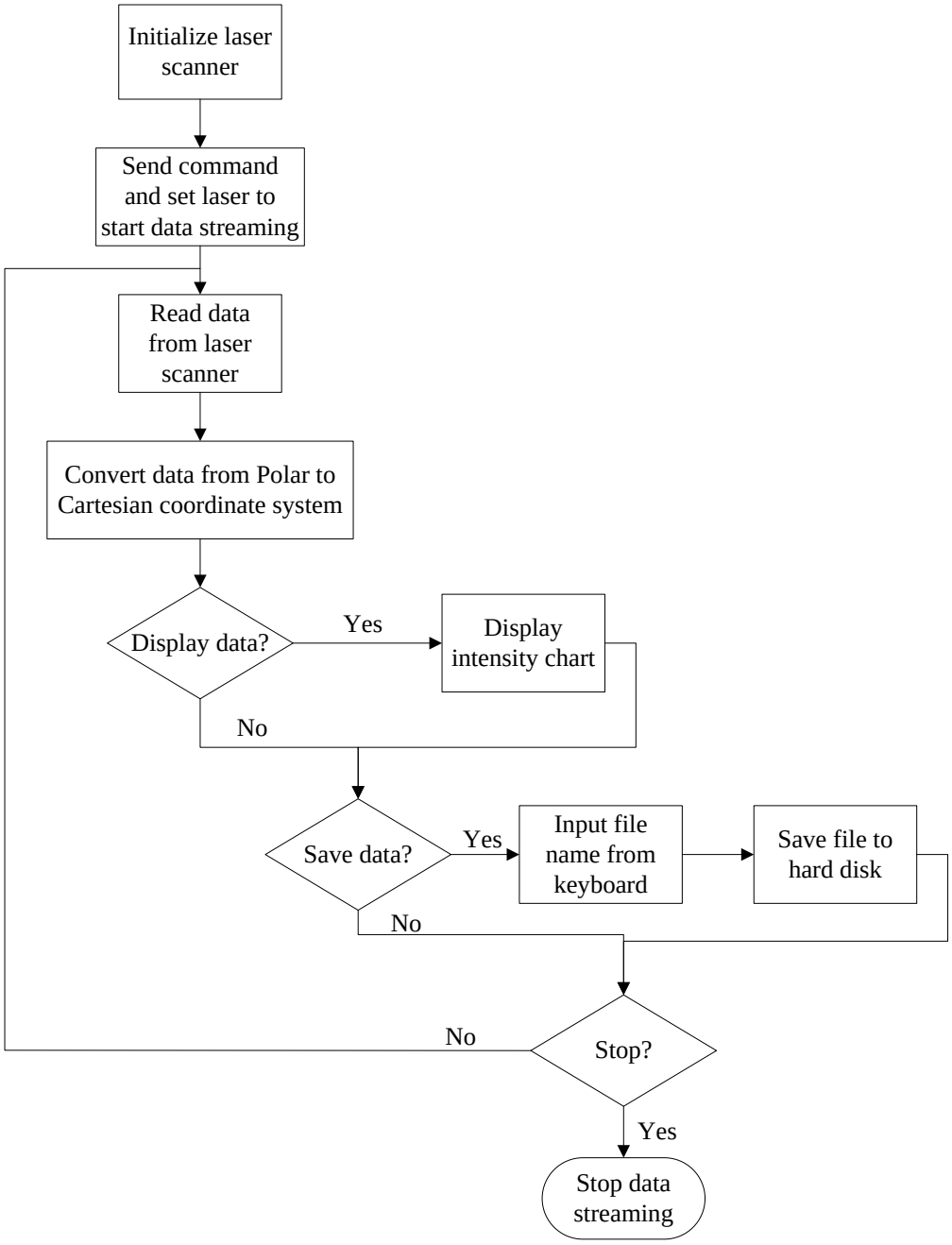

Figure 2.6. Laser communication software flow chart

2.2 Algorithm to characterize tree canopy

The core of the software component for the intelligent sprayer is an intelligent algorithm to characterize a tree canopy based on the laser sensor detection and for calculating an optimal output flow rate in correspondence to the computed canopy profile and density.

2.2.1 Basic terms and definitions used in the algorithm design

The data collected by the laser sensor reflects the distance of individual points on the canopy surface to the sensor's central point. This distance is then used to determine the distance between the tree vertical center line and the detected point on the canopy surface. The tree vertical center line is determined beforehand by using the "top point rule" which will be explained in the following sections. However, obtaining foliage density information from range values can be more challenging and will be discussed first.

The major part of the work in this canopy characterization algorithm is to predict foliage density using distance/range measurements from the laser scanner. The density algorithm was designed based on two assumptions:

1) In a short/limited height *h* (height range covered by one nozzle), the densest possible canopy of a tree will appear to be a flat surface, parallel to the plane defined by the tractor forward direction and tree vertical center line.

2) For a small volume of the canopy viewed from the sensor, the surface topology will vary but there is no empty space or hollowness inside of the canopy.

To describe the design of the algorithm, especially the design of density calculation, several terms are defined below. Figure 2.8 presents a graphical illustration of these terms.

Frame: During canopy detection, the laser scanner spins and scans 180° vertically to obtain an array of distance data, and each data point represents a distance between the scanner and the point detected on the canopy surface for a certain angular interval. This array of data is called a ***Frame*.** For example, in the 180° range and 0.5° angular resolution scanning mode, one frame of data contains 361 data points, and each data point represents the distance between the scanner and the canopy surface for the angular intervals of 0°, 0.5°, 1°, 1.5°… 179.5° and 180°.

Slice: A *Frame* is a basic unit of data collection. However, it cannot be directly utilized to do computation because canopy characteristics must be derived from a contiguous space range, and a single frame cannot provide sufficient information about the space topology of the canopy. Therefore, multiple contiguous *Frames* (such as 10 frames) is concatenated into a bigger 2-D array, called a ***Slice*** which represents a contiguous space range in the tree canopy, and is used as the unit of calculation to compute the tree canopy parameters over a contiguous space.

Segment: A slice of data points is equally divided into 20 height groups of points from the ground upward across the height with an increment of the height covered by the spray discharged from one nozzle (e.g. 13.5 cm). Each of such a group of points is called

a ***Segment.*** Each *segment* may not contain the same number of data points but has the same height. A *segment* is physically covered by its corresponding spray nozzle.

Density: Density in this scenario is defined with the assumption that, the ideal segment of the densest canopy should be 100% filled with tree-substances (leaves, twigs, branches, etc.) from the canopy surface inward to the trunk of the tree. Looking from the laser sensor, this segment will appear as a cube with purely flat surface and with a depth equal to the cross-section width of the canopy from the surface perpendicular to tree vertical center line. The ***density*** of a *segment* is defined as the ratio between actual volume filled with tree substances and the maximum possible volume.

For an ideal segment with density equal to 100%, all points on the canopy surface have the same distance to the tree vertical center line equal to the cross-segment width of the tree. In reality, a segment may have some holes and hollows on its surface (due to the lack of leaves, etc.). As a result, the volume of substances inside the segment is less than the maximum possible volume which corresponds to 100% density. This is illustrated in Figure 2.7. In the figure each data point is represented by a bar, with the length of the bar equal to the distance of that point to the tree vertical center line. Each bar in a same segment has the same normalized bottom area, so that its volume can be calculated by multiplying the bottom area with its depth. Summing up all bars in a segment yields the total volume of that segment. The maximum volume of a segment can be computed by filling that segment using the bar with the largest depth in that segment. The segment's density is derived by dividing its actual volume over the maximum possible volume of that segment.

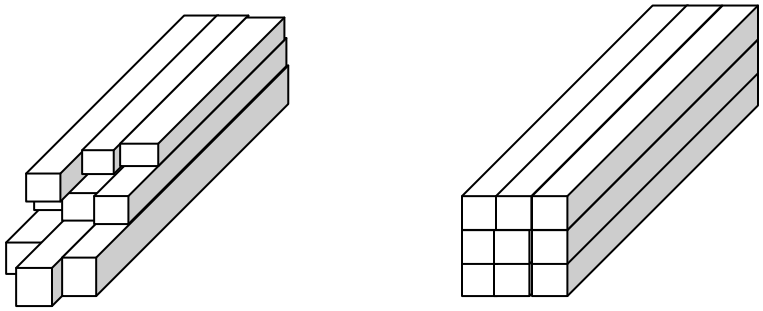

A real segment with density < 100% An ideal segment with density=100%

Figure 2.7. Two segments with different densities

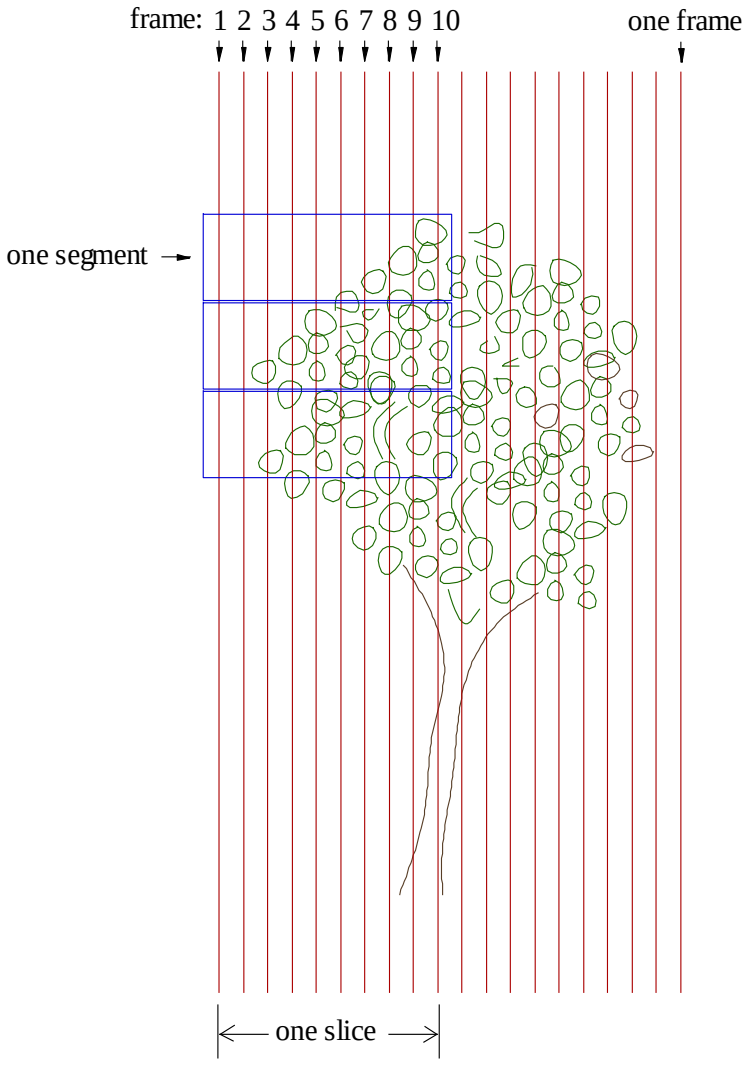

Figure 2.8. Illustration of definitions used in the algorithm

2.2.2 Algorithm design

The density-calculation algorithm consists of multiple stream-lined components that form a cascade of processing, as is shown in Figure 2.9 (details as shown in Appendix D and E).

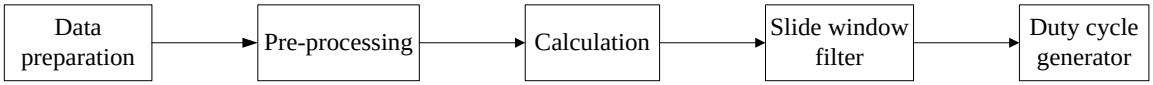

Figure 2.9. Density algorithm design flow chart

2.2.2.1 Data preparation

Since data from the laser scanner is formatted in polar coordinates, a conversion is needed before data can be processed further. As shown in Figure 2.10, range values are converted to Cartesian coordinates using their angles. Converted data points are saved in two buffers and then delivered to the computation module.

The computational module accepts input in unit of frame. In the data-preparation component, a double-buffer is prepared to accommodate the input frames. Each of the double buffers has the same size as a slice. The data frames are concatenated into the first buffer. Once the accumulated frames form a complete slice, this slice is delivered to the next stage in the chain, while input frames are redirected to the second buffer. By the time the second buffer is filled up, the data processing in the first buffer will be completed. Then, the first buffer will be switched to receive new data while the data in

the second buffer is delivered to the next stage for processing. In this way, a Ping-pong cycle is formed. The double-buffering mechanism guarantees concurrent data processing with data buffering, which provides the efficiency to achieve real-time processing in the density algorithm.

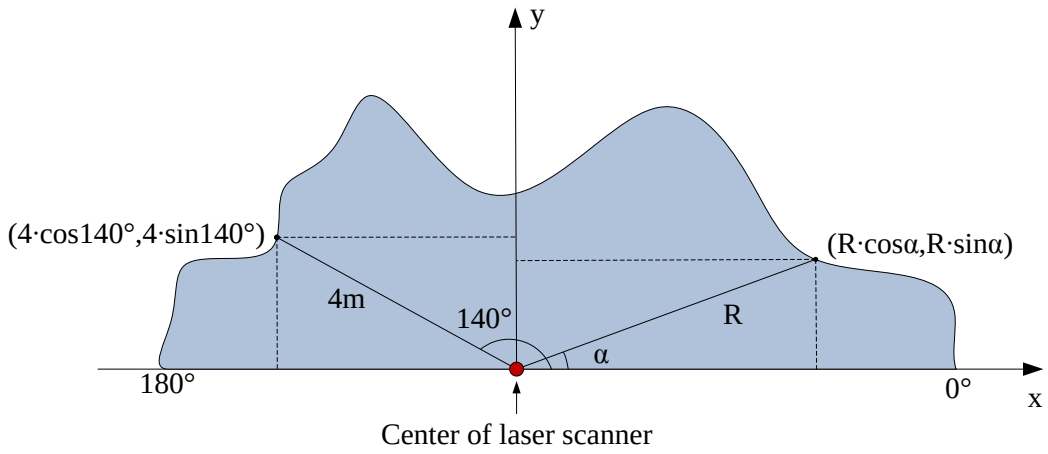

Figure 2.10. Conversion from polar coordinates to Cartesian coordinates

2.2.2.2 Data Pre-processing

The slices generated by “Data preparation” module will enter “Data-preprocessing” component. Each frame of data generated by laser scanner corresponds to a scan that covers a 180° half-circle range scanning from the ground to the sky, while the section of interest in the range is only the part where the canopy resides. Therefore, in the “Pre-processing” part, the head and tail of each data frame will be trimmed off, which

leaves the main body of a frame corresponding to the tree canopy. In an outdoor environment, the data frames usually contain some "outlier" values caused by environment noises such as sun glare. If not filtered out, they will bring some uncertainty into the density computation. The "Pre-processing" part also eliminates these "outliers" by resetting their values to 0.

The value of each data point represents the distance from laser sensor to that point detected on the canopy. However, the calculation of canopy density is based on each point's distance from the canopy surface to the tree center. In order to derive this distance, the position of the tree center needs to be calculated first. A simple yet effective procedure to find tree center distance from the laser sensor was designed as below:

1) After trimming off head and tail of each data frame and filtering out outlier values, each data frame was scanned from the top, and the first point with non-zero value was found. This point was regarded as the "top-of-canopy" for that frame. Each point was captured in a pair of values: the height of that point, and the distance from that point to laser sensor.
2) All the "top-of-canopy" points within one slice were then compared to find the point with the greatest height value. That point becomes the "center point" for the current slice, and its "distance to the laser sensor" was used as that slice's "center distance" to the laser sensor.
3) A sliding window which contains the center points for the past 5 slices was maintained in the memory. Once the "center point" for the current slice was found, it was shifted into the sliding window and the oldest point was retired from the sliding

window. Then the 5 points was compared in this sliding window and the largest distance value to the laser sensor was found. This value was output as the "distance from the laser sensor to the tree center" for the current slice.

After acquiring the tree center distance for a slice, all surface data points in the slice was subtracted from the center distance to get their distances to the tree center. These distance values were then pipelined to the next stage to be used to calculate tree canopy density.

2.2.2.3 Calculation

After pre-processing, the data slice is split into multiple segments (each segment corresponding to one nozzle's height) and computation is performed on each segment to calculate its density. The calculation can be divided into the following stages.

1) Data segmentation

Since the intelligent sprayer has multiple nozzles to cover different parts of the tree canopy, the tree canopy needs to be split into multiple segments of equal height that are covered by the spray from one nozzle. Given the number of nozzles, the height that one nozzle covers and distance from laser sensor to the tree center, the split strategy to divide one data slice into multiple segments can be derived. For each working mode (e.g. different angular resolution mode and angular range mode) of the intelligent sprayer this split strategy is different, and this strategy is called a ***template***.

Given a working mode (such as 0° to 180° scanning range with 0.5° angular resolution mode used in the field tests including in this dissertation) of the intelligent sprayer, the template remains the same and does not need to be computed for every data frame. Therefore templates for every possible working mode of the intelligent sprayer are calculated and prepared beforehand. Before the sprayer starts to work, its working mode will be predetermined and sent to the algorithm, and the algorithm will pick the data split template appropriately for that specific mode. For a slice of data, the split template is applied into each frame and then each frame is divided it into multiple sub-frames. All the sub-frames in the same position of a slice form a segment.

From basic geometry, the radius covered by each segment is different since each segment is of the same height. However, the laser sensor generates data points at equal angle intervals. As a result, each segment covers varied number of data points.

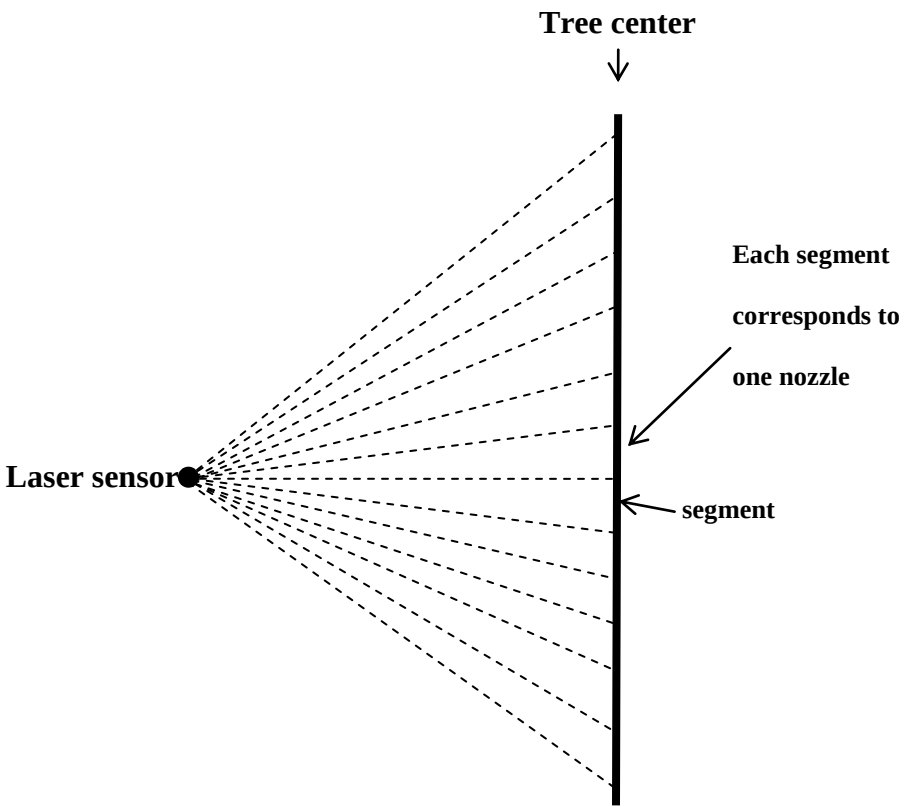

Figure 2.11. Illustration of data segmentation

2) Density computation

Now the data slice has been split into segments, and the value of a data point represents its distance to the tree center. According to our definition, density of a segment is determined by the actual canopy volume over the maximum volume of that segment. As illustrated in Figure 2.7, the basic idea is to treat each data point as a bar. All the bars in the same segment have the same normalized bottom size/area, while depth of the bar is the distance from its surface point to the tree center. By summing up the volume of all

the small bars, the volume of this segment is calculated. In the assumption stated earlier, it is assumed that for the maximum possible volume of this segment, it is filled with bars with the largest depth of all the data points in the segment and forms a cubic. The volume of this cubic is easily derived by multiplying the bottom area with the largest depth. Thus the density of the segment is calculated with the ratio of its actual volume over its maximum possible volume.

$$\rho_i = \frac{V_{act}}{V_{max}} = \frac{\sum_{j=0}^{n} W_j}{W_{max} \times n} \tag{2.1}$$

Where:

ρ_i : Canopy density for segment i (corresponding to nozzle i),

V_{act}: Actual volume of the canopy section detected by laser scanner,

V_{max}: Maximum possible volume if this section has the maximum density,

W_j: Width (depth) of every data point in segment i,

n: Number of effective data points in segment i,

W_{max}: Maximum width (depth) of segment i,

2.2.2.4 Improvements of density definition

From the above definition, the algorithm is extended to cover several special cases.

1) To handle a transition slice

As the sprayer moves along the tree row line, the laser sensor will detect consecutive tree canopies interspersed with empty spaces. When the sensor moves from an empty space to an area covered by canopy or from canopy area to empty space, the slice will be a partially empty; this is called a transition slice. Figure 2.12 illustrates a segment in a transition slice. This segment consists of 4 sub-frames. The sub-frame 0 is at the transition area from empty space to canopy, and it contains only 1 valid data point. If sub-frame 0 is included in calculation, it will expand the bottom area of this segment and hence increase the maximum volume of this segment, which results in a smaller computed density than a typical human being would perceive.

In order to improve the accuracy of density computation, any highly sparse sub-frame that contains too few valid data points from a segment was filtered out. A threshold value T_t was chosen, and if number of valid data points in a sub-frame is smaller than this threshold number, this sub-frame is excluded from the segment. In the example in Figure 2.12, if T_t is set to be 2, then sub-frame 0 will be eliminated, and the bottom area of this segment becomes 4×3 instead of 4×4. This filtering mechanism helps to preclude polluted data at the transition area from the computation, and hence improve the density accuracy.

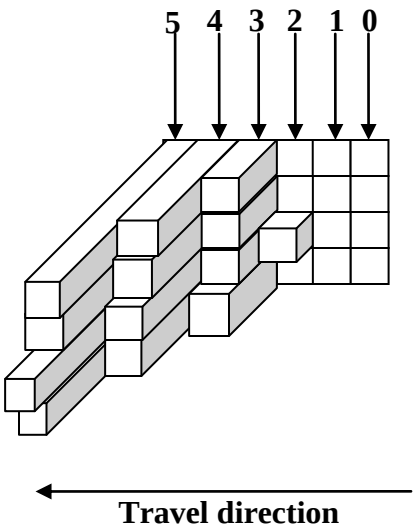

Figure 2.12. Illustration of a segment in a transition slice

2.2.2.5 Sliding Window Output

The density algorithm computes a density value for each segment in a slice. These density values of a slice form an array, and this array is transferred to the next stage to determine the sprayer flow rate for each nozzle. The operator can directly utilize the current slice's density values to control the flow rate, and this usually produces satisfactory results in low wind situation. However, under unfavorable windy conditions, this strategy may not provide satisfactory match between optimal spray and target canopy. If the wind contains a strong component perpendicular to spray direction, the spray liquid from the sprayer may be blown away from the original designed path and end up not residing on the correct location on the canopy. As illustrated in Figure 2.13, the canopy is scanned to form three slices, and the sprayer sprays pre-calculated amount

of liquid for each slice. Due to the strong wind component perpendicular to the spray direction, however, the liquid aimed at slice 1 is blown toward to 1', liquid for slice 2 ends up on slice 1, and slice 3 cannot receive any spray.

To overcome this mis-targeting problem caused by wind conditions, a sliding window mechanism to offset possible negative impacts is designed. A sliding window at the output side of the computation is prepared. This sliding window contains a circular buffer to hold the density results for the past three slices including current slice. The computed density from section 2.2.2.3 is shifted into this slide window as current slice, and the oldest slice in the buffer is retired and replaced by the newest result. Then the three arrays in the sliding window are compared to form a new **output array**. Every element in this **output array** is the largest value of the three elements at corresponding positions from the three past arrays. Eventually, this sliding window will provide the capability of "remembering" the computation result in the past. Consequently, the mis-targeting problem is compensated by adjusting the delay unit (described in section 2.5), and opening the nozzles ahead of time for one slice and delay the turning-off for one slice.

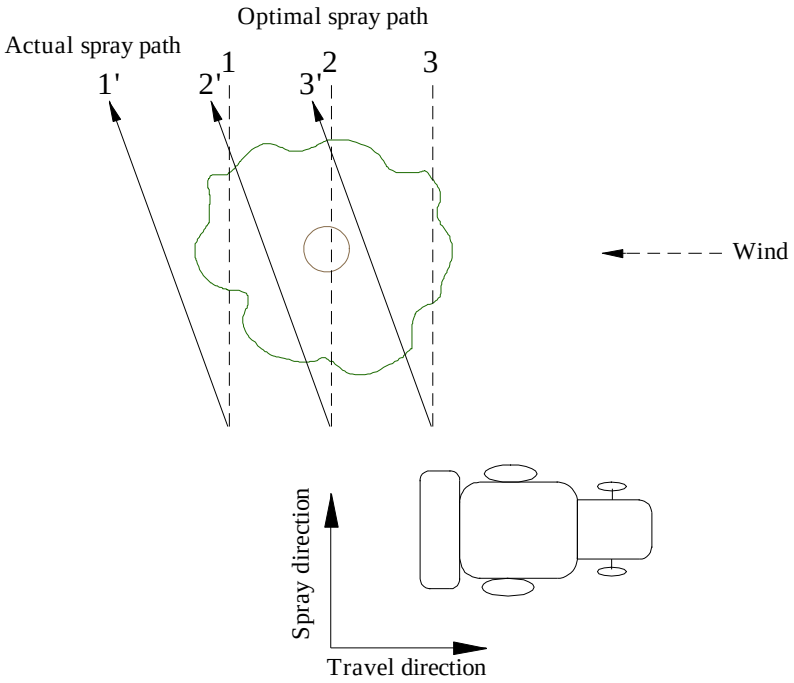

Figure 2.13. Potential wind effect on spray path

2.2.3 Evaluation of the algorithm

Tests were performed using an artificial target to evaluate the accuracy of the density algorithm. The artificial target was designed to mimic the surface roughness of different densities.

2.2.3.1 Laboratory experiment setup

An indoor moving track was built to move the laser scanner and scan at a selected speed. The laser scanner was mounted on a 6.1 m steel track and a string was attached to the laser mount. A step motor was attached to the end of the track and was used to pull the string to transport the laser scanner. The laser scanner could move in two directions at a selected controllable speed. The speed was adjusted by changing the motor speed and duration of pulse signal. After a short travel distance the laser scanner reached a desired steady speed. The target was placed within the sections where laser speed is steady and at 1.8 m in front of the track. In this study, the laser scanning data was moving at a travel speed of 3.22 km/h. The scanned data was processed using the designed algorithm to calculate the density of each pattern.

2.2.3.2 Using artificial target to test the performance of the density algorithm

2.2.3.2.1 Design of the artificial target

To validate the accuracy of density algorithm, artificial targets made of 3.5×3.5×60 cm (assuming a typical leaf size is 3.5×3.5 cm) lumber blocks were used The targets were formed with 23 rows by 13 columns of lumber blocks as shown in Figure

2.14. A strip of wood was added on top of the lumber blocks and was used to mimic the tree center line. By pushing each lumber block outward or inward, different patterns and thus different densities/surface roughness were obtained.

To map the height that the nozzles cover, the array of lumber blocks was divided vertically into four sections and each section activated one nozzle corresponding to that height. The laser scanned the lumber blocks several times and the data was saved and analyzed using the designed density algorithm. The density of each section was calculated accordingly by the following equation:

$$\rho_i = \frac{V_{act}}{V_{max}} \tag{2.2}$$

Where:

ρ_i : Density for the section of blocks in the ith height,

V_{act}: Actual volume of lumber inside of this section of block,

V_{max} : Maximum possible volume for this section of blocks, when considering the target to be a solid rectangular that included every lumber blocks.

(a) front view

(b) side view

Figure 2.14. Lumber block as artificial target

2.2.3.2.2 Pattern arrangements and relevant density

The patterns of the lumber blocks used are shown in Figure 2.15 (a) to (e). The density for each pattern was calculated and presented in the figure caption.

In Figure 2.15 (a), the pattern was designed by placing one lumber block at its original surface and the other three adjacent blocks pushed inward (behind the simulated tree centerline). Thus for this pattern, the density was,

$$\rho = \frac{1}{1+3} = 0.25.$$

In Figure 2.15 (b), for each block on its original surface, two adjacent blocks were pushed inward behind the center line (created by the wood board on top of the blocks). Thus for this pattern, the density was,

$$\rho = \frac{1}{1+2} = 0.33.$$

Similarly, in Figure 2.15 (c), the density was,

$$\rho = \frac{1}{1+1} = 0.5.$$

In Figure 2.15 (d), the density was,

$$\rho = \frac{4}{4+2} = 0.66.$$

In Figure 2.15 (e), the density was,

$$\rho = \frac{3}{3+1} = 0.75.$$

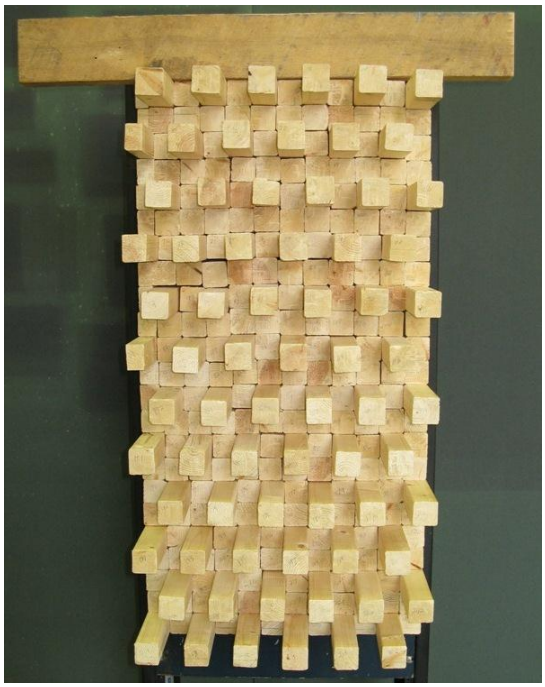

(a) Lumber block with density 0.25

(b) Lumber block with density 0.33

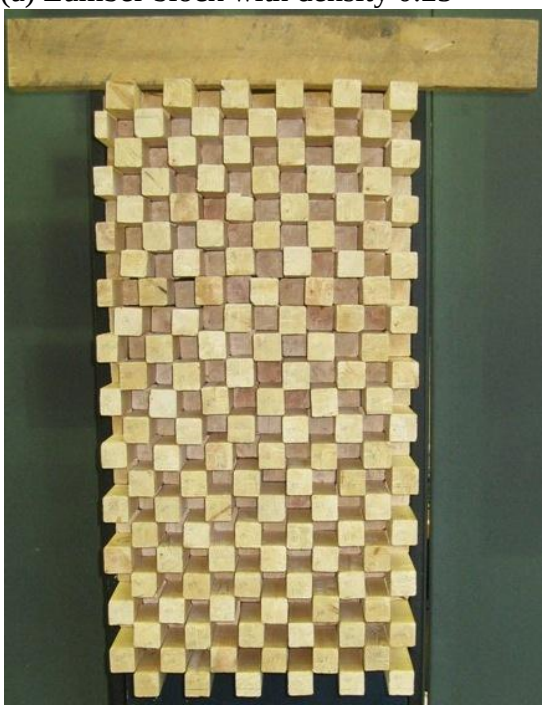

(c) Lumber block with density 0.5

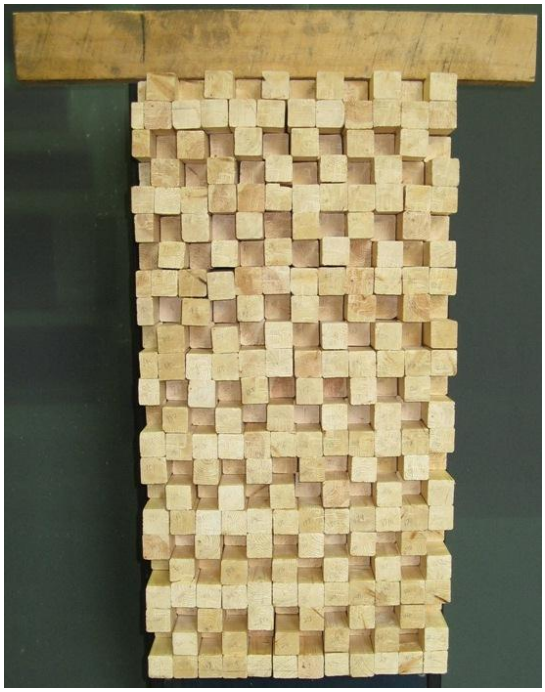

(d) Lumber block with density 0.66

(continued)

Figure 2.15. Lumber blocks with different densities

(Figure 2.15 continued)

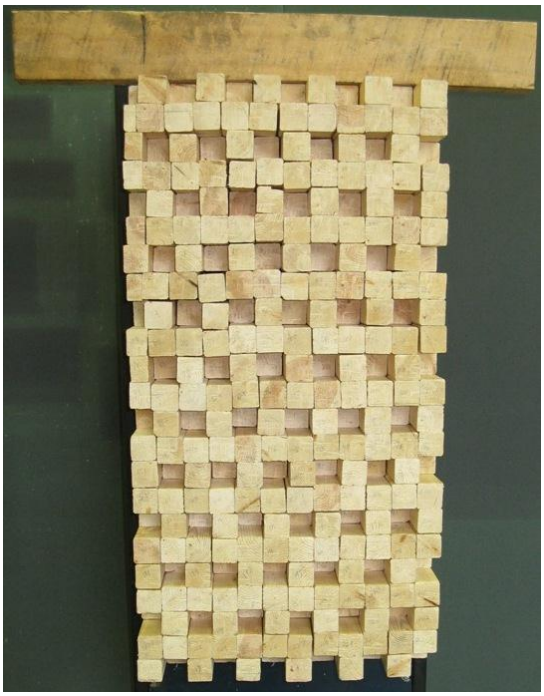

(e) Lumber block with density 0.75

2.3 Flow-Rate Control System

2.3.1 Controller components

Solenoid valve assemblies (Capstan Ag Inc., Topeka, KS, US) were used for controlling the flow rate (output) of each port of the multiport air assisted nozzles. One solenoid valve was connected to one nozzle outlet to control each nozzle output independently in a fast and reliable manner.

Pulse Width Modulation (PWM) signals were used to control the solenoid valves making possible changing of the flow rate output of each nozzle. The PWM duty cycle was defined as T_{on}/T_{off} (%) in one period and the range is 0% - 100%. Changing the duty cycle of the PWM signals controlled the open time of the solenoid valve, and thus altered the flow rate of nozzles.

A USB-4304 9513-based counter/timer board (Measurement Computing Co., Norton, MA, US) shown in Figure 2.15 was used to generate PWM signals with configurable duty cycles. It has 10 channels of counter output that can be used for generating PWM signals through a custom designed computer program. Two USB-4304 boards were used to generate 20 channels of PWM control signals for 20 nozzle outlets on one side of the intelligent sprayer.

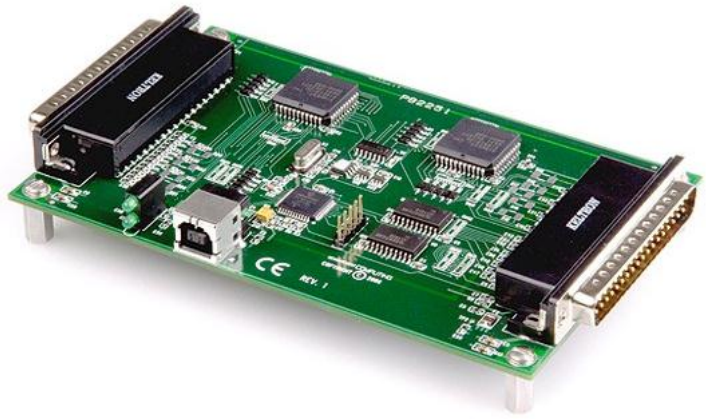

Figure 2.16. USB-4304 board (courtesy from mccdaq.com)

This counter board was connected with a laptop computer through a USB cable (<5 m length limit) for data communication and also for supplying +5 VDC power to the board. Each board could draw up to 500 mA current. To satisfy the need for multiple USB boards, a powered USB 2.0 hub (Belkin, Playa Vista, CA, US) was used and was powered with a 12 VDC to 5 VDC converter VHK 100W-Q24-S5 (CUI Inc., Tualatin, OR, US) using a self-made 1.35 mm DC power plug connector.

The two USB 4304 10 channel timer/counter boards (Measurement Computing Co., Norton, MA, US) were used to generate PWM signals for 20 ports on one side of the intelligent sprayer. The PWM signals then went through amplification and switching circuit to open and close the solenoids that were attached to the nozzles to control the rate of spray outputs. One N-MOSFET was used to switch one 12 VDC solenoid on or off according to the high or low level of the 5 VDC TTL (Transistor–transistor logic) PWM signal that was sent by the counter board.

2.3.2Software design for generating PWM signals

A logic program was specially developed to control USB 4304 counter board to generate 10 channels of PWM signals with independent duty cycles using LabVIEW software (National Instruments Co., Austin, TX, USA). Figure 2.17 shows the flow chart for generating PWM signals with the desired duty cycle and frequency (details as shown in Appendix C).

2.3.3 Switching/amplification circuit using PWM signals

Since the PWMs signals generated from the counter board are +5 VDC TTL (Transistor–transistor logic) signals, they are required to be amplified in order to be able to control the solenoid valves that are powered at 12 VDC. Custom switching/amplification circuits designed for four functions: 1) supporting +12 VDC power from external tractor battery and also receiving +5 VDC power from USB port through USB 4304 power pins; 2) connecting 10 channels of independent PWM signals generated from USB 4304 board to the corresponding program; 3) switching from +5 V TTL to +12 V signals to activate solenoid valves; 4) limiting the reverse kick-back current from solenoid coil using *Zener* diodes (details as shown in Appendix B).

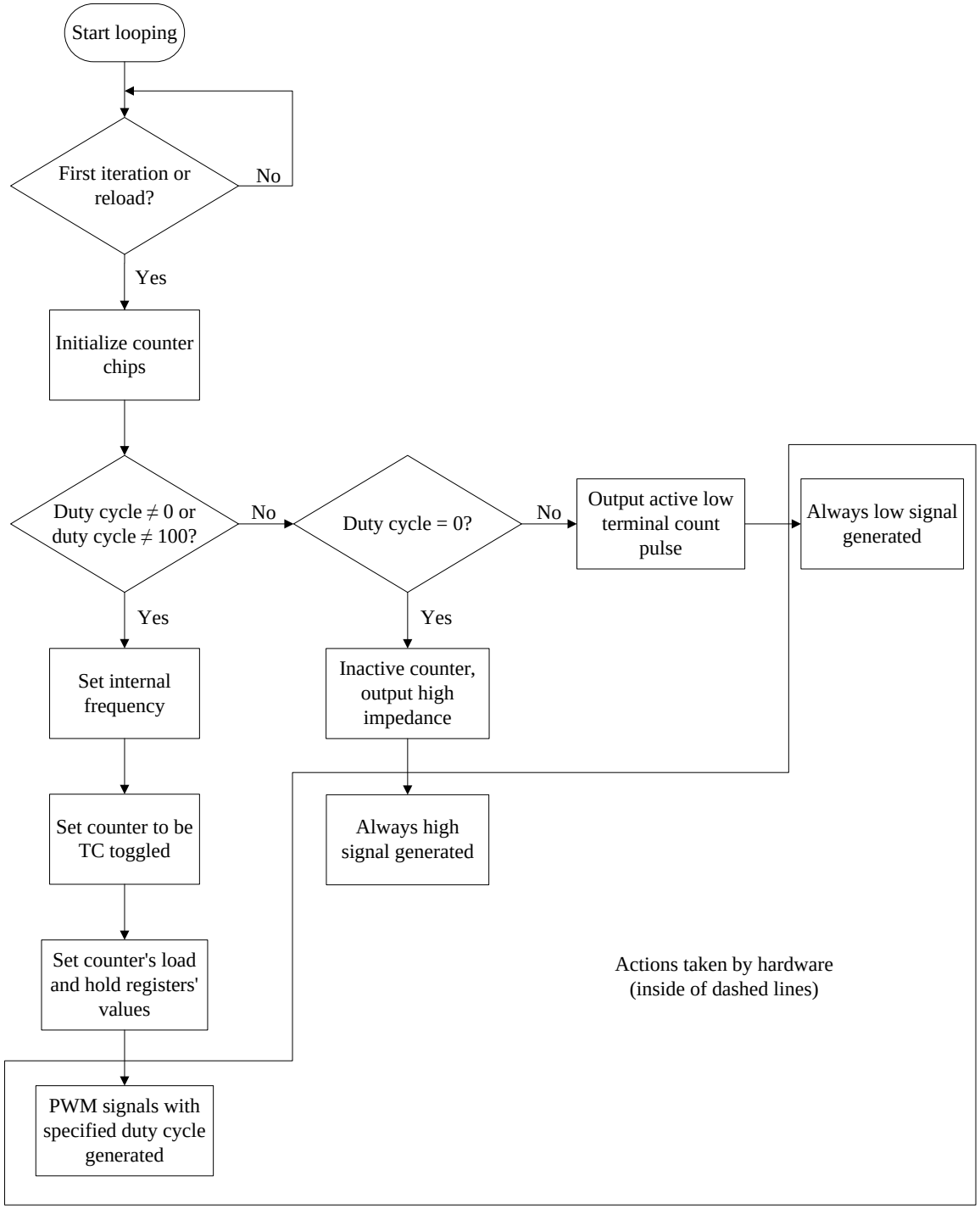

Figure 2.17. Flow chat for generating PWM signals

2.3.4 Experiment station for one five-port air assisted nozzle

An experiment station was built to test the variable rate control software and hardware and also to calibrate the five-port air-assisted nozzle. Figure 2.18 shows the schematic of the design of the experiment station for independent control of one five-port air-assisted nozzle.

The experiment station included a tank and a pump for supplying liquid, a pressure regulator and a mechanical pressure gauge for adjusting the liquid pressure manually, a pressure transducer and a flow sensor connected to a data acquisition board (USB-1608FS, Measurement Computing Co., Norton, MA, US) shown in Figure 2.19. The acquisition board was used for acquiring real time pressure and flow rate values and also for storing them in a portable computer. A five-port nozzle (air was not supplied for all tests done with this experiment station) was connected and controlled by five solenoid valves, one for each port. An operator used a custom computer program designed with LabVIEW (interface shown in Figure 2.20) to change the duty cycle of 5 independent channels of PWM signals generated and amplified by the control circuits (shown in Figure 2.21) to drive five individual solenoid valves.

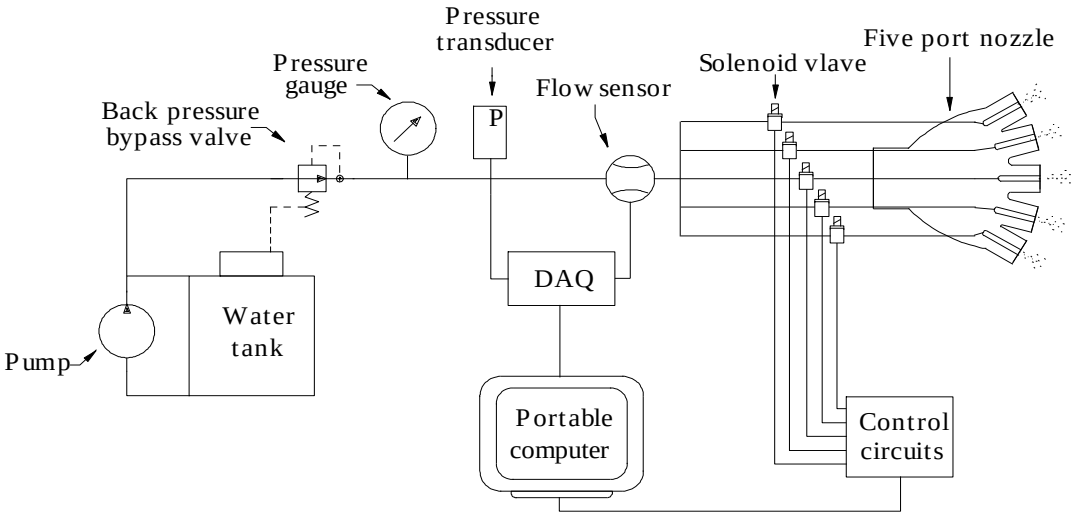

Figure 2.18. Schematic for five port nozzle experiment station

Figure 2.19. USB-1608FS data acquisition board (courtesy from mccdaq.com)

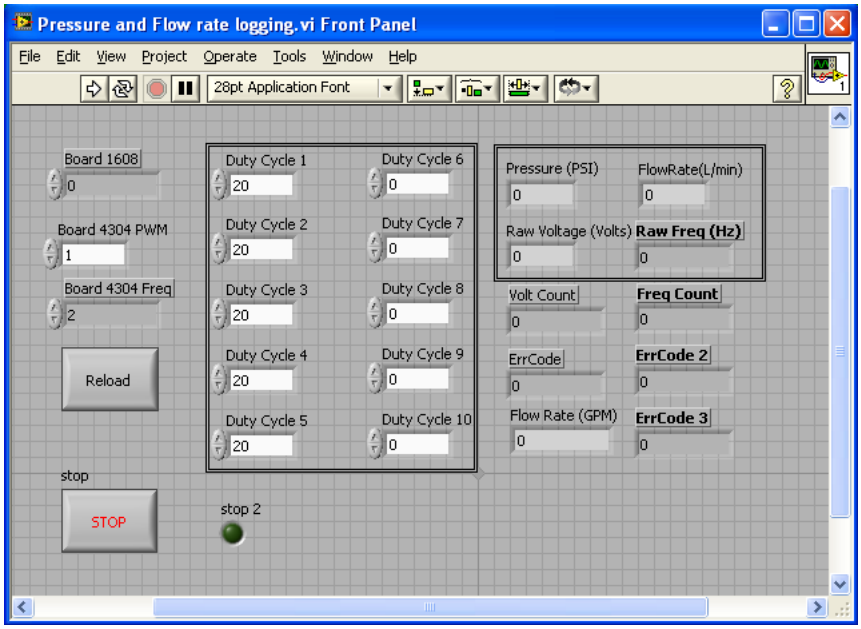

Figure 2.20. Computer interface for calibration of five port nozzle

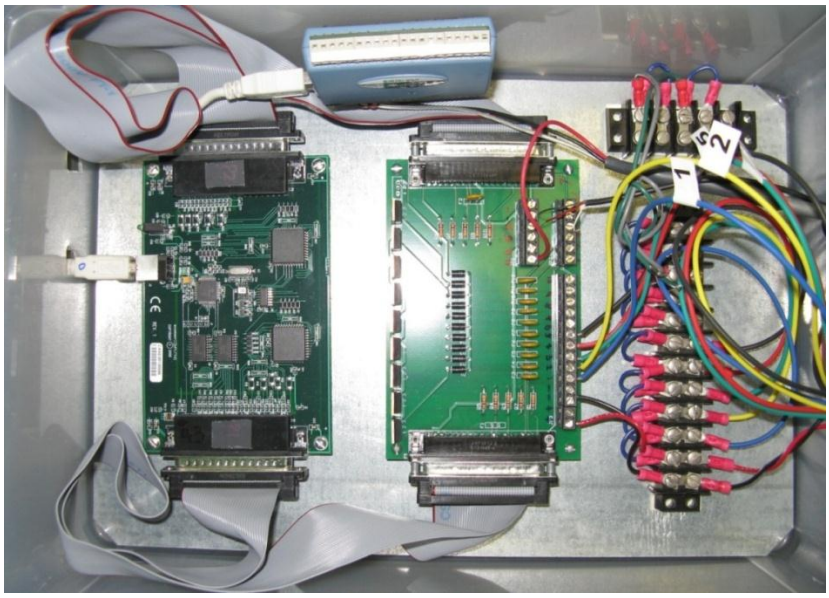

Figure 2.21. Control circuits for generating and amplifying PWM signals

2.3.5 Pressure transducer and flow sensor

2.3.5.1 Pressure transducer

A pressure transducer (model MSP-400-100-P-4-N-1, Measurement Specialties Inc., Hampton, VA) was used in the experiment system to monitor and log the pressure change in real time. When supplied with 12 VDC power, this pressure transducer outputs 1 ~ 5 VDC voltage signal which is proportional to 0 ~ 690 kPa operating pressure.

The analog to digital (A/D) converter was a 16 bit USB-1608FS analog to digital converter and -5 V to +5 V was chosen as the full scale range, the resolution of the A/D converter was:

$$\text{Res} = \frac{\text{FSR}}{2^{\text{n}}} = \frac{5-(-5)}{2^{16}} = \frac{10}{65536} = 0.0001526 \text{ (Volt/bit)} \tag{2.3}$$

Where,

Res :Resolution, Volt/bit,

FSR: Full scale range, Volt,

N: Bits resolution, bit.

Thus the pressure sensitivity of the pressure transducer is:

$$\text{P}_{\text{sen}} = \frac{\text{V}_{\text{h}} - \text{V}_{\text{l}}}{\text{P}_{\text{h}} - \text{P}_{\text{l}}} = \frac{5-1}{690-0} = 0.0058 \text{ (Volt/kPa)} \tag{2.4}$$

Where,

P_{sen}: Pressure sensitivity, $\mathrm{Volt/kPa}$,

V_h: Output high voltage, Volt,

V_l: Output low voltage, Volt,

P_h: Highest pressure to measure, kPa,

P_l: Lowest pressure to measure, kPa.

Thus the smallest pressure change that the A/D converter can measure is:

$$\Delta P = \frac{\mathrm{Res}}{P_{sen}} = \frac{0.0001526\mathrm{V}}{\mathrm{bit}} \cdot \frac{\mathrm{kPa}}{0.0058\mathrm{V}} = 0.02631\ (\mathrm{kPa/bit}) \tag{2.5}$$

Where,

ΔP: The pressure resolution that the A/D converter can measure, $\mathrm{kPa/bit}$.

Thus, the pressure measured can be calculated from digital counts converted by analog voltage input.

$$P(\mathrm{counts}) = \text{pressure at } 0 \text{ counts} + \Delta P \cdot \mathrm{counts} = \frac{\Delta P}{2} + \Delta P \cdot \mathrm{counts}$$

2.3.5.2 Flow sensor

A flow sensor (model DFS-2 Digiflow Systems, Hudson, MA) was used to calibrate the relationship between the duty cycle of the PWM control signal and the flow rate output from the ports on the five-port nozzle. The resolution (also called K-factor)

for this flow rate sensor is 62,417 pulses/Liter. Thus the relationship between the output frequency (reverse of pulses) and the flow rate was suggested to be:

$$q = \text{freq}\left(\frac{\text{pulse}}{\text{sec}}\right) \cdot \frac{1000\ (\text{ml})}{62417\ (\text{pulses})} \cdot \frac{60\ (\text{sec})}{1\ (\text{min})} = \text{freq} \cdot \frac{60000}{62417}\ (\text{ml/min}) \qquad (2.6)$$

Where,

q: measured flow rate, ml/min,

freq: Frequency output from the flow sensor, Hz.

To increase the accuracy of the flow sensor, the above relationship between flow sensor output and the actual flow rate was determined by changing the duty-cycle of the PMW solenoid valves on an 8002 XR flat fan nozzle tip at 207 kPa. Liquid output was manually collected over a period of time and the measured flow rate was calculated by dividing the liquid volume over time.

2.3.6 Pressure fluctuation caused by the variable flow rate

In the duty cycle vs. flow rate calibration test, pressure fluctuation was observed when the solenoids were activated on and off at a certain rate (e.g. at 10 Hz frequency). The level of the pressure fluctuation increased with the increase of the flow rate and was observed to be about 100 kPa when there was one active five-port nozzle. If more five-port nozzles were activated at the same time, the pressure fluctuation could easily exceed 100 kPa.

The intelligent sprayer prototype, described in more detail in the later chapters, consisted of 20 solenoid valves on each side. Turning all the nozzles on and off to achieve variable rate for matching target characteristics will eventually create the pressure fluctuation greater than 100 kPa. Since the nozzle flow rate is directly affected by the operating pressure, the pressure fluctuation should be minimized to obtain a constant flow rate for the same control signals. Therefore, to limit the pressure fluctuation at the nozzle tips, and to minimize the error of the nozzle flow rate, a back pressure bypass unit consisting of a pressure regulator was added in the spray line to stabilize the pressure by discharging excessive fluid back to the tank, as shown in Figure 2.18.

The adjustable pressure regulating valve and the check valve were tested to compare their performance in reducing pressure fluctuation caused by flow rate changes. When conducting tests to determine the effect of two back pressure bypass valves, all the nozzles were fully open for 300 ms and then close for 300 ms all at the same time. Pressure was acquired from the pressure transducer every 50 ms using USB-1608FS data acquisition board and was saved to a portable computer using the program interface shown in Figure 2.20. This represents the most extreme case for the intelligent sprayer to face while in operation, though it is unlikely to happen. However, testing under this condition could provide a reference for the upper limits of pressure fluctuation when using a check valve or an adjustable valve for the back pressure path.

2.4 Spray model for optimal flow rate calculation

2.4.1 Spray model derivation

As shown in Figure 2.22, for each segment of the tree canopy corresponding to one nozzle port on the intelligent sprayer, the volume of the canopy segment is:

$$Vol_{segment} = h \cdot W \cdot v \cdot t \tag{2.7}$$

The effective volume of this tree canopy segment is:

$$Vol_{effective} = h \cdot W \cdot v \cdot t \cdot \rho \tag{2.8}$$

Where,

W: Width (depth) of the canopy section (segment maximum width), m,

v: Tractor forward speed, m/s,

t: Time passed, s,

ρ: Density of the canopy segment, 0 ~ 1,

h: Average height that each nozzle covers, m, (0.12 to 0.135 cm based on sprayer dimension measured).

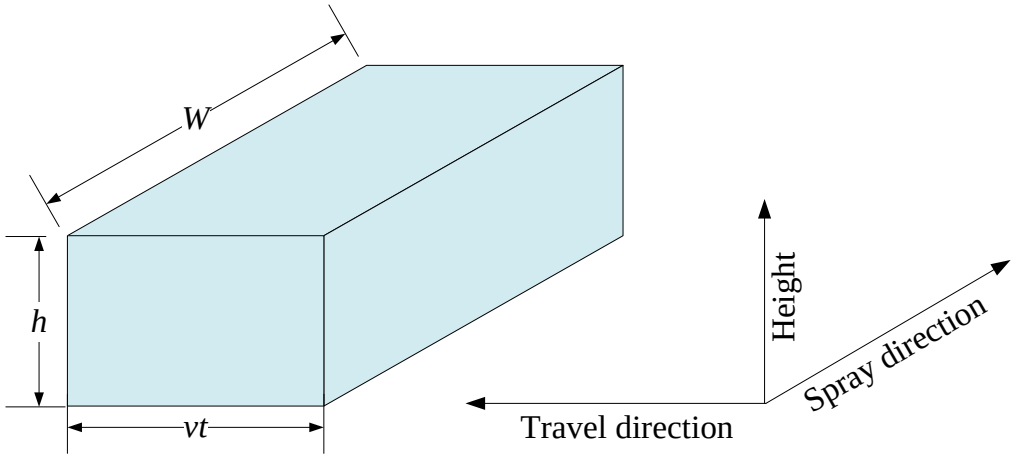

Figure 2.22. The volume of a canopy segment that is sprayed by one nozzle within time t

The needed spray volume (ml) is:

$$E_{vol} = Vol_{effective} \cdot \nabla = h \cdot W \cdot v \cdot t \cdot \rho \cdot \nabla \quad (2.9)$$

For one nozzle, the flow rate (ml/min) required is:

$$q = \frac{E_{vol}}{t} = h \cdot W \cdot v \cdot \rho \cdot \nabla \quad (2.10)$$

According to the flow meter calibration at 207 kpa (see result in Equation 3.1 in section 3.2 in the next Chapter):

$$q = 6.56 \times DC - 73.88$$

Where,

DC is the duty cycle of the flow rate control signal, and ∇ is the spray rate or the amount of spray to treat a unit of tree canopy volume (L/m^3).

Thus to match the need of the effective volume of the tree canopy segment, the required Duty cycle of the control signal should be:

$$DC = \frac{h \cdot W \cdot v \cdot \rho \cdot \nabla + 73.88}{6.56} \tag{2.11}$$

The recommended optimal spray rates for orchards are 0.1 L and 0.13 L of spray mixture per 1.0 m^3 of tree canopy for pruned and unpruned trees, respectively (Jenkins and Hines, 2003). For the tests conducted in this study, ∇ was chosen to be 0.1. Therefore, the duty cycle of the control signal can be determined with the known segment height that one nozzle port covers (h), the tractor speed (v), the calculated maximum segment width (W) and the density of the canopy segment (ρ).

2.4.2 Laboratory (indoor) sprayer evaluation of the intelligent sprayer

To evaluate the accuracy of using the laser scanner and computational algorithm to measure tree canopy characteristics and to assess the performance of the spray model designed for the Intelligent sprayer, sectional volume of four trees with two different species was measured by the laser scanner and then was compared with manual measurements.

The two tree species were *Tsuga Canadensis* and *Emerald Green Thuja* (Figure 3.11), and they were purchased from local commercial nurseries. The two *Tsuga*

Canadensis trees were 228 cm and 320 cm high and were designated as Tree 1 and Tree 2, respectively. The two *Emerald Green Thuja* trees were 271 cm and 263 cm high and were designated as Tree 3 and Tree 4, respectively.

The widths at a 12 cm height interval of each tree were manually measured to calculate sectional volume. Trees were also scanned by the laser scanner to determine the sectional volume for comparison. Sectional density and optimal spray rate for each nozzle corresponding to that section were then calculated by the computer program using the density algorithm and the spray model described earlier. For each of the 20 sections/nozzles, density calculated from laser data was multiplied by the sectional volume based on the manual measurement to obtain effective tree volume corresponding to each nozzle. The optimal spray rate calculated by the algorithm was then divided by the effective tree volume to obtain the actual spray constant (Equation 2.12) used for each nozzle.

The procedure for this indoor evaluation test was:

1. Manually measure the tree width at every 12 cm height interval (the height for each nozzle to cover, assumed) for all four trees (shown in Figure 2.23).
2. Calculate the canopy volume for each height section (corresponding to one nozzle) using the following equation:

$$\mathrm{Vol_i} = \frac{1}{3} \cdot \pi \cdot \mathrm{h} \cdot (\mathrm{R}^2 + \mathrm{rR} + \mathrm{r}^2) \qquad (2.12)$$

Where,

Vol_i: Volume for the ith section of canopy,

H: Height interval, equals to 12 cm in this experiment,

R: Radius of the lower part of the section, also equals to half the lower part width ($\frac{D}{2}$),

r: Radius of the upper part of the section, also equals to half the upper part width ($\frac{d}{2}$).

3. Scan all trees with laser scanner and save the range data.

4. Use the algorithm to calculate tree maximum width and each sectional canopy density from the range data.

5. Use the spray model to calculate the flow rate for each canopy section, calculate the spray volume by multiplying flow rate with time.

6. Divide spray volume result by the effective canopy volume (or manually- measured volume multiplies by the calculated canopy density) for each canopy section.

$$\nabla_i = \frac{Q_i \times t}{Vol_i \times \rho_i} \tag{2.13}$$

Where,

i: The canopy section number, 1 to 20 (from bottom to top),

∇_i: Spray rate for the ith section of the canopy (L/m^3),

Q_i: Flow rate for the ith nozzle, L/min,

t: Time used for spraying the ith section of canopy, min,

Vol_i: Volume for the ith section of canopy, m^3,

ρ_i: Density for the ith section of canopy, calculated by the density algorithm.

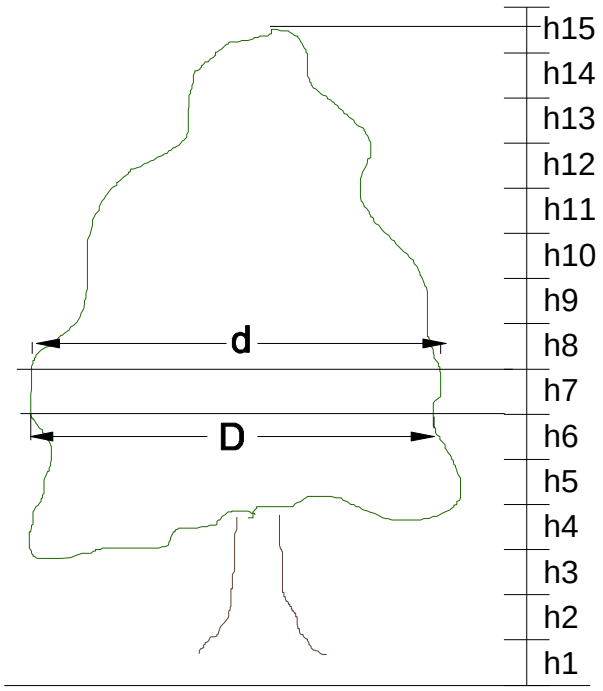

Figure 2.23.Illustration of the manual tree section measurement

For this test, the center of the sprayer was 1.2 m high above the ground, and thus 12 cm nozzle height interval was used in this test, while for the later tests described in Sections 2.6 and 2.7, a 13.5 cm nozzle height interval was used because the center of the sprayer was raised to 1.35 m high.

2.5 Sprayer Modification

The intelligent sprayer was modified from a vineyard sprayer (model ZENIT B11, HARDI Inc., Davenport, IA) with a 0.81 m axial fan to deliver air to eight spray dischargers on both sides of the sprayer. The modifications to the sprayer were done in three steps: nozzle replacement, sensor and controller mounting, pressure regulating and system response calibration.

2.5.1 Nozzle replacement

The original eight spray dischargers on two sides of the sprayer were replaced with eight, five-port air-assisted nozzles, and each nozzle consisted of five ports to discharge five streams of sprays. The nozzle tip in each port was a modified Teejet 11003VB flat fan tip (Spraying Systems, Wheaton, IL) and was mounted at the center of each port. Details of the modified nozzle tips for the five-port nozzle were given by Zhu et al., (2006). These nozzles were used for the intelligent sprayer development to potentially improve spray penetration and spray deposition uniformity over conventional spray delivery design.

The maximum air velocity of five-port air assisted nozzles was measured with constant temperature anemometer (CTA) employing 0.15 mm cylindrical hot-film sensors (Model 1210-60, TSI Inc., St. Paul, MN). The sensors were located at 1 cm away from the port outlets. During the air velocity measurement, the fan was set at the high speed mode (same as field test setting).

2.5.2 Sensor and controller mounting

The laser scanner was mounted on the spray tank frame between the tractor cab and spray nozzles. Both the scanner and nozzles on the same side were pointed to the same direction. The distance between the laser scanner and the nozzles was 1.45 m. This distance was chosen because it was easy for the connection between the sensor and the spray tank frame. The error caused by the distance was compensated by adding a delay in the controller and thus not affecting the real-time matching of the flow rate to the target.

A water proof controller box was mounted beneath the water tank of the intelligent sprayer. All electrical circuits, power converters and cables were mounted inside the secured controller box and were sealed from water leakage damage.

2.5.3 Pressure regulating (back pressure bypass)

As indicated previously, the spray pressure near the nozzle tip fluctuates when the solenoid valves were switched on and off at a 10 Hz rate. The pressure fluctuation could cause unintended changes in flow rate output and droplet size. To reduce the pressure fluctuation near the nozzle tip, a back pressure regulating unit described in section 2.3 was added to discharge extra fluids through the bypass to the spray tank.

2.5.4 System response calibration using high speed camera system

Real-time automatic spray application is the one of the major goals in the design of the intelligent sprayer. Because it takes time for the laser scanner to scan the target, the data buffer to accumulate frames for calculation, the algorithm to calculate canopy width,

density and optimal flow rate for each nozzle, and the hydraulic-mechanical response to the control signal, there is a time delay between the target being detected by the laser scanner and the liquid actually being sprayed. Knowing this system delay time is very important because it is a reference to determine minimum distance between the laser scanner and nozzle outlets. It is also used to calculate the control delay needed for matching the correct spray flow rate to the target structure.

A SILICON VIDEO® 642M camera (EPIX, Inc., Buffalo Grove, IL, USA) was used to measure the system response time. This high speed camera can capture an image sequence with a time mark on each frame. This enables one to determine the time difference between any two images by simple subtraction of times associated with two images.

A laser pointer was mounted beside the camera in a position such that it would produce a dot on a recognizable location on the laser scanner at the exact time when the laser beam aligned with the edge of the target tree. In this way, the "seeing" of the target was identified by capturing the laser pointer dot on the specific location (calibrated beforehand) on the laser scanner. Following this, the time of actual spraying was captured in the camera and recorded. Therefore the system response was the time between the actions captured when laser "sees" the target and when the liquid began to flow.

2.6 Field Evaluations of intelligent sprayer

The field tests were conducted over three typical growth periods in a Gala and Golden Delicious apple orchard at an OARDC research field (Wooster, OH). The first test was carried out in early spring (April 12) when trees just started leafing. The second test was done on May 3 when half foliage was developed. The third test was conducted on June 8 when the trees had fully-established canopies. The weather conditions during the field tests during the three days are listed in Table 2.2. Before the tests, the droplet size and outlet air velocity were measured with a particle/droplet laser image analysis system (Oxford Lasers VisiSizer and PIV, Oxford Shire, UK) and a constant temperature anemometer (model IFA-300, TSI, Inc., St. Paul, MN), respectively.

Test date	Average wind velocity (m/s)	Wind direction	Ambient temperature (°C)	Relative humidity (%)
April 12, 2010	3.2	ENE	15	25
May 3, 2010	3.1	WNW	22	48
June 8, 2010	1.7	ESE	21	43

Table 2.2. Weather data during the field tests

2.6.1 Artificial targets mounting

Artificial targets were used in the field tests to evaluate the spray performance of the intelligent sprayer with automatic control (S1) comparing to intelligent sprayer without automatic control (S2) and a conventional air-blast sprayer (S3).

As shown in Figure 2.24, one tree row in the orchard was randomly picked. From that row, three groups of three trees were randomly selected. The middle tree of each three-tree group was used as the major spray target.

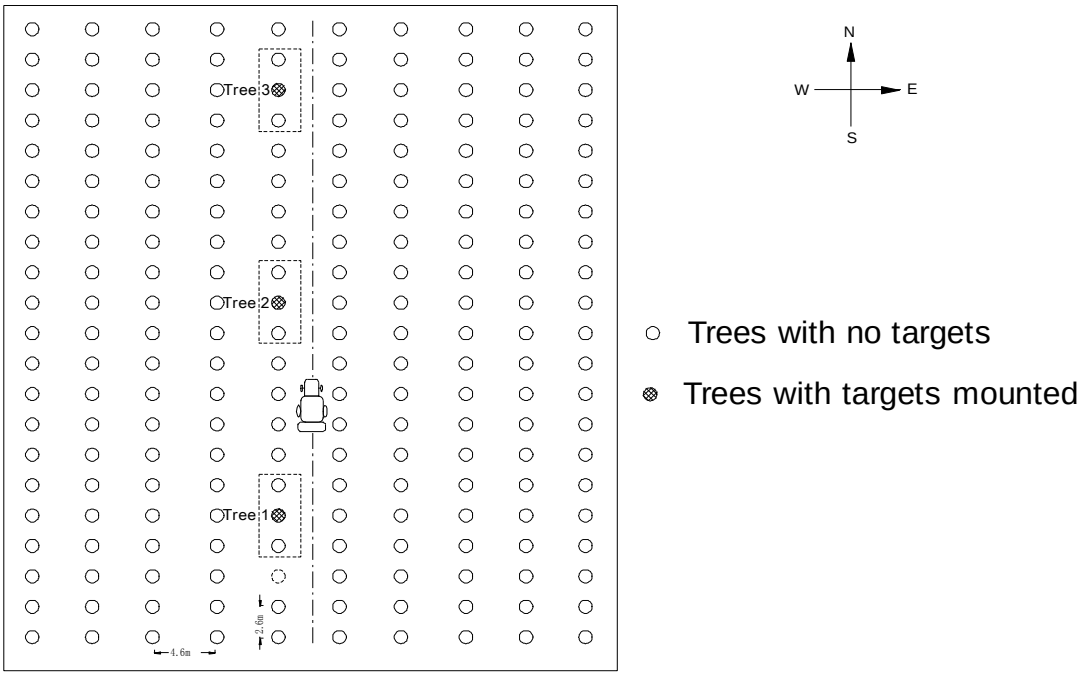

Figure 2.24. Arrangement of the orchard used in the field tests

Three types of artificial targets were chosen: (1) water sensitive papers (WSP, two sizes: 26 mm×76 mm, and 26 mm×508 mm, Spray Systems Co., Wheaton, IL, USA), (2) Monofilament nylon screens (50 mm×50 mm, Filter Fabrics Inc., Goshen, IN, USA), and

(3) plastic plates (26 mm×76 mm). They were mounted at the following five different locations to evaluate the coverage and deposition of each spray treatment:

1. Inside target tree canopies,
2. on the ground under canopies of the target tree and its adjacent trees,
3. at different heights on poles behind the tree canopies,
4. along gaps between the two trees,
5. Spray drift at different heights downwind 5 m, 15 m and 35 m away from the center of the test tree row (for the tests conducted in May and June).

For location 1, both water sensitive papers (26 mm×76 mm) and nylon screens were mounted at different heights and depths inside the target tree canopies to document the spray coverage and deposit uniformity inside the canopies (shown in Figure 2.29). The targets samples were mounted at different heights and different horizontal positions (at the edge of tree canopies, in the middle and half way inside the canopies). However, since the apple trees used in this field test did not have many branches, not all designated points had a supporting branch to mount the target sample. Therefore, targets were mounted with the same distribution plan but their exact locations had to be slightly changed from the protocol established according to the availability of supporting branches. All artificial targets were mounted first and then their locations were measured (with the coordinate systems described in Figures 2.25 and 2.26) manually with three perpendicularly placed tape measures. Since the wind direction (west wind) in Test two

(May, 2010) was different from the wind directions (east wind) in Test one (April, 2010) and Test three (June, 2010), the spray direction and thus the definition of X direction in test two was different from those in Test one and Test three.

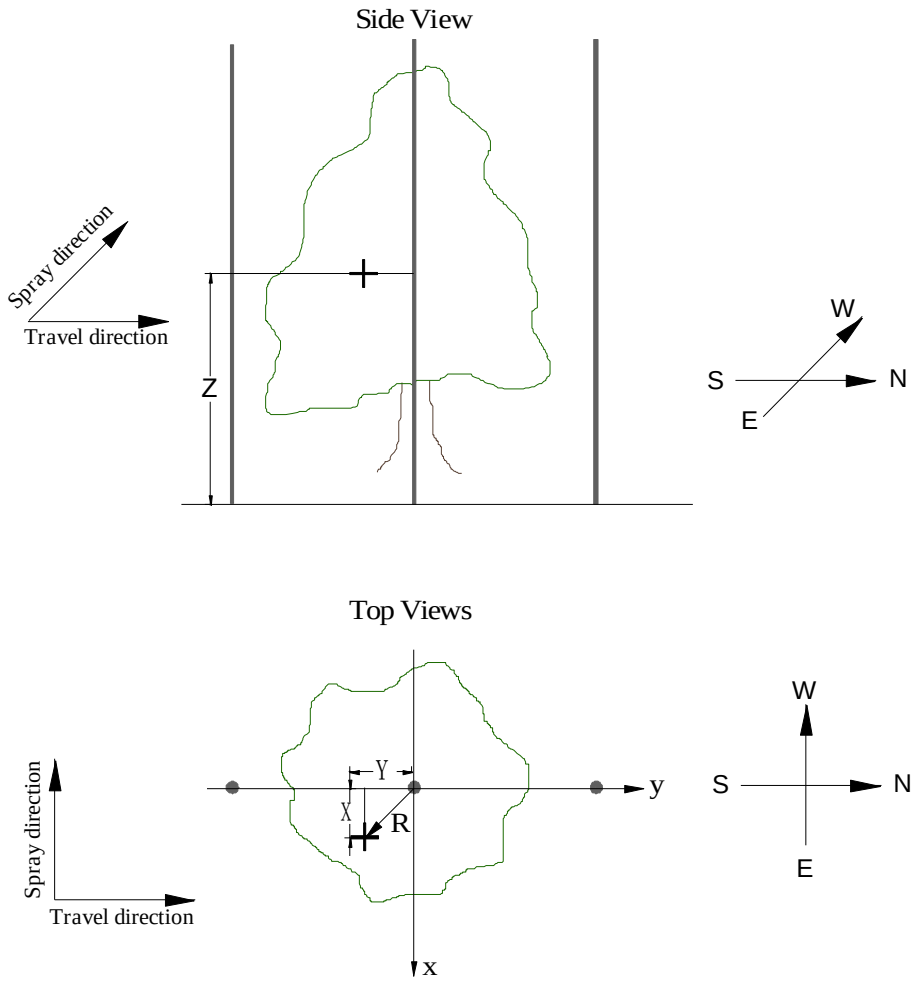

Figure 2.25. Coordinate system for sample locations in trees (April and June, 2010)

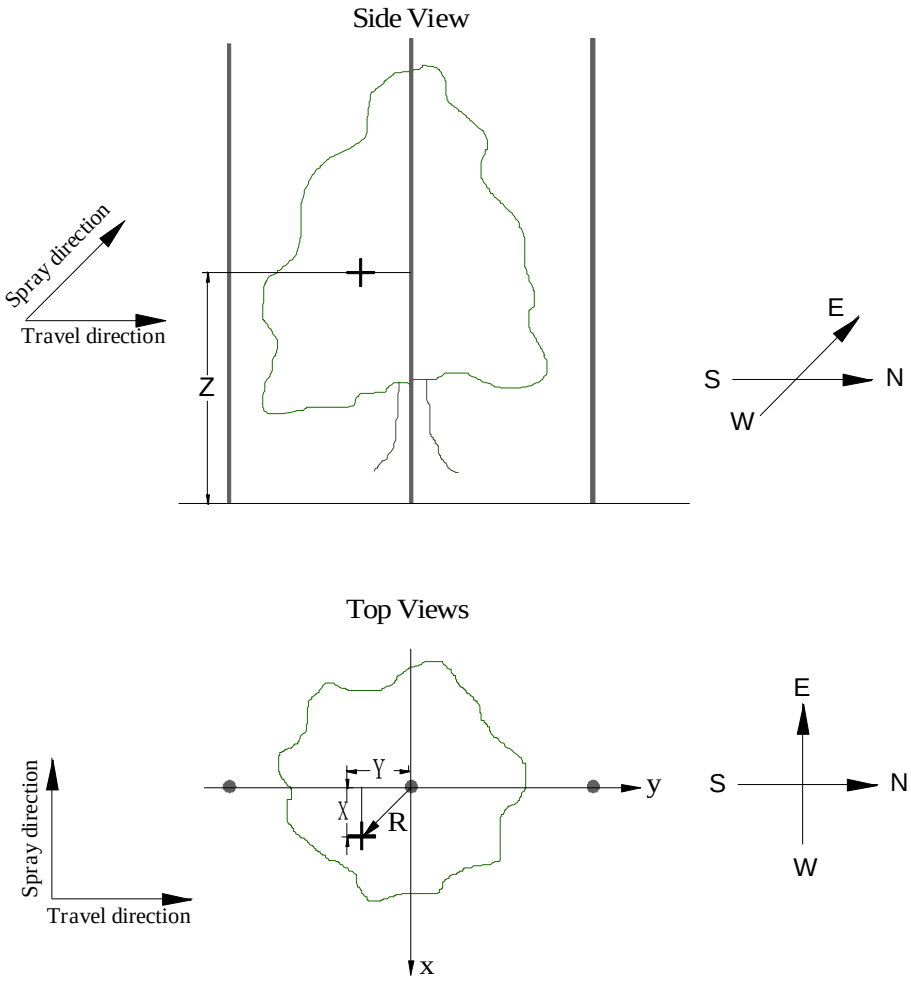

Figure 2.26. Coordinate system for sample locations in trees (May, 2010)

For locations 2 and 3, as shown in Figures 2.27, 2.28 and 2.29, seven pieces of wood boards (150 mm×330 mm) were placed under each set of the three trees, and three poles were installed behind the tree canopies. Water sensitive papers (26 mm×76 mm) and plastic plates were clipped on the wood boards on the ground to evaluate the spray

deposits lost on the ground. Water sensitive papers (26 mm×76 mm) and Nylon screens were mounted on the poles behind tree canopies to compare the spray loss between, above and behind tree canopies.

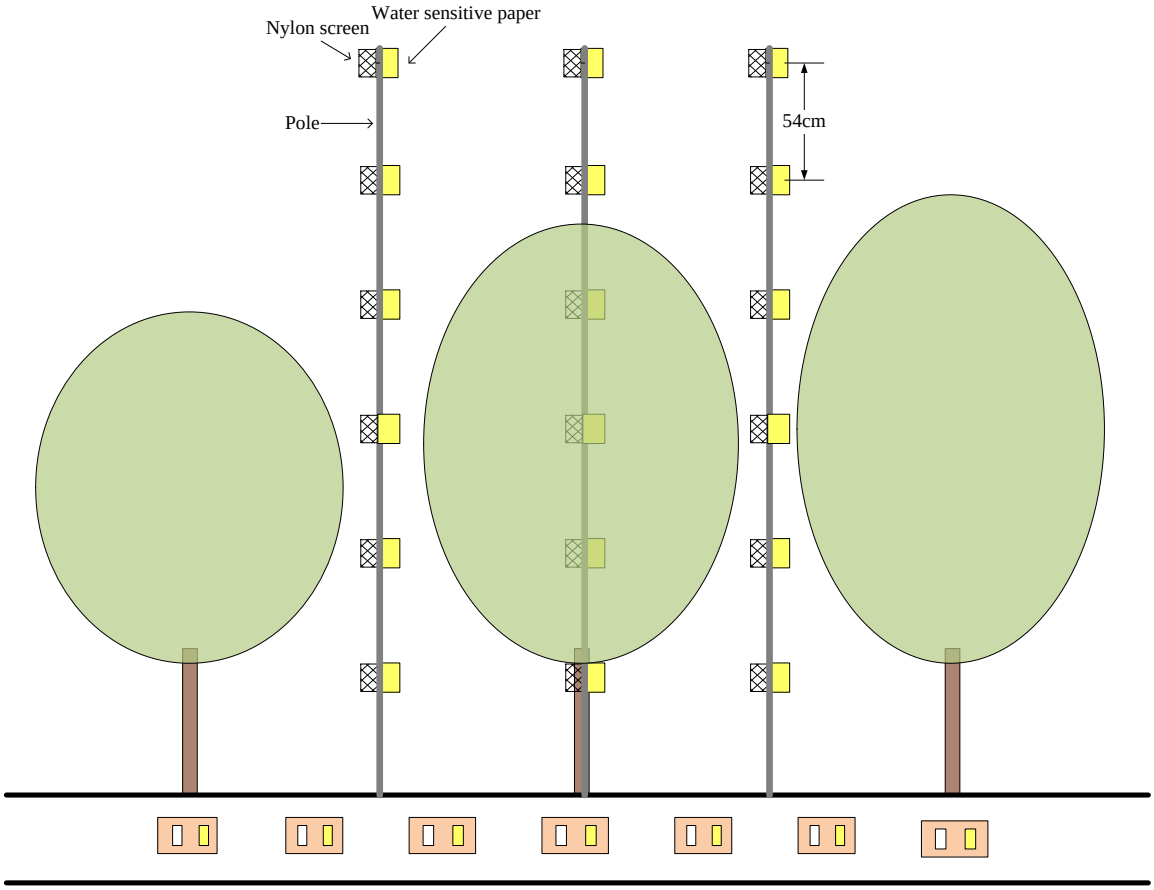

Figure 2.27. Artificial targets on the ground and poles – side view

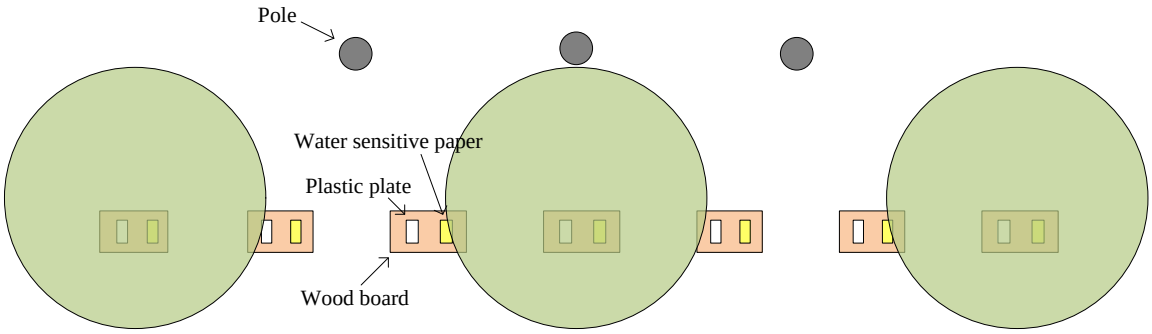

Figure 2.28. Artificial targets on the ground and poles – top view

For location 4, as shown in Figure 2.29, four pieces of long water sensitive papers (26 mm×508 mm) were mounted on a 2 m long wood piece at three heights (0.4 m, 0.96 m and 2 m) to document the transition of spray coverage from tree canopy to gap and then to tree canopy.

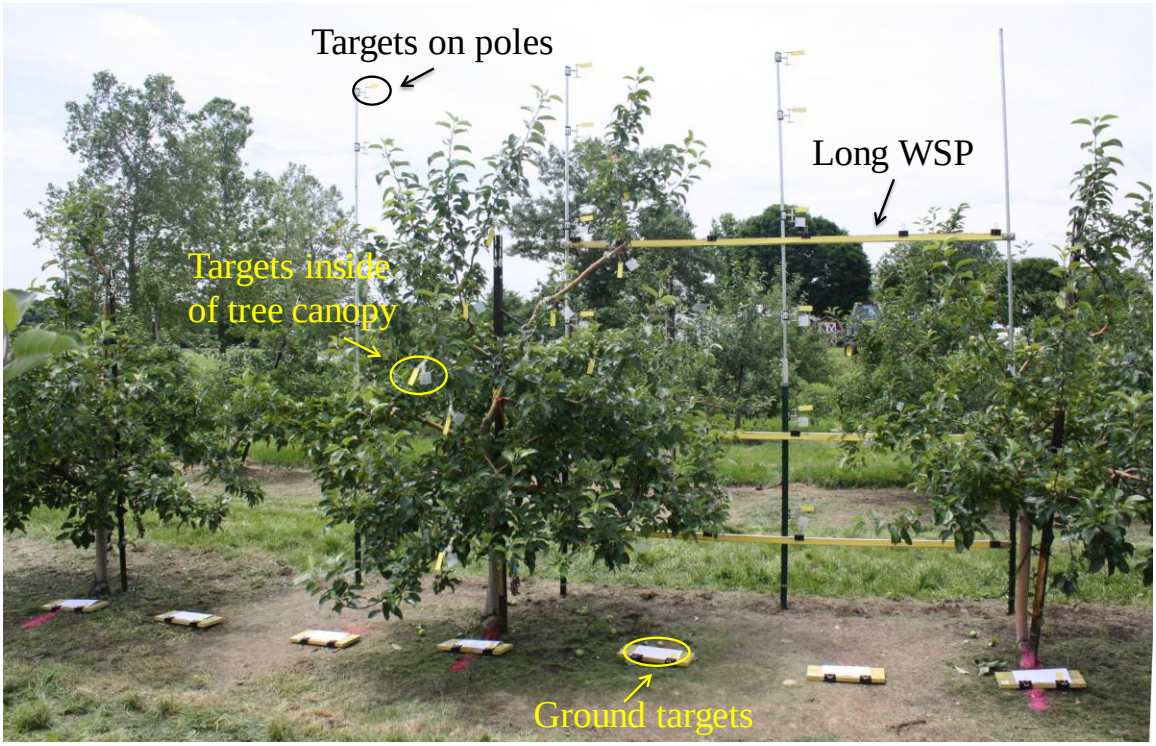

Figure 2.29. Artificial target mounting positions

For location 5 (done for May and June tests), Nylon screens (50 mm×50 mm) were mounted at 54 cm intervals on poles installed downwind 5 m, 15 m and 35 m away from the test tree row centerline to record off-target spray movement.

2.6.2 Sprayer settings

The spray mixture used in the field tests was 2 g of Brilliant Sulfaflavine (MP Biochemicals, Inc., Aurora, OH) per liter of water for all the sprays tests. Tank mixture samples with known concentration (2 g/L) were collected before and after each spray as references for calculating the deposits on nylon screen samples.

The sprayers and their test settings are shown in Table 2.3. A Durand Wayland 1500 sprayer represented conventional air blast orchard sprayer was used and was called S3.

Sprayer	Pressure (kPa)	Number of opened nozzles on each side	Nozzle tip	Flow rate per nozzle (L/min)	Ground speed (km/h)	Application rate (L/ha)
Intelligent sprayer with automatic control (S1)	207	20	8002	≤ 0.68	3.22	≤ 554
Intelligent sprayer without automatic control (S2)	207	20	8002	0.68	3.22	554
Conventional air blast sprayer (S3)	248	8	D5 DC25	1.36	3.22	443

Table 2.3. Sprayer field test settings

Flow rates all nozzles were calibrated under the test sprayer setup before field experiments. The spray application rate for the sprayer without intelligent function and the conventional air-blast sprayer were,

$$Liters\ per\ hectare = \frac{600.2 \cdot N \cdot q}{W \cdot V} \tag{2.14}$$

Where:

N =Number of the nozzles used,

q =Flow rate of one nozzle, L/min,

W =Distance between two tree row centerlines, m, 4.575 m in the test field,

V =Ground speed, km/h.

Thus for intelligent sprayer without automatic control (S2), the application rate (L/ha) is:

$$Liters\ per\ hectare = \frac{600.2 \times 20 \times 0.68}{4.575 \times 3.22} = 554.$$

For the Conventional air blast sprayer (S3), the application rate (L/ha) is:

$$Liters\ per\ hectare = \frac{600.2 \times 8 \times 1.36}{4.575 \times 3.22} = 443.$$

2.7 Sprayer test on container trees

The four container trees used in the indoor tests described in section 2.4 had denser canopies than the apple trees used in the field tests. The container plants were used in an outdoor test to evaluate the performance of the intelligent sprayer for dense canopies.

The container trees were placed side by side from north to south. During this outdoor test, the average wind velocity was 3.5 m/s from northwest, the ambient temperature was 8.5 °C, and the relative humidity was 50%.

2.7.1 Location of water sensitive paper mounting

Water sensitive papers (26 mm by 76 mm) were mounted inside each container tree canopy to measure spray coverage at different locations inside tree canopies. The guideline for mounting of the water sensitive papers was shown in Figure 2.30. With this design, tree canopy was divided into five sections in two horizontal directions (e.g. from spray direction and sprayer travel direction). Water sensitive papers were distributed along the tree height directions with a height interval of 27 cm. In this way, spray deposition could be evaluated from three directions. Since these trees had different heights and structures, the total number of water sensitive papers was not the same for all trees.

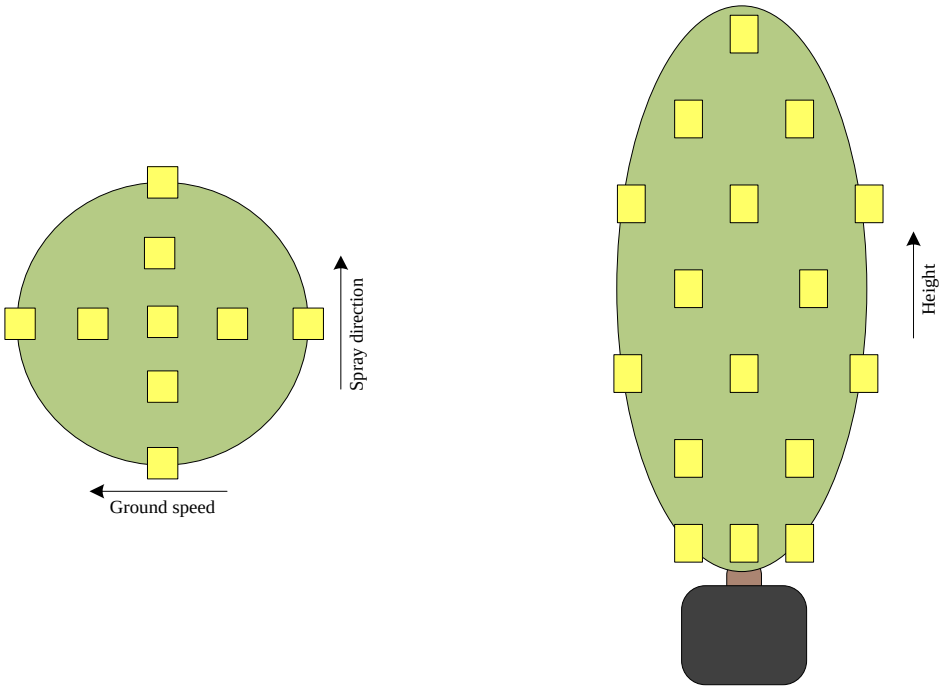

(a) Water sensitive paper locations– top view (b) Water sensitive paper locations– side view

Figure 2.30. Water sensitive paper locations for container trees

2.7.2 Sprayer setup

As shown in Table 2.4, the intelligent sprayer was set to operate under 207 kPa and with twenty 8002 nozzles under control. The intelligent sprayer sprayed the trees at two ground speeds (3.22 km/h and 6.44 km/h) for three replications for each speed. Water was used in this spray test.

Sprayer	Pressure (kPa)	Number of nozzles on each side	Nozzle tip	Flow rate per nozzle (L/min)	Ground speed (km/h)
Intelligent sprayer with automatic control	207	20	8002	≤ 0.68	3.22
Intelligent sprayer with automatic control	207	20	8002	≤ 0.68	6.44

Table 2.4. Sprayer settings for container tree tests

2.8 Calculations of liquid consumption

One of the major goals of this study to determine if the intelligent sprayer operation would result in considerable reductions in pesticide consumption by better targeting and variable rate application. Tests were conducted to document the savings in spray mixture containing water and chemicals, when using the intelligent sprayer.

For the intelligent sprayer without automatic control and the conventional air-blast sprayer, the flow rate discharged from each nozzle remained the same after liquid pressure was set, and the total spray volume could be calculated by multiplying flow rate by the spray time. Thus, for the non-variable rate sprayer, the liquid consumption is:

$$Vol = n \times q \times t \tag{2.15}$$

Where:

Vol: Total liquid volume sprayed, ml

n: Number of nozzles used during spray,

q: Flow rate for each nozzle used, ml/min

t: Sprayed time, min.

For the Intelligent sprayer, the data associated with duty cycles of nozzles was saved after each application. The actual flow rate of each nozzle, and the total spray volume of the sprayer was calculated using the saved duty cycles of control signals for each spray, the calibrated relationship between duty cycle, flow rate for the nozzles used, and the time interval used for each control signal.

From the nozzle calibration result described in Equation 3.1 in section 3.3, the relationship between duty cycle and output flow rate of the nozzles is:

$$q = 6.56 \times \mathrm{DC} + 73.88$$

Where,

q: Flow rate of one nozzle, ml/min,

DC: Duty cycle of the spray control PWM signal (0~100).

Therefore the total liquid consumption is:

$$Vol = \sum_{j=1}^{n} \sum_{i=1}^{20} q_{ij} \times \Delta t \qquad (2.16)$$

Vol: Total volume of liquid sprayed by the intelligent sprayer, mL,

q_{ij}: Flow rate of the ith nozzle (out of the total of 20) at the jth slice, mL/min

Δt: Time interval of the control signals. The control signal refreshes every 0.26 second for all tests in this dissertation, so $\Delta t = \frac{0.26}{60} = 0.0043$ (minutes).

The liquid savings were calculated by dividing the liquid consumption from the intelligent sprayer by the amount discharged from the intelligent sprayer without control or from the conventional air-blast sprayer. Of course the "liquid" mentioned here includes water as carrier, and pesticides and other chemicals added to the spray mixture to enhance the efficiency of a spray application. Therefore, any savings in spray liquid

consumption should lead to higher net income and less impact on the environment and human safety.

Chapter 3: Results and discussion

In the previous chapter, components of the intelligent sprayer that can adjust its spray flow rate in accordance with the canopy characteristics were described. A prototype of the intelligent sprayer has been implemented, including a laser sensor to scan the foliage canopy, a real time algorithm to calculate the canopy characteristics using the data from the laser sensor, and a variable rate controller to convert the computation results into PWM control signals to activate solenoid valves to change the nozzle flow rate. A series of tests were designed and conducted to validate each part of the design. Both field and controlled outdoor tests were also conducted to evaluate performance of the entire intelligent sprayer system. In this chapter, all tests results are presented and analyzed.

3.1 Validation result on wooden block (artificial target) density

An indoor experiment was designed (described in section 2.2) using an artificially target to evaluate the accuracy of the density calculation algorithm. In this test, lumber blocks were assembled together to form shapes with pre-defined density. Then the artificial target with known density was scanned using a laser sensor. Measurement data was then sent to the proposed intelligent algorithm to compute the density created by these artificial targets. The computation results were compared with the corresponding known density of that arrangement of the artificial target.

Since the intelligent sprayer prototype has 20 nozzles on one side to be controlled, the algorithm divides the laser scanning range into 20 groups corresponding to the 20 nozzles. The lumber blocks with known densities used in this density validation test had a height that could be covered by four nozzles. Thus, the lumber blocks were divided into four sections: sections 1, 2, 3 and 4.

After the laser sensor scanned the lumber blocks 30 times, the densities of each section were calculated for these 30 runs, and the calculated densities for each section were averaged (Figures 3.1 through 3.4). Figures 3.1 through 3.4 also illustrate the relationship between the calculated density from laser scanner data and the actually known density of the artificial target (lumber block section). The regression equations were:

$\text{Calculated density} = 0.9544 \cdot \text{Known density} + 7.8555$, with R^2=0.9817 for section 1,

$\text{Calculated density} = 0.9418 \cdot \text{Known density} + 7.8184$, with R^2=0.9799 for section 2,

$\text{Calculated density} = 0.9784 \cdot \text{Known density} + 5.0706$, with R^2=0.9869 for section 3,

$\text{Calculated density} = 1.0066 \cdot \text{Known density} + 1.9041$, with R^2=0.9942 for section 4.

From the linear regression equations, the slopes for the four sections were 0.9544, 0.9418, 0.9784, and 1.0066. All the slopes were very close to one. Although the calculated density is slightly larger than the known density, their difference was very small. Therefore, the designed density algorithm was effective in estimating density of a three dimensional object using the roughness of its surface.

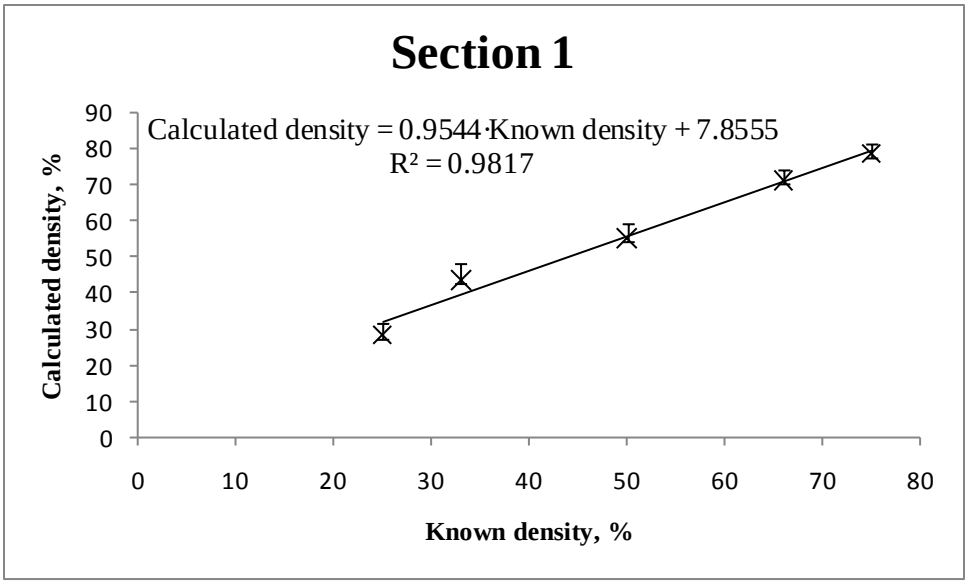

Figure 3.1. Regression result of calculated density (%) using laser data and density algorithm over known density (%) of section 1 of the lumber block

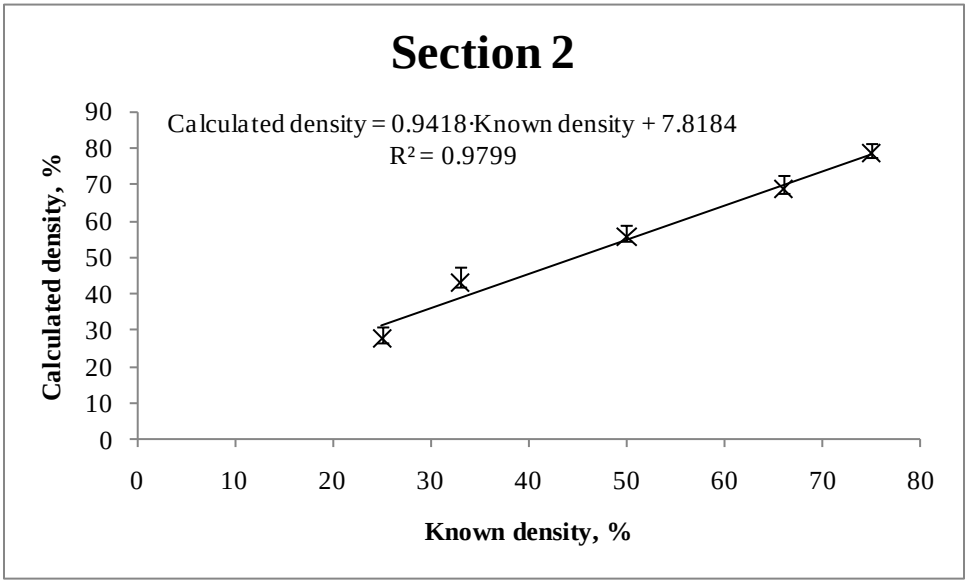

Figure 3.2. Regression result of calculated density (%) using laser data and density algorithm over known density (%) of section 2 of the lumber block

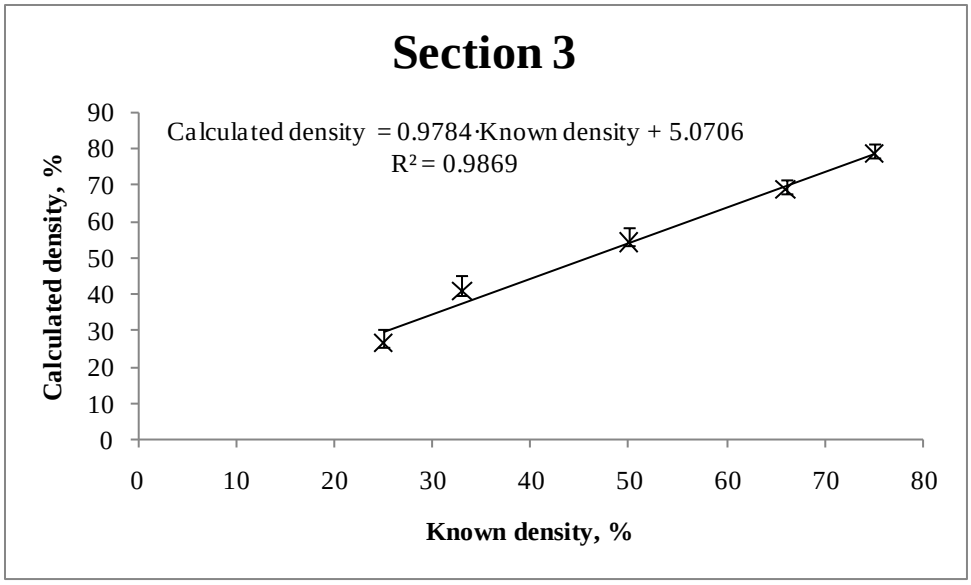

Figure 3.3. Regression result of calculated density (%) using laser data and density algorithm over known density (%) of section 3 of the lumber block

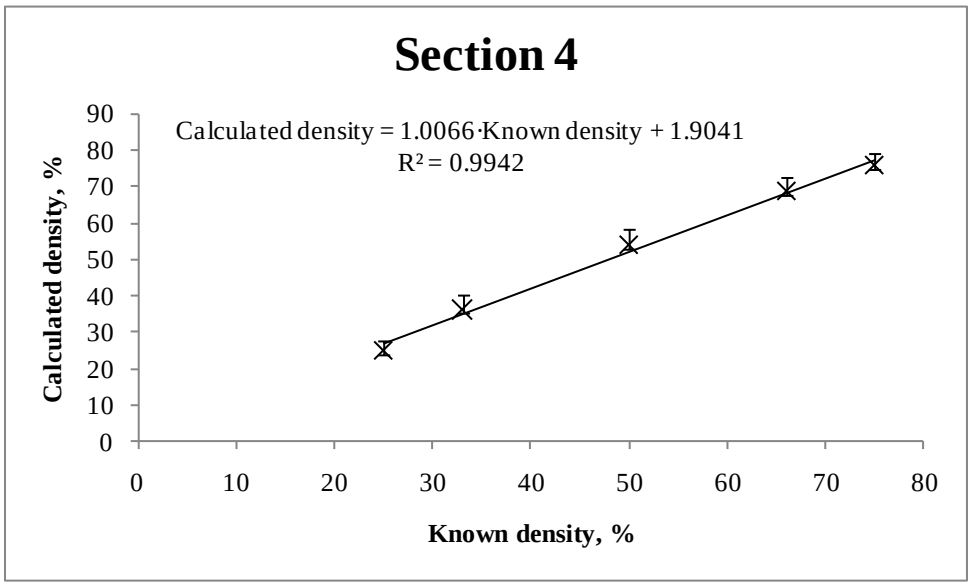

Figure 3.4. Regression result of calculated density (%) using laser data and density algorithm over known density (%) of section 4 of the lumber block

3.2 Nozzle calibration results

To achieve accurate control of the flow rate output at the spray nozzles, they must be calibrated to include the system variables (such as duty cycle of the PWM control signals). All the calibrations in this section were completed with the set-up described in section 2.3.

3.2.1 Flow rate sensor calibration

Figure 3.5 shows the calibration of the DFS-2 flow rate sensor operated at 207 kPa with one of the five-port 8002 XR nozzle tips as the liquid discharger. The amount of liquid from each run was measured manually and then compared with the frequency output from the flow sensor. The flow rate of liquid passing through the flow sensor had a linear relationship with the frequency generated by the flow sensor. The regression equation was: $\text{Flow rate} = 1.1566 \cdot \text{Frequency} - 78.343$, with $R^2 = 0.9965$.

3.2.2 Calibration of pulse width modulated solenoid valve

Solenoid valves modulated with PWM signaled for controlling the liquid flow through each 8002 XR nozzle tip mounted at the center of a five-port nozzle was calibrated with different duty cycles of the PWM signals at 207 kPa. Figure 3.6 shows the linear relationship between duty cycle and frequency for the flow rate of liquid passing through the solenoid valve. The regression equation was: $\text{Frequency} = 5.6746 \cdot \text{DutyCycle} + 131.69$, with $R^2 = 0.9906$.

3.2.3 Relationship between duty cycle and nozzle flow rate

From the calibration results presented in Figures 3.5 and 3.6, the relationship between flow rate and duty cycle was:

$$Q = 6.56 \times DC + 73.88 \quad (3.1)$$

Where,

Q: Liquid flow rate from 8002 XR nozzle tip, ml/min.

DC: Duty cycle of the input PWM control signal.

Equation 3.1 was used in section 2.4 when deriving the spray model for the intelligent sprayer.

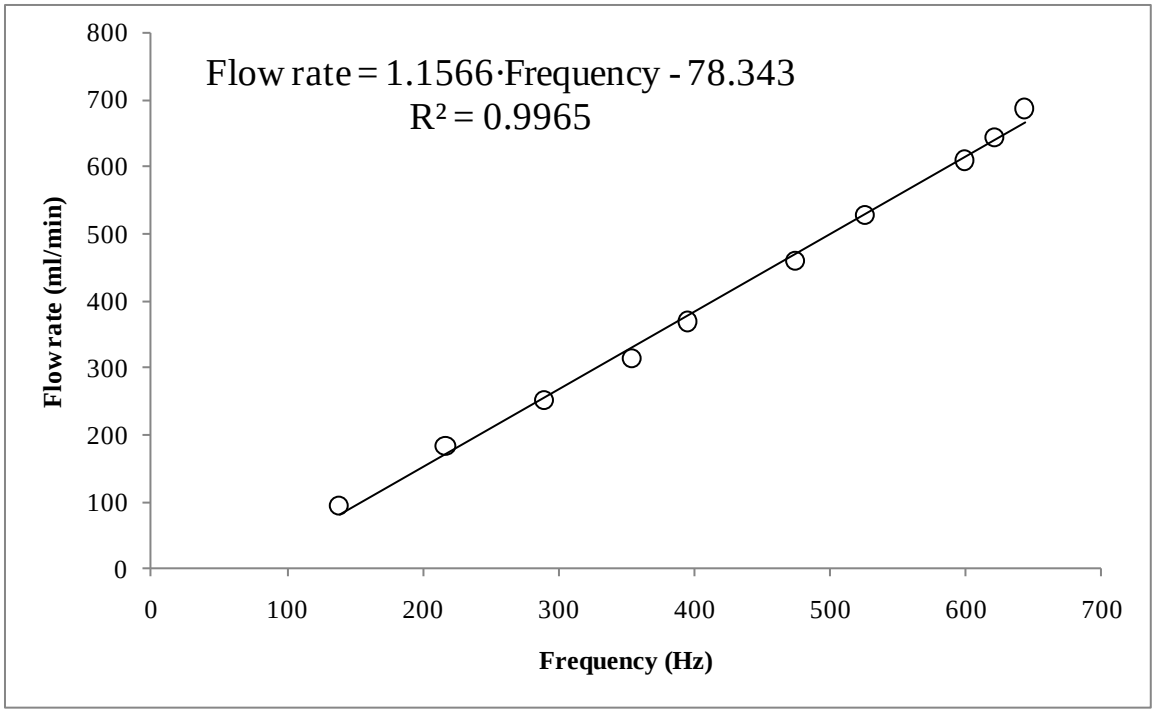

Figure 3.5. Calibration of flow rate as a function of frequency from DFS-2 flow rate sensor (with 8002 XR tip at 207 kPa)

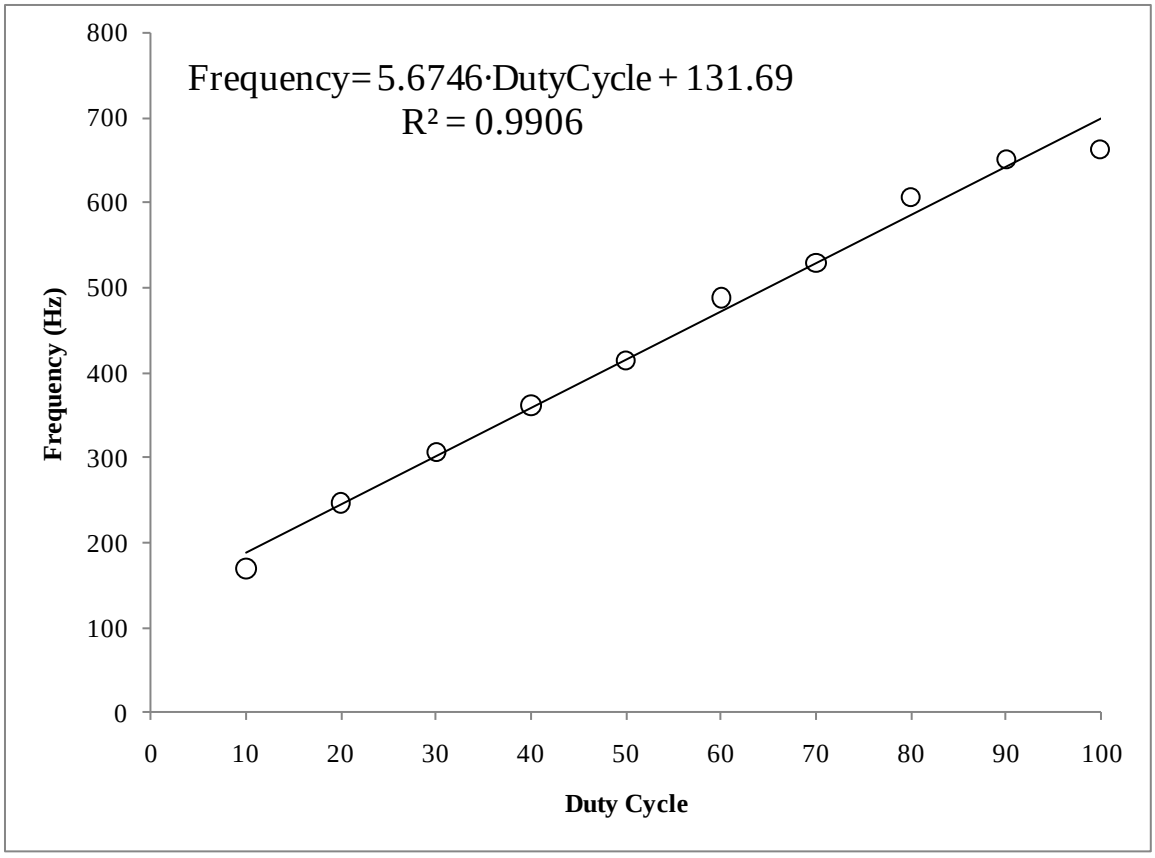

Figure 3.6. Calibration of frequency as a function of duty cycle for the PWM solenoid valve controlled 8002 XR nozzle tip used on the sprayer

3.3 Back pressure effect comparison result

As describe in section 2.3, pressure fluctuation was observed when operating the solenoid valves using PWM signals. Pressure fluctuation can induce error in flow rate output and droplet size that the nozzle produces. A back pressure bypass test unit was designed and described in section 2.3. The adjustable valve and check valves were tested to compare their ability to limit pressure fluctuations.

Figures 3.7 and 3.8 show the change of nozzle pressure when using the check valve and the adjustable valve in the back pressure unit to manipulate two five-port nozzles. Figure 3.7 shows that, when using the check valve to manipulate two five-port nozzles, the pressure fluctuation might reach 85 kPa. Figure 3.8 shows that, when using the adjustable valve to manipulate two five-port nozzles, the pressure fluctuation could go up to 35 kPa.

Figures 3.9 and 3.10 show the change in nozzle pressure with using the check valve and the adjustable valve in the back pressure unit to manipulate four five-port nozzles. Figure 3.9 shows that, when using the check valve to manipulate four five-port nozzles the pressure fluctuation could go up to 89 kPa. Figure 3.10 shows that, when using the adjustable valve to manipulate four five-port nozzles the pressure fluctuation could go up to 66 kPa.

Figures 3.7 to 3.11 indicate that the adjustable valve performs better than the check valve in limiting the pressure fluctuation and is more suitable to be used in the back pressure unit to minimize the nozzle pressure changes caused by the constant pulsing of the solenoid valves.

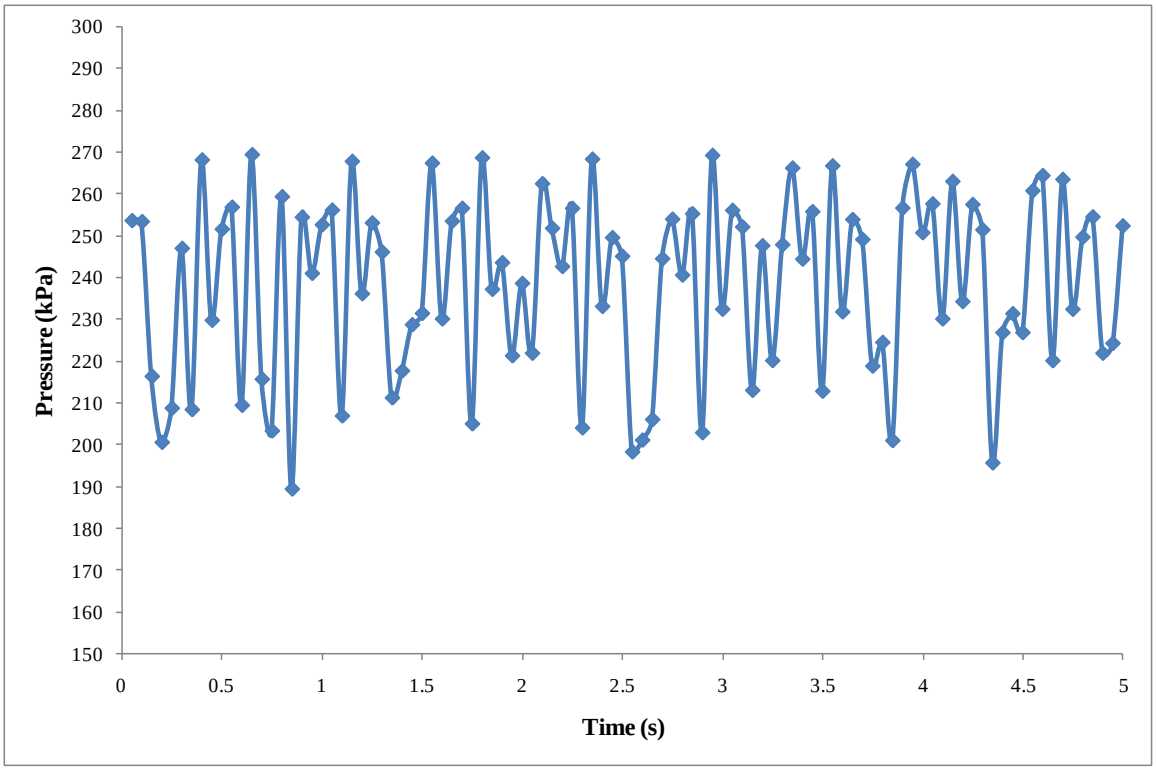

Figure 3.7. Pressure fluctuation observed using a check valve in the back pressure unit to manipulate two operating multi-port nozzles

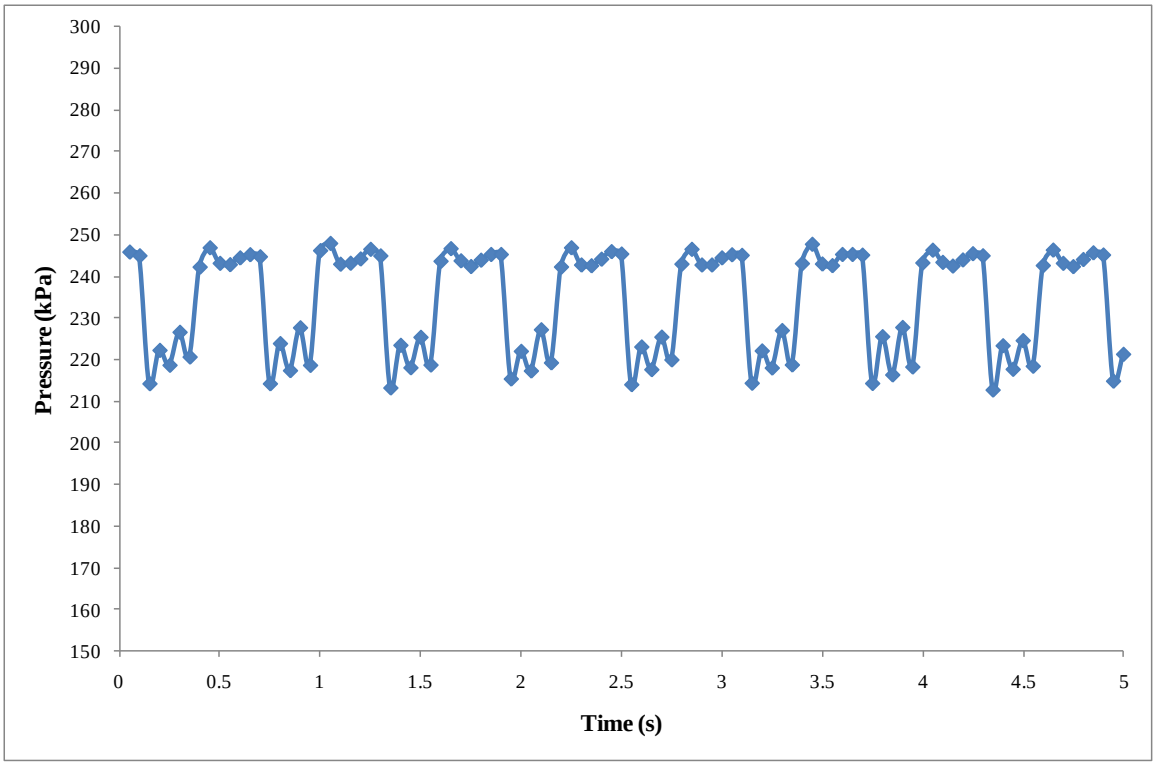

Figure 3.8. Pressure fluctuation observed using an adjustable valve in the back pressure unit to manipulate two operating multi-port nozzles

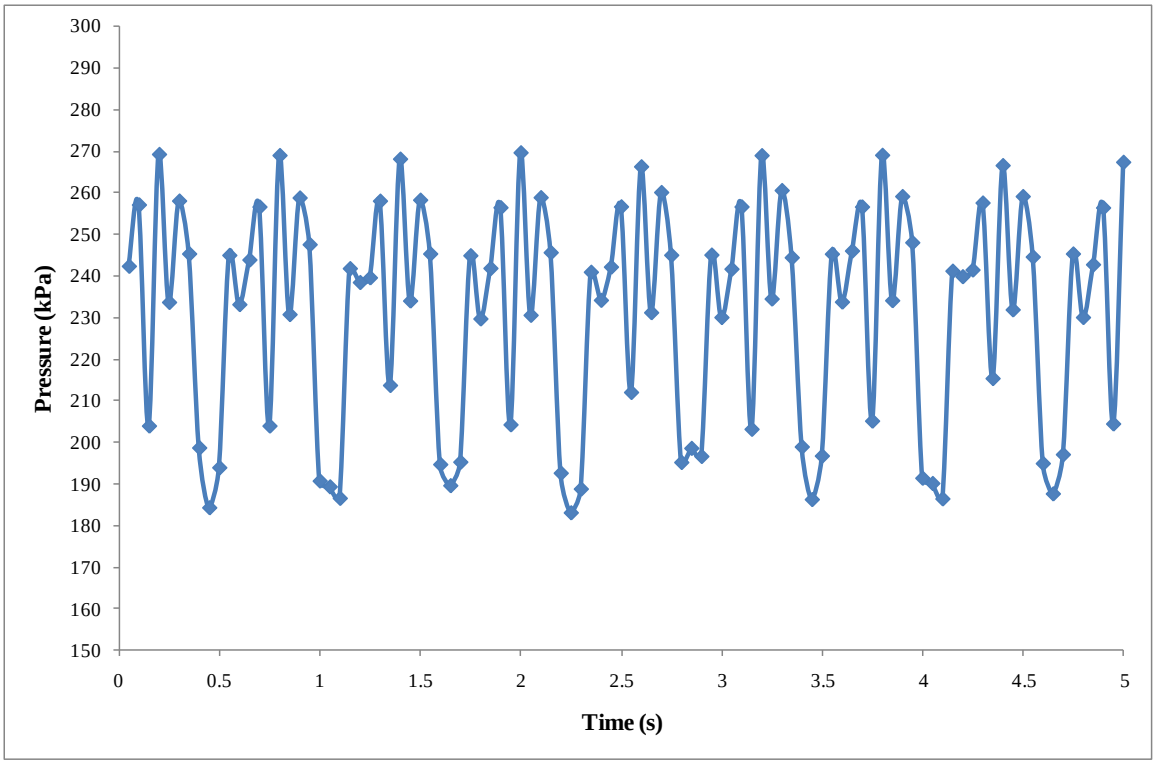

Figure 3.9. Pressure fluctuation observed using a check valve in the back pressure unit to manipulate four operating multi-port nozzles

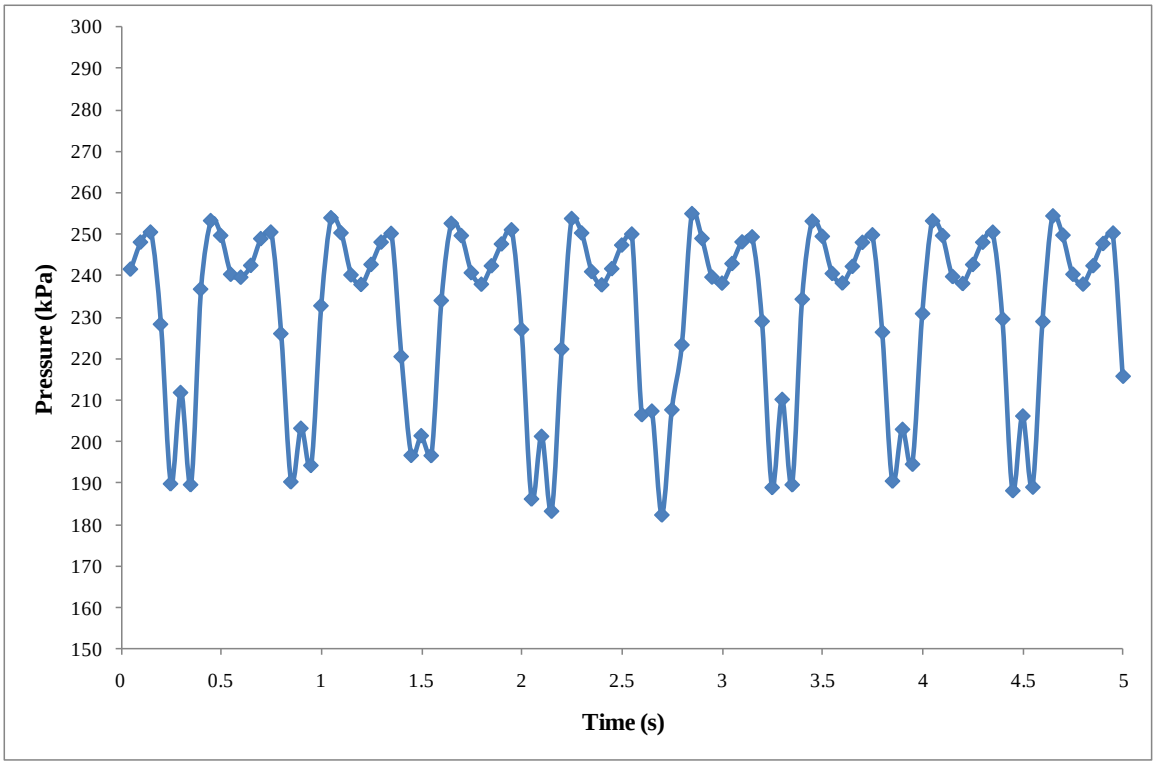

Figure 3.10. Pressure fluctuation observed using an adjustable valve in the back pressure unit to manipulate four operating multi-port nozzles

3.4 Indoor spray rate test

Before outdoor field tests were conducted, indoor experiments using controlled targets was designed and performed. As described in section 2.4, laboratory tests were carried out to evaluate the sprayer performance in terms of the algorithm design and spray model design. Four trees were scanned by the laser scanner and also measured manually for the volume evaluation. The pictures and the laser scanned image of the four trees are shown in Figures 3.11 (a) to (h). Tree 1 and tree 2 were of the same species (*Tsuga Canadensis*). Tree 1 was shorter and narrower than tree 2. Tree 3 and tree 4 were *Emerald Green Thuja*. Tree 3 was taller and a little narrower than tree 4.

(a) Tree 1 picture

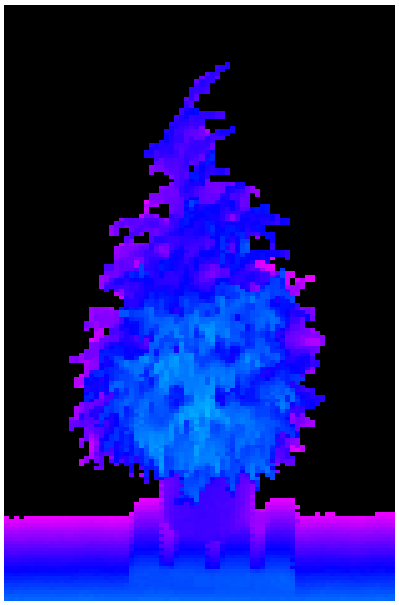

(b) Tree 1 scanned by laser

(c) Tree 2 picture

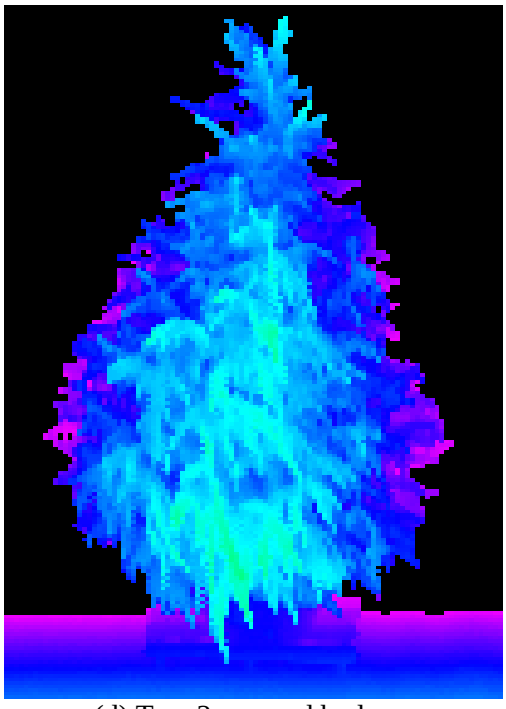

(d) Tree 2 scanned by laser

(continued)

Figure 3.11. Pictures of trees used for the tree volume evaluation and images scanned by laser

(Figure 3.11 continued)

(e) Tree 3 picture

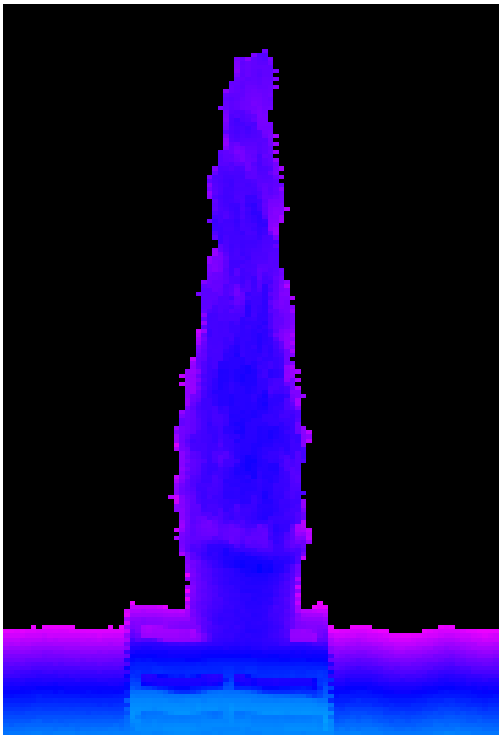

(f) Tree 3 scanned by laser

(g) Tree 4 picture

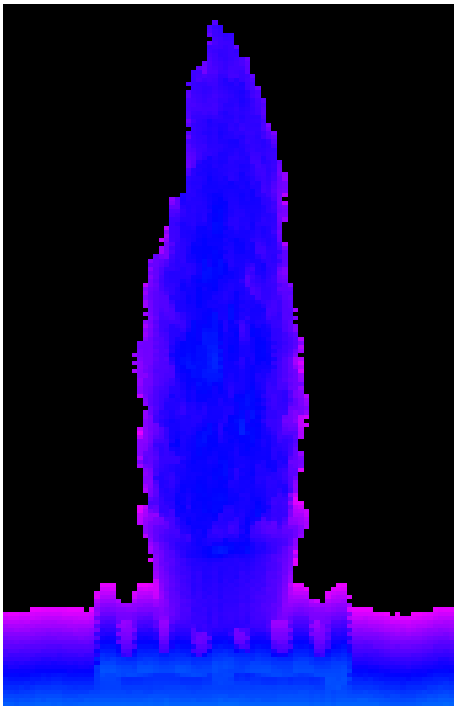

(h) Tree 4 scanned by laser

Table 3.1 shows the actual heights of each tree and the container in which the tree was planted. In this test, only tree canopies were of the interest, so the result on the height of containers were not discussed. The nozzles that should be opened to spray tree canopy for each tree are also listed in Table 3.1. This was verified by the calculated results from the algorithm.

Table 3.2 shows the result of spray constants calculated by the algorithm for each section of the tree covered by one nozzle, nozzles are ordered 1 to 20 from bottom to the top. The bottom few nozzles that faced the tree containers were not considered. Spray constants, as defined in section 2.4, were Liters of spray liquid per m^3 of effective tree volume (volume times density). The effective tree volume in this test was calculated from the manually measured volume multiplied by the density factor calculated from the density algorithm. The average spray constants were 0.155, 0.142, 0.251 and 0.194 L/m^3 for trees 1, 2, 3 and 4, respectively, and they all were greater than 0.1 L/m^3. The reason for this over estimation is explained as below.

Targeted, variable-rate application of pesticides is expected to result in savings in consumption of pesticides. However, the amount of savings may be a critical issue for some growers who may not want to take the risk of not spraying enough chemicals on the target. The main goal behind development of the intelligent sprayer was that it should apply the optimum amount of chemicals while achieving satisfactory efficacy expected from the products applied. As a safety measure, to make sure that sprayed product reaches deep into the canopy, and coverage is more than adequate, the density algorithm used for the intelligent sprayer was designed such that the densities predicted would be

intentionally increased by using the assumption of no hollowness under canopy surface, and the spray model allowing increases in the flow rate using the maximum segment width, as described in section 2.4.

The spray constant used in the spray model (described in section 2.4) was 0.1 L/m^3. To ensure that no target will be missed the concept described above (to spray a little more than what is actually needed) was used in the design of algorithm and the spray model. This explains why almost every spray constant calculated in Table 3.2 was larger than the designed value of 0.1 L/m^3. Even doing so, significant savings in spray liquid consumption resulted from using the intelligent sprayer compared to a conventional sprayer, as discussed later in section 3.9.

	Tree height (cm)	Container height (cm)	Nozzles that has canopy to spray
Tree 1	228	55	6 - 19
Tree 2	320	72	7 - 20
Tree 3	271	55	6 - 20
Tree 4	263	60	6 - 20

Table 3.1. Tree and container heights and nozzles necessary to spray these trees for the tree volume evaluation test

Nozzle #	Tree 1	Tree 2	Tree 3	Tree 4
20	Nozzle close	0.260 (0.028)	0.291 (0.218)	0.356 (0.056)
19	0.236 (0.086)	0.226 (0.032)	0.278 (0.063)	0.290 (0.104)
18	0.221 (0.065)	0.301 (0.025)	0.241 (0.153)	0.247 (0.032)
17	0.204 (0.025)	0.154 (0.009)	0.333 (0.249)	0.210 (0.025)
16	0.163 (0.033)	0.129 (0.014)	0.334 (0.211)	0.196 (0.008)
15	0.139 (0.102)	0.129 (0.009)	0.344 (0.015)	0.189 (0.004)
14	0.143 (0.069)	0.121 (0.008)	0.353 (0.252)	0.184 (0.067)
13	0.129 (0.040)	0.118 (0.009)	0.224 (0.118)	0.154 (0.054)
12	0.101 (0.009)	0.105 (0.011)	0.231 (0.118)	0.135 (0.046)
11	0.117 (0.025)	0.089 (0.010)	0.282 (0.141)	0.161 (0.054)
10	0.145 (0.033)	0.082 (0.007)	0.272 (0.121)	0.144 (0.045)
9	0.125 (0.033)	0.088 (0.010)	0.164 (0.054)	0.152 (0.049)
8	0.136 (0.022)	0.094 (0.012)	0.162 (0.067)	0.165 (0.050)
7	0.144 (0.010)	0.093 (0.011)	0.141 (0.050)	0.163 (0.047)
6	0.161 (0.023)	Container	0.116 (0.048)	0.159 (0.061)
5	Container		Container	Container
4				
3				
2				
1				

Table 3.2. Average spray constant (L/m^3), calculated by the algorithm for each section of the tree covered by its corresponding nozzle. Standard deviations are represented in parenthesis.

3.5 Calibration of sprayer components

After the sprayer prototype was made, several calibration tests were conducted to give the basic parameters of the sprayer, such as the air velocity and droplet size the sprayer ports and nozzles could produce. System response time was also calibrated so that it can be used to match the spray output to the targeted canopy sections.

3.5.1 Air velocity and droplet size from the intelligent sprayer

The average air velocity measured near the outlets of the 20 ports on one side of the intelligent sprayer was 49 m/s. Droplet size distributions ($D_{V.1}$, $D_{V.5}$ and $D_{V.9}$) from the 8002 nozzle tips for different control duty cycles operated at 207 kPa pressure and 50 m/s air velocity are shown in Table 3.3. As shown, while the $D_{V.1}$ values remained relatively similar (with the exception of increasing duty cycle from 10% to 20%), in general $D_{V.5}$ and $D_{V.9}$ values showed a slight reduction as the duty cycle increased.

Duty cycle	Dv.1 (μm)	Dv.5 (μm)	Dv.9 (μm)
10%	77	203	411
20%	111	199	404
40%	110	201	381
50%	110	199	376
60%	110	198	351
80%	108	194	341
100%	107	187	328

Table 3.3. Droplet sizes from 8002 nozzle tip operated at 207 kPa pressure, 50 m/s air velocity and various duty cycles.

3.5.2 Sprayer system response time

The intelligent sprayer consists of many different aspects, ranging from computational algorithms to hydraulic mechanics. Different components are cascaded to form a complete system. Each component introduces certain latency into the whole system. In this experiment, the overall response time of the intelligent sprayer system was measured.

As described in section 2.5, videos were recorded to document the response time from when the sprayer starts spraying targets, until the laser detected the target. Figures 3.12 (a) to (d) show the four frames taken from video files of the response time measurement. The time difference of 0.119 s (0.196 s – 0.076 s) between Figures 3.12 (a) and (c) is the lag time between the time when laser detected the target and the time liquid discharged from the nozzle. This lag time included software computation time, electronic response time and hydraulic-mechanical response time.

Since the laser was mounted 1.45 m ahead of nozzles (half-way between the cab location and the nozzles), there was sufficient time between when the laser "sees" the target and when the sprayer is operated under the typical travel speeds. Therefore, to match the optimal spray to the intended target canopy, a delay was added to the model between the point when the software performs all the necessary calculations and develops an output, and when the solenoid valve control was reloaded. The delay count was calculated as:

$$\Delta = \frac{\frac{L}{v} - t_{response}}{t_{refresh}} \quad (3.2)$$

Where,

L: Distance from the center of the laser to the center of the nozzle port, which was measured to be 1.45 m.

v: Tractor forward speed, which was 3.22 km/h (0.89 m/s).

$t_{response}$: System response time, which was calibrated above (0.119 s).

$t_{refresh}$: Refresh time for the solenoid valves, which was 0.26 s for all the tests performed in this study.

Substituting values of parameters into equation (3.2) yields $\Delta \approx 6$. Thus, a delay count of 6 was used in the field tests so that the highest amount of the spray solution discharged from the intelligent sprayer is intercepted by the target canopy.

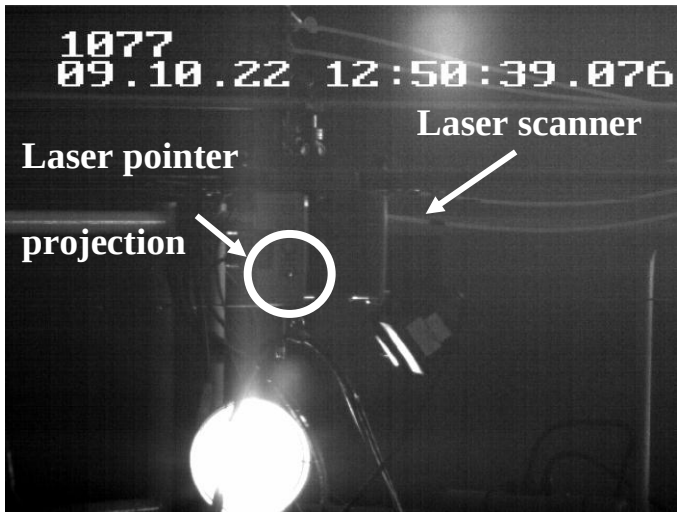

(a) Laser scanner "sees" the target

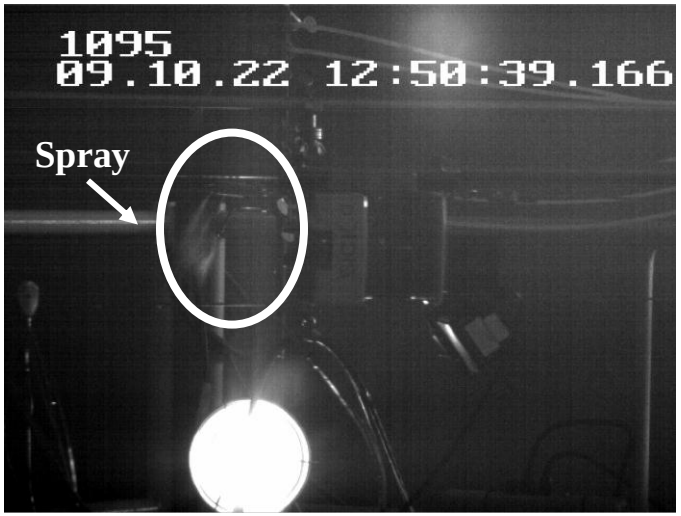

(b) Nozzles start spraying

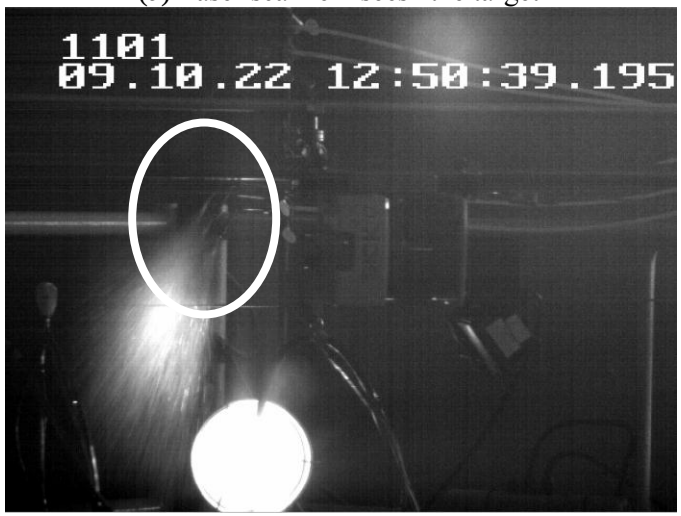

(c) Full spray discharged from nozzles

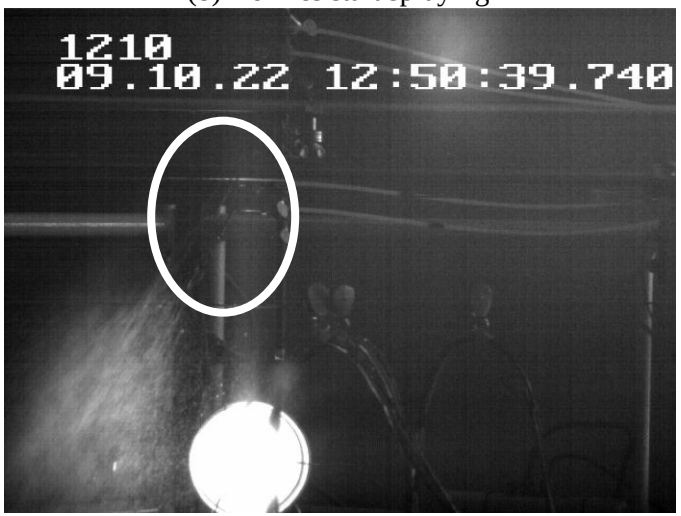

(d) Nozzle finish spraying

Figure 3.12. Screenshots from high speed video camera for measurement of sprayer system response time

3.6 Field tests

3.6.1 Uniformity of spray deposition and coverage inside tree canopies

As described in section 2.6, a 3D Cartesian coordinate system was defined for locating each sample mounted inside the tree canopy. With the defined 3D Cartesian coordinate system, every water sensitive paper and nylon screen mounted inside tree canopies was given one set of X, Y and Z values based on manual measurement. Accordingly, the samples collected from each tree were grouped in three directions: tree height direction (vertically), spray direction (horizontally), and tractor travel direction (horizontally). In this way, the uniformity of spray deposition and coverage from each direction could be evaluated separately. For example, target locations were grouped into four X sections (Tables 3.4 to 3.9) with about equal width according to the samples' X coordinates (as shown in Figures 2.25 and 2.26). The "front" is closest to the spray nozzle, and the "back" section is the furthest away from the spray nozzles. Similarly, "middle front and middle back" represents the sections located in the middle parts of the canopy with "middle front" closer to the spray nozzles and "middle back" away from the spray nozzles. Due to the change in spray direction in the spray test performed in May and the growing of tree width, actual range of the four X location sections varies for each test. In the same way, target locations were grouped into four Y sections and three Z sections. "Right, middle right, middle left and right" (Tables 3.10 to 3.15) represent four horizontal location sections along the tractor travel direction with "right" having the largest Y values and "left" having the smallest Y values. "High, middle and low" (Tables

3.16 to 3.21) represent three vertical sections with “high” having the largest Z values and low having the smallest Z value.

For the first test conducted in April when trees were just starting to leaf out, the average coverage inside canopies were 41%, 88% and 70%, and the average deposit inside the canopies were 1.31, 6.61 , and 3.91 μL/cm^2 for S1, S2 and S3, respectively.

For the second test conducted in May when the apple trees canopies were at half of the full foliage, the average coverage inside canopies were 39%, 74% and 53%, and the average deposit inside the canopies were 0.87, 3.64, and 1.56 μL/cm^2 for S1, S2 and S3, respectively.

For the third test conducted in June when the foliage was fully developed, the average coverage inside canopies were 36%, 56% and 42%, and the average deposit inside the canopies were 0.92, 2.96 , and 1.27 μL/cm^2 for S1, S2 and S3, respectively.

Tables 3.4 to 3.9 show the coverage and deposition result for the samples mounted at different X locations inside the tree canopies. In earlier months when the tree canopies were not fully developed, both values of spray coverage and deposit for S1 were significantly lower than those for S2 and S3. In June when the canopies were fully developed, the three sprayers do not have significant differences in spray coverage and deposit performance. These tables also show that in general S2 has the best uniformity (fewest differences in deposit and coverage) along the X direction (spray direction) and S1 has the second best. When just looking at the half of canopies closer to the spray nozzles, S1 has uniform spray coverage and deposition along the spray direction for all

tests and all trees. Therefore, it suggests that S1 works better when used to spray every row than when used in alternative row spraying.

Tables 3.10 to 3.15 show the coverage and deposition result for the samples mounted at different Y locations inside the tree canopies. The uniformity of S1 and S2 on Y direction (parallel to spray travel direction) are better than that of S3 which S1 has better uniformity on Tree 1 and 2, while S2 has better uniformity on Tree 3.

Tables 3.16 to 3.21 show the coverage and deposition result for the samples mounted at different Z locations inside the tree canopies. It is shown that S1 generally has the best uniformity along the Z direction (vertical direction) among three sprayers.

It is also shown from Tables 3.4 to 3.21 that for the first two tests while the tree canopies were not fully developed, almost all the coverage and deposit values for S2 and S3 were significantly larger than those for S1. Many samples sprayed by S2 and S3 in the first two tests, had coverage from 80% to 100%, which are more than what the canopies needed. However, the results of S1 were sufficient for all tests, and were not too high.

The spray coverage and deposit from S1 were sufficient except for one position on Tree 2 in May test (Table 3.5 at the back location of the tree) where the average coverage was 3% and was lower than the recommended 15% (based on Dr. Heping Zhu's experience with visual observation of spray coverage on water sensitive papers). The results from the other two sprayers, S2 and S3, at this location were also lower than 15%, which indicates that this location was hard to reach by itself (on the back of the canopy, farthest from spray nozzles), especially when the trees reached about half-full canopies.

Target location on tree canopy	Average Spray Coverage (%)[1]								
	April			May			June		
	S1[2]	S2[3]	S3[4]	S1	S2	S3	S1	S2	S3
Front	53 (20) cdA	100 (0) aA	86 (16) abAB	38 (12) dAB	89 (15) abA	71 (18) bcA	75 (18) bcA	88 (14) abA	83 (11) abA
Middle front	41 (20) dA	96 (12) aA	75 (17) abcAB	45 (18) dA	82 (28) abA	52 (21) cdAB	45 (32) dAB	65 (36) bcdA	59 (28) bcdAB
Middle back	48 (22) bcA	100 (0) aA	87 (16) aA	25 (23) dB	65 (16) bA	40 (15) cdBC	47 (21) bcAB	58 (31) bcA	37 (21) cdBC
Back	46 (28) bcdA	93 (15) aA	64 (22) abcB	19 (19) dB	72 (35) abA	26 (19) cdC	32 (29) cdB	52 (35) bcdA	18 (20) dC

Table 3.4. Spray coverage on water sensitive papers within different X location sections inside Tree 1 canopy for the field tests in April, May and June using intelligent sprayer with automatic spray control, intelligent sprayer without automatic control and conventional air blast sprayer. Standard deviations are given in parentheses.

[1] Means in a row followed by different lowercase letters are significantly different ($p < 0.05$). Means in a column followed by different uppercase letters are significantly different ($p < 0.05$).

[2] S1 = Intelligent sprayer with automatic control.

[3] S2 = Intelligent sprayer without automatic control.

[4] S3 = Conventional air blast sprayer.

Target location on tree canopy	Average Spray Coverage (%)[1]								
	April			May			June		
	S1[2]	S2[3]	S3[4]	S1	S2	S3	S1	S2	S3
Front	45 (4) cdA	89 (19) abA	68 (3) bcAB	52 (19) cdA	91 (19) aA	73 (8) abA	38 (6) dA	71 (2) abcA	84 (14) abA
Middle front	33 (18) dA	62 (27) abcA	76 (17) abA	52 (19) bcdA	88 (21) aA	72 (26) abA	31 (22) dA	57 (30) bcdA	36 (15) cdB
Middle back	42 (29) bcA	79 (36) aA	76 (12) abA	16 (12) cB	52 (31) abcB	41 (22) bcB	27 (28) cA	45 (34) bcA	27 (26) cB
Back	42 (23) bcA	81 (38) aA	59 (14) abB	3 (0) dB	11 (5) cdC	13 (10) cdC	16 (4) cdA	55 (24) bA	25 (17) cdB

Table 3.5. Spray coverage on water sensitive papers within different X location sections inside Tree 2 canopy for the field tests in April, May and June using intelligent sprayer with automatic spray control, intelligent sprayer without automatic control and conventional air blast sprayer. Standard deviations are given in parentheses.

[1] Means in a row followed by different lowercase letters are significantly different ($p < 0.05$). Means in a column followed by different uppercase letters are significantly different ($p < 0.05$).

[2] S1 = Intelligent sprayer with automatic control.

[3] S2 = Intelligent sprayer without automatic control.

[4] S3 = Conventional air blast sprayer.

Target location on tree canopy	Average Spray Coverage (%)[1]								
	April			May			June		
	S1[2]	S2[3]	S3[4]	S1	S2	S3	S1	S2	S3
Front	55 (14) aA	91 (16) abAB	77 (20) abAB	58 (20) abA	91 (16) aAB	81 (16) abA	61 (38) abAB	69 (27) abA	59 (38) abA
Middle front	44 (25) dA	100 (0) aA	81 (15) abcA	51 (29) cdA	90 (45) abA	59 (32) cdAB	53 (39) cdA	64 (37) bcdA	76 (19) abcdA
Middle back	39 (23) bcAB	94 (13) aA	61 (25) bB	33 (29) cA	52 (35) bcAB	30 (23) cC	32 (30) cAB	53 (32) bcA	30 (20) cB
Back	20 (6) bcB	70 (30) aB	28 (7) bcC	33 (20) bcA	46 (33) abA	33 (32) bcBC	16 (23) bcB	36 (24) bA	7 (7) cC

Table 3.6. Spray coverage on water sensitive papers within different X location sections inside Tree 3 canopy for the field tests in April, May and June using intelligent sprayer with automatic spray control, intelligent sprayer without automatic control and conventional air blast sprayer. Standard deviations are given in parentheses.

[1] Means in a row followed by different lowercase letters are significantly different ($p < 0.05$). Means in a column followed by different uppercase letters are significantly different ($p < 0.05$).

[2] S1 = Intelligent sprayer with automatic control.

[3] S2 = Intelligent sprayer without automatic control.

[4] S3 = Conventional air blast sprayer.

Target location on tree canopy	Average Spray Deposit (μL/cm^2)[1]								
	April			May			June		
	S1[2]	S2[3]	S3[4]	S1	S2	S3	S1	S2	S3
Front	1.16 (0.51) efA	7.69 (2.89) aA	4.11 (1.53) bcA	0.61 (0.36) fA	3.16 (1.53) bcdeA	1.77 (0.64) defA	2.37 (0.84) cdefA	4.81 (1.74) bA	3.53 (1.3) bcdA
Middle front	0.93 (0.32) cA	8.67 (3.78) aA	4.64 (0.83) bA	0.55 (0.32) cA	3.74 (1.9) bA	1.27 (0.52) cAB	1.6 (1.4) cAB	4.06 (1.58) bA	1.19 (0.76) cB
Middle back	1.42 (0.84) cA	8.91 (2.58) aA	4.72 (1.49) bA	0.6 (0.62) cA	3.63 (2.73) bA	0.89 (0.55) cB	0.95 (0.47) cBC	3.85 (2.96) bA	0.99 (0.55) cB
Back	1.6 (1.12) cA	7.4 (2.04) aA	4.46 (1.24) bA	0.44 (0.63) cA	5.74 (5.15) abA	0.73 (0.48) cB	0.37 (0.16) cC	1.8 (1.27) cA	0.52 (0.44) cB

Table 3.7. Spray deposits collected by nylon screens within different X location sections inside Tree 1 canopy for the field tests in April, May and June using intelligent sprayer with automatic spray control, intelligent sprayer without automatic control and conventional air blast sprayer. Standard deviations are given in parentheses.

[1] Means in a row followed by different lowercase letters are significantly different ($p < 0.05$). Means in a column followed by different uppercase letters are significantly different ($p < 0.05$).

[2] S1 = Intelligent sprayer with automatic control.

[3] S2 = Intelligent sprayer without automatic control.

[4] S3 = Conventional air blast sprayer.

Target location on tree canopy	Average Spray Deposit (μL/cm^2)[1]								
	April			May			June		
	S1[2]	S2[3]	S3[4]	S1	S2	S3	S1	S2	S3
Front	1.43 (0.14) cdA	3.16 (1.48) abcA	3.94 (0.37) abA	0.8 (0.4) dA	4.41 (2.26) aA	2.64 (0.98) bcA	1.07 (0.38) cdA	2.77 (1.43) abcA	2.44 (0.36) bcdA
Middle front	1.13 (0.39) cA	3.19 (2.68) abA	3.5 (0.61) abA	1.08 (0.43) cA	3.93 (2.38) aA	2.52 (0.67) bcAB	0.57 (0.39) cAB	1.23 (0.45) cA	0.88 (0.44) cB
Middle back	1.92 (1.34) cA	7.29 (3.04) aA	4.17 (0.68) bA	0.36 (0.19) cB	1.23 (0.6) cB	1.12 (0.29) cBC	0.71 (0.82) cBC	2.68 (2.4) bcA	0.9 (0.88) cB
Back	1.69 (1.04) cdA	5.89 (3.03) aA	3.53 (1.08) bA	0.11 (0.04) cB	0.59 (0.34) cdB	0.43 (0.03) cdC	0.28 (0.2) cdC	2.57 (2.72) bcA	0.66 (0.58) cdB

Table 3.8. Spray deposits collected by nylon screens within different X location sections inside Tree 2 canopy for the field tests in April, May and June using intelligent sprayer with automatic spray control, intelligent sprayer without automatic control and conventional air blast sprayer. Standard deviations are given in parentheses.

[1] Means in a row followed by different lowercase letters are significantly different ($p < 0.05$). Means in a column followed by different uppercase letters are significantly different ($p < 0.05$).

[2] S1 = Intelligent sprayer with automatic control.

[3] S2 = Intelligent sprayer without automatic control.

[4] S3 = Conventional air blast sprayer.

Target location	Average Spray Deposit (μL/cm^2)[1]								
	April			May			June		
on tree canopy	S1[2]	S2[3]	S3[4]	S1	S2	S3	S1	S2	S3
Front	1.4 (0.73) cA	5.85 (3.05) aA	3.82 (1.12) abcAB	1.88 (1.13) cA	4.28 (1.25) abA	2.34 (0.99) bcA	2 (2.11) bcA	3.05 (3.12) abcA	2.55 (0.36) bcA
Middle front	1.21 (0.79) dA	6.07 (2.63) aA	4.07 (0.92) bA	1.54 (0.97) dA	4.5 (2.35) bA	1.63 (0.77) dAB	1.4 (1.29) dA	3.32 (2.48) bcA	2.08 (0.88) cdA
Middle back	1.12 (0.6) cdA	7.52 (3.66) aA	3.43 (1.49) bAB	0.87 (0.78) cdA	3.01 (3.07) bcA	0.89 (0.84) cdB	0.71 (0.72) dA	3.71 (3.51) bA	1.01 (0.68) cdB
Back	0.73 (0.2) dA	4.48 (2.89) aA	2.49 (1.31) bcB	0.87 (0.44) bdA	3.43 (2.2) abA	1.04 (0.56) bdB	0.48 (0.5) dA	1.22 (1.31) bcdA	0.47 (0.45) dB

Table 3.9. Spray deposits collected by nylon screens within different X location sections inside Tree 3 canopy for the field tests in April, May and June using intelligent sprayer with automatic spray control, intelligent sprayer without automatic control and conventional air blast sprayer. Standard deviations are given in parentheses.

[1] Means in a row followed by different lowercase letters are significantly different ($p < 0.05$). Means in a column followed by different uppercase letters are significantly different ($p < 0.05$).

[2] S1 = Intelligent sprayer with automatic control.

[3] S2 = Intelligent sprayer without automatic control.

[4] S3 = Conventional air blast sprayer.

Target location on tree canopy	Average Spray Coverage (%)[1]								
	April			May			June		
	S1[2]	S2[3]	S3[4]	S1	S2	S3	S1	S2	S3
Right	45 (23) cdA	100 (0) aA	72 (22) bcA	41 (24) dA	89 (18) abA	59 (12) cdA	49 (26) cdA	65 (30) bcdAB	46 (25) cdA
Middle right	51 (26) bcA	92 (15) aA	81 (21) aA	33 (16) cA	77 (27) abA	53 (27) bcA	36 (26) cA	48 (35) cB	32 (28) cA
Middle left	43 (13) deA	100 (0) aA	86 (15) abA	24 (19) eA	66 (25) bcdA	34 (23) eA	64 (26) bcdA	83 (21) abcA	62 (32) cdA
Left	46 (34) bA	100 (0) aA	67 (8) abA	48 (25) bA	84 (27) abA	52 (13) abA	37 (30) bA	50 (36) bAB	46 (33) bA

Table 3.10. Spray coverage on water sensitive papers within different Y location sections inside Tree 1 canopy for the field tests in April, May and June using intelligent sprayer with automatic spray control, intelligent sprayer without automatic control and conventional air blast sprayer. Standard deviations are given in parentheses.

[1] Means in a row followed by different lowercase letters are significantly different ($p < 0.05$). Means in a column followed by different uppercase letters are significantly different ($p < 0.05$).

[2] S1 = Intelligent sprayer with automatic control.

[3] S2 = Intelligent sprayer without automatic control.

[4] S3 = Conventional air blast sprayer.

Target location	Average Spray Coverage (%)[1]								
	April			May			June		
on tree canopy	S1[2]	S2[3]	S3[4]	S1	S2	S3	S1	S2	S3
Right	25 (24) cB	67 (39) abA	67 (9) abA	43 (20) bcA	85 (24) aAB	76 (14) aA	19 (26) cA	33 (25) cB	26 (24) cB
Middle right	51 (19) bcA	83 (31) aA	66 (19) abA	46 (28) bcdA	81 (34) aA	66 (22) abA	23 (21) dA	64 (30) abA	30 (23) cdB
Middle left	41 (11) bcdAB	85 (30) aA	73 (18) abA	10 (7) dB	38 (30) cdB	17 (10) dB	39 (5) cdA	68 (27) abcAB	70 (23) abcA
Left	29 (28) bcAB	75 (34) aA	74 (7) aA	41 (24) abcAB	65 (42) abAB	58 (30) abA	10 (6) cA	29 (17) bcB	32 (21) bcB

Table 3.11. Spray coverage on water sensitive papers within different Y location sections inside Tree 2 canopy for the field tests in April, May and June using intelligent sprayer with automatic spray control, intelligent sprayer without automatic control and conventional air blast sprayer. Standard deviations are given in parentheses.

[1] Means in a row followed by different lowercase letters are significantly different ($p < 0.05$). Means in a column followed by different uppercase letters are significantly different ($p < 0.05$).

[2] S1 = Intelligent sprayer with automatic control.

[3] S2 = Intelligent sprayer without automatic control.

[4] S3 = Conventional air blast sprayer.

Target location on tree canopy	Average Spray Coverage (%)[1]								
	April			May			June		
	S1[2]	S2[3]	S3[4]	S1	S2	S3	S1	S2	S3
Right	57 (23) bA	100 (0) aA	79 (32) abA	48 (31) bA	80 (19) abA	60 (20) bA	76 (36) abA	84 (22) abA	71 (16) abA
Middle right	30 (18) cdB	84 (22) aA	52 (29) bcA	52 (25) bcA	83 (44) aA	60 (30) bA	29 (30) cdB	57 (24) bAB	24 (23) dB
Middle left	33 (24) bAB	86 (27) aA	61 (24) abA	44 (29) bA	61 (41) abA	41 (42) bA	35 (31) bB	29 (35) bB	41 (36) bAB
Left	44 (22) bAB	100 (0) aA	67 (8) abA	25 (25) bA	55 (38) abA	37 (32) bA	19 (28) bB	48 (38) bAB	63 (42) abA

Table 3.12. Spray coverage on water sensitive papers within different Y location sections inside Tree 3 canopy for the field tests in April, May and June using intelligent sprayer with automatic spray control, intelligent sprayer without automatic control and conventional air blast sprayer. Standard deviations are given in parentheses.

[1] Means in a row followed by different lowercase letters are significantly different ($p < 0.05$). Means in a column followed by different uppercase letters are significantly different ($p < 0.05$).

[2] S1 = Intelligent sprayer with automatic control.

[3] S2 = Intelligent sprayer without automatic control.

[4] S3 = Conventional air blast sprayer.

Target location on tree canopy	Average Spray Deposit (μL/cm^2)[1]								
	April			May			June		
	S1[2]	S2[3]	S3[4]	S1	S2	S3	S1	S2	S3
Right	1.49 (0.77) cA	9.68 (2.65) aA	5.05 (0.9) bA	0.52 (0.42) cA	3.84 (2.15) bA	1.46 (0.55) cA	0.81 (0.55) cA	4.6 (3.17) bA	1.08 (0.67) cA
Middle right	1.53 (1.03) cdA	7.44 (2.12) aA	4.43 (1.64) bA	0.53 (0.33) dA	3.93 (2.8) bA	1.35 (0.78) cdA	0.84 (0.65) cdA	2.32 (1.94) cA	0.89 (0.93) cdA
Middle left	0.96 (0.28) eA	8.5 (3.53) aA	4.56 (1.2) bA	0.39 (0.27) eA	2.88 (1.6) cdA	0.71 (0.35) eA	1.76 (1.22) deA	4.28 (0.94) bcA	2.02 (1.71) deA
Left	1.04 (0.68) bA	7.67 (2.98) aA	3.8 (0.07) abA	1.17 (0.83) bA	6.76 (5.05) aA	1.41 (0.39) bA	1.81 (1.71) bA	3.65 (3.1) abA	1.37 (0.77) bA

Table 3.13. Spray deposits collected by nylon screens within different Y location sections inside Tree 1 canopy for the field tests in April, May and June using intelligent sprayer with automatic spray control, intelligent sprayer without automatic control and conventional air blast sprayer. Standard deviations are given in parentheses.

[1] Means in a row followed by different lowercase letters are significantly different ($p < 0.05$). Means in a column followed by different uppercase letters are significantly different ($p < 0.05$).

[2] S1 = Intelligent sprayer with automatic control.

[3] S2 = Intelligent sprayer without automatic control.

[4] S3 = Conventional air blast sprayer.

Target location on tree canopy	Average Spray Deposit (μL/cm^2)[1]								
	April			May			June		
	S1[2]	S2[3]	S3[4]	S1	S2	S3	S1	S2	S3
Right	1.28 (1.24) bcA	4.65 (3.31) aA	3.47 (0.68) abA	0.84 (0.49) cA	3.48 (2.59) abAB	2.14 (0.76) bcA	0.6 (0.94) cA	1.8 (2.47) bcA	0.83 (0.72) cB
Middle right	2.01 (0.94) cdeA	6.01 (3.31) aA	3.69 (0.8) bcA	0.84 (0.54) deA	3.87 (2.74) bA	2.36 (1.28) bcdA	0.42 (0.38) eA	2.49 (2.4) bcdA	0.81 (0.77) deB
Middle left	1.25 (0.29) bcA	3.73 (2.4) aA	3.96 (1.22) aA	0.24 (0.16) cB	1.13 (0.49) bcB	0.63 (0.35) bcB	0.85 (0.44) bcA	3.2 (2.02) aA	2.19 (0.63) abA
Left	1.21 (1.2) bcA	6.55 (2.66) aA	4.01 (0.97) abA	0.61 (0.23) cAB	2.77 (1.73) abcAB	1.86 (0.78) bcA	0.3 (0.26) cA	1.76 (2.51) bcA	1.05 (0.8) cB

Table 3.14. Spray deposits collected by nylon screens within different Y location sections inside Tree 2 canopy for the field tests in April, May and June using intelligent sprayer with automatic spray control, intelligent sprayer without automatic control and conventional air blast sprayer. Standard deviations are given in parentheses.

[1] Means in a row followed by different lowercase letters are significantly different ($p < 0.05$). Means in a column followed by different uppercase letters are significantly different ($p < 0.05$).

[2] S1 = Intelligent sprayer with automatic control.

[3] S2 = Intelligent sprayer without automatic control.

[4] S3 = Conventional air blast sprayer.

Target location on tree canopy	Average Spray Deposit (μL/cm^2)[1]								
	April			May			June		
	S1[2]	S2[3]	S3[4]	S1	S2	S3	S1	S2	S3
Right	1.8 (0.63) cdA	7.47 (0.87) aA	4.02 (1.53) bcA	1.33 (0.9) dA	5.78 (2.42) abA	1.8 (0.48) cdA	2.67 (1.53) cdA	5.72 (3.44) abA	1.98 (0.86) cdAB
Middle right	0.87 (0.31) deB	6.17 (3.22) aA	3.38 (1.29) bcA	1.25 (0.74) deA	3.73 (2.16) bA	1.48 (0.92) deA	0.58 (0.58) eB	2.16 (2.01) cdB	0.98 (0.74) deB
Middle left	0.92 (0.78) bB	5.08 (4.53) aA	3.18 (1.68) abA	1.81 (1.46) bA	3.36 (2.65) abA	1.52 (1.41) bA	0.82 (0.76) bB	2.56 (3.11) abAB	1.21 (1.11) bAB
Left	1.14 (0.64) bcdAB	6.39 (2.32) aA	3.38 (0.7) bA	0.84 (0.66) cdA	2.85 (1.87) bcA	1.24 (0.95) bcdA	0.46 (0.63) dB	2.52 (2.3) bcdAB	2.17 (1.14) bcdA

Table 3.15. Spray deposits collected by nylon screens within different Y location sections inside Tree 3 canopy for the field tests in April, May and June using intelligent sprayer with automatic spray control, intelligent sprayer without automatic control and conventional air blast sprayer. Standard deviations are given in parentheses.

[1] Means in a row followed by different lowercase letters are significantly different ($p < 0.05$). Means in a column followed by different uppercase letters are significantly different ($p < 0.05$).

[2] S1 = Intelligent sprayer with automatic control.

[3] S2 = Intelligent sprayer without automatic control.

[4] S3 = Conventional air blast sprayer.

Target location on tree canopy	Average Spray Coverage (%)[1]								
	April			May			June		
	S1[2]	S2[3]	S3[4]	S1	S2	S3	S1	S2	S3
High	49 (23) cA	100 (0) aA	72 (20) bcA	23 (16) dA	88 (23) abA	52 (18) cAB	69 (10) bcA	100 (0) aA	61 (13) cA
Middle	51 (22) cdA	100 (0) aA	83 (20) abA	27 (14) dA	68 (23) bcA	35 (24) dB	47 (35) cdA	69 (29) bcAB	38 (35) dA
Low	43 (22) bA	95 (12) aA	79 (19) aA	42 (23) bA	79 (26) aA	56 (21) bA	42 (25) bA	49 (29) bB	48 (30) bA

Table 3.16. Spray coverage on water sensitive papers within different Z location sections inside Tree 1 canopy for the field tests in April, May and June using intelligent sprayer with automatic spray control, intelligent sprayer without automatic control and conventional air blast sprayer. Standard deviations are given in parentheses.

[1] Means in a row followed by different lowercase letters are significantly different ($p < 0.05$). Means in a column followed by different uppercase letters are significantly different ($p < 0.05$).

[2] S1 = Intelligent sprayer with automatic control.

[3] S2 = Intelligent sprayer without automatic control.

[4] S3 = Conventional air blast sprayer.

Target location on tree canopy	Average Spray Coverage (%)[1]								
	April			May			June		
	S1[2]	S2[3]	S3[4]	S1	S2	S3	S1	S2	S3
High	48 (17) deAB	100 (0) aA	47 (11) deB	62 (5) cdA	100 (0) aA	76 (2) bcA	15 (8) fA	88 (21) abA	40 (18) eA
Middle	53 (14) dA	100 (0) aA	77 (17) bcA	52 (19) dA	96 (10) abA	71 (28) cdA	23 (18) eA	59 (30) cdAB	23 (20) eA
Low	30 (24) deB	62 (34) abB	70 (9) aA	27 (24) eB	54 (35) abcB	49 (28) abcdA	24 (23) eA	39 (25) cdeB	42 (30) bcdeA

Table 3.17. Spray coverage on water sensitive papers within different Z location sections inside Tree 2 canopy for the field tests in April, May and June using intelligent sprayer with automatic spray control, intelligent sprayer without automatic control and conventional air blast sprayer. Standard deviations are given in parentheses.

[1] Means in a row followed by different lowercase letters are significantly different ($p < 0.05$). Means in a column followed by different uppercase letters are significantly different ($p < 0.05$).

[2] S1 = Intelligent sprayer with automatic control.

[3] S2 = Intelligent sprayer without automatic control.

[4] S3 = Conventional air blast sprayer.

Target location on tree canopy	Average Spray Coverage (%)[1]								
	April			May			June		
	S1[2]	S2[3]	S3[4]	S1	S2	S3	S1	S2	S3
High	28 (11) cdB	100 (0) aA	29 (7) cdC	44 (19) bcAB	66 (29) bA	51 (28) bcA	29 (23) cdB	54 (11) bcA	10 (6) dB
Middle	59 (9) cdA	100 (0) aA	85 (12) abcA	71 (17) bcdA	91 (15) abA	54 (33) dA	71 (31) bcdA	70 (38) bcdA	50 (15) dAB
Low	32 (23) aB	84 (23) aA	60 (26) aB	38 (27) aB	65 (34) aA	52 (34) aA	28 (32) aB	48 (33) aA	46 (37) aA

Table 3.18. Spray coverage on water sensitive papers within different Z location sections inside Tree 3 canopy for the field tests in April, May and June using intelligent sprayer with automatic spray control, intelligent sprayer without automatic control and conventional air blast sprayer. Standard deviations are given in parentheses.

[1] Means in a row followed by different lowercase letters are significantly different ($p < 0.05$). Means in a column followed by different uppercase letters are significantly different ($p < 0.05$).

[2] S1 = Intelligent sprayer with automatic control.

[3] S2 = Intelligent sprayer without automatic control.

[4] S3 = Conventional air blast sprayer.

Target location on tree canopy	Average Spray Deposit (µL/cm^2)[1]								
	April			May			June		
	S1[2]	S2[3]	S3[4]	S1	S2	S3	S1	S2	S3
High	1.2 (0.43) cA	10.3 (1.73) aA	5.45 (0.46) bA	0.32 (0.24) cA	6.03 (3.3) bA	1.42 (0.65) cA	1.44 (0.74) cA	5.2 (1.16) bA	2.06 (0.74) cA
Middle	1.61 (1.11) cA	7.69 (1.49) aA	4.41 (1.7) bA	0.34 (0.24) cA	3.25 (1.71) bA	0.89 (0.46) cA	1.27 (1.38) cA	3.21 (1.72) bA	1.16 (1.24) cA
Low	1.1 (0.51) cA	8.14 (3.49) aA	4.35 (0.98) bA	0.77 (0.51) cA	3.67 (2.95) bA	1.28 (0.69) cA	1.17 (0.96) cA	3.46 (2.71) bA	1.26 (1.32) cA

Table 3.19. Spray deposits collected by nylon screens within different Z location sections inside Tree 1 canopy for the field tests in April, May and June using intelligent sprayer with automatic spray control, intelligent sprayer without automatic control and conventional air blast sprayer. Standard deviations are given in parentheses.

[1] Means in a row followed by different lowercase letters are significantly different ($p < 0.05$). Means in a column followed by different uppercase letters are significantly different ($p < 0.05$).

[2] S1 = Intelligent sprayer with automatic control.

[3] S2 = Intelligent sprayer without automatic control.

[4] S3 = Conventional air blast sprayer.

Target location on tree canopy	Average Spray Deposit (µL/cm^2)[1]								
	April			May			June		
	S1[2]	S2[3]	S3[4]	S1	S2	S3	S1	S2	S3
High	2.18 (1.19) cdeA	7.92 (1.13) aA	3.58 (1.37) bcdA	1.05 (0.04) deA	5.78 (1.11) abA	2.93 (0.11) cdeA	0.22 (0.12) eA	4.77 (3.77) bcA	1.22 (0.96) deA
Middle	1.85 (0.51) cdA	7.1 (1.42) aA	4.08 (1.01) bA	0.9 (0.47) dA	3.95 (2.05) bAB	2.85 (1.09) cA	0.5 (0.36) dA	2.75 (1.91) bcAB	0.83 (0.75) dA
Low	1.3 (1.13) bcA	3.78 (3.15) aB	3.59 (0.64) aA	0.53 (0.46) cA	2.16 (2.27) bB	1.42 (0.84) bcB	0.59 (0.69) cA	1.58 (1.81) bcB	1.18 (0.93) bcA

Table 3.20. Spray deposits collected by nylon screens within different Z location sections inside Tree 2 canopy for the field tests in April, May and June using intelligent sprayer with automatic spray control, intelligent sprayer without automatic control and conventional air blast sprayer. Standard deviations are given in parentheses.

[1] Means in a row followed by different lowercase letters are significantly different ($p < 0.05$). Means in a column followed by different uppercase letters are significantly different ($p < 0.05$).

[2] S1 = Intelligent sprayer with automatic control.

[3] S2 = Intelligent sprayer without automatic control.

[4] S3 = Conventional air blast sprayer.

Target location on tree canopy	Average Spray Deposit (µL/cm^2)[1]								
	April			May			June		
	S1[2]	S2[3]	S3[4]	S1	S2	S3	S1	S2	S3
High	0.85 (0.33) dA	9.19 (2.59) aA	3.39 (1.11) bcAB	1.33 (0.56) dA	4.7 (1.72) bA	1.18 (0.44) dA	0.8 (0.52) dA	2.64 (1.34) cdAB	0.89 (0.39) dA
Middle	1.61 (0.55) cA	8.67 (2.96) aA	4.87 (0.76) bA	1.73 (1.14) cA	4.85 (3.34) bA	1.35 (0.89) cA	1.43 (0.99) cA	5.19 (2.81) bA	1.17 (0.7) cA
Low	0.96 (0.62) aA	4.73 (2.43) aB	3 (1.23) aB	1.22 (1) aA	3.39 (2.1) aA	1.63 (1.08) aA	0.89 (1.28) aA	2.26 (2.72) aB	1.54 (1.13) aA

Table 3.21. Spray deposits collected by nylon screens within different Z location sections inside Tree 3 canopy for the field tests in April, May and June using intelligent sprayer with automatic spray control, intelligent sprayer without automatic control and conventional air blast sprayer. Standard deviations are given in parentheses.

[1] Means in a row followed by different lowercase letters are significantly different ($p < 0.05$). Means in a column followed by different uppercase letters are significantly different ($p < 0.05$).

[2] S1 = Intelligent sprayer with automatic control.

[3] S2 = Intelligent sprayer without automatic control.

[4] S3 = Conventional air blast sprayer.

3.6.2 Spray loss on to the ground

As shown in Figures 3.13 and 3.14, S1 had the smallest amount of spray loss on the ground, and S3 had the most. The differences are significant between three sprayers. Even though the lowest nozzle on S3 was manually closed during all three spray tests, the conventional sprayer (S3) still had much greater spray deposition on the ground than the intelligent sprayer prototype (S1 and S2). This result shows that, the spray trajectories from the intelligent sprayer were more toward the canopies than the radial spray pattern from the conventional air blast sprayer.

As for each individual sprayer itself, the spray loss on the ground had very little variation among the three tests conducted in April, May and June.

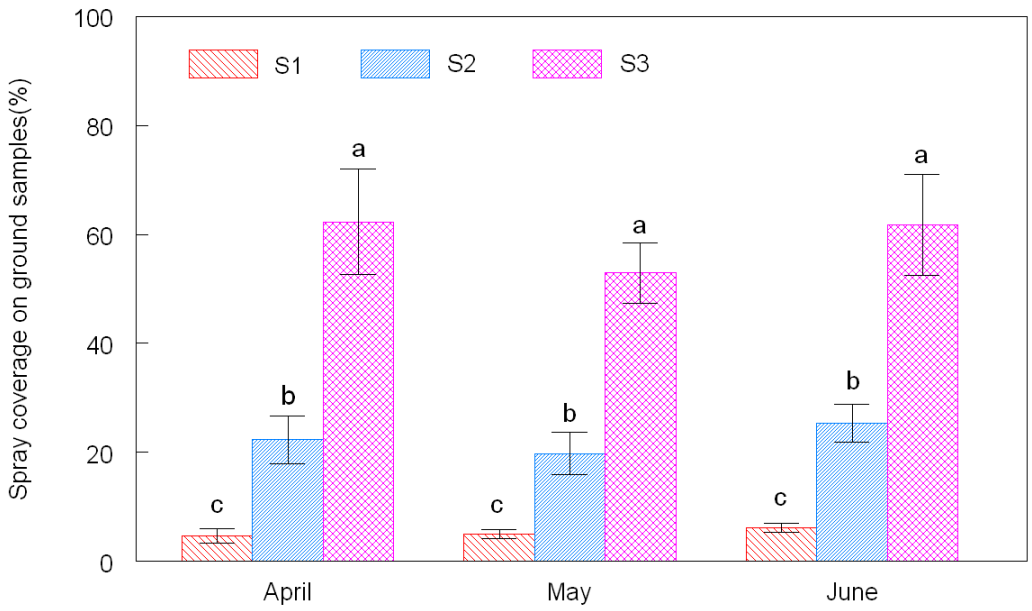

Figure 3.13. Mean spray coverage (%) on water sensitive papers placed on the ground for tests with intelligent sprayer with automatic control (S1), intelligent sprayer without automatic control (S2) and conventional air blast sprayer (S3). Standard deviations are represented by the error bars. Means marked with different lower case letters are significantly different ($p < 0.05$).

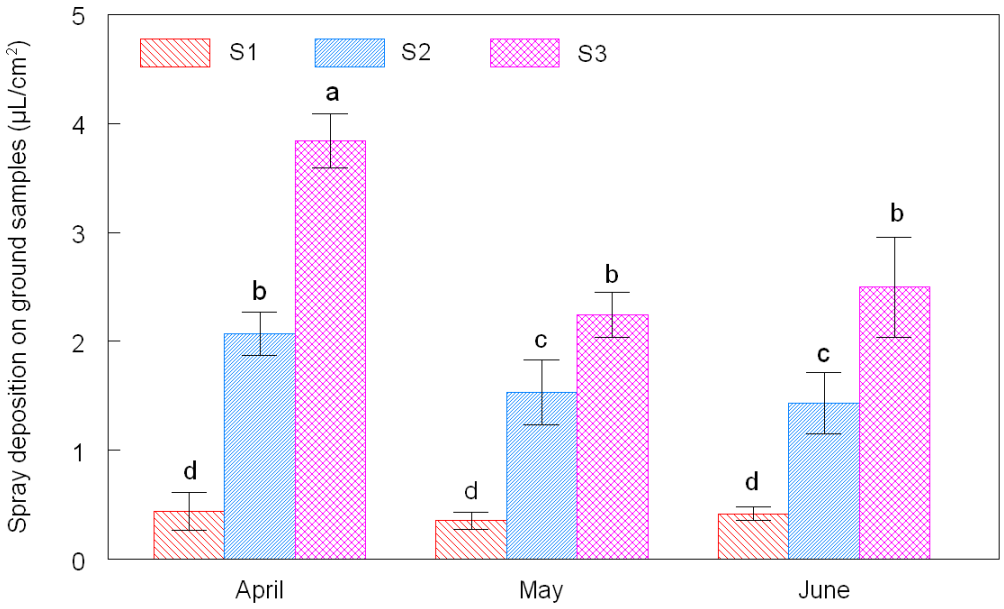

Figure 3.14. Mean deposition (µL/cm^2) on the plastic plates placed on the ground for tests with intelligent sprayer with automatic control (S1), intelligent sprayer without automatic control (S2) and conventional air blast sprayer (S3). Standard deviations are represented by the error bars. Means marked with different lower case letters are significantly different ($p < 0.05$).

3.6.3 Spray loss through tree gaps between tree canopies and above tree canopies

To determine potential spray losses through the gaps between trees, above and behind tree canopies, water sensitive paper and nylon screen samplers were mounted 54cm apart vertically on three poles 1.45 m behind the tree row centerline (as describe in section 2.6).

Since the conventional sprayer (S3) and the intelligent sprayer without automatic control (S2) did not stop spraying for gaps between trees and they also did not close any nozzles that discharged sprays over the top of the canopy, it was expected that these sprayers would produce considerably higher amounts of deposits on the samplers positioned beyond canopies than the intelligent sprayer with automatic control (S1).

As shown in Figures 3.15, and 3.16, the samplers sprayed by S1 have significantly smaller coverage and fewer deposits than those sprayed by S2 and S3 in April and May. In June, the spray coverage and deposit from S1 is less than those from S2 and S3, but the difference is not statistically significant.

For S2 and S3 treatments, spray deposits on the samplers mounted on poles tended to decrease as the growing season extended from April to June. This was because the tree foliage became denser and more collectors were in the shadow of the canopy. Thus more spray was intercepted by the foliage and less reached the collector. However, this trend was not observed for S1. This result is due to the automatic increase in spray applied by S1 when its sensor detected a denser canopy.

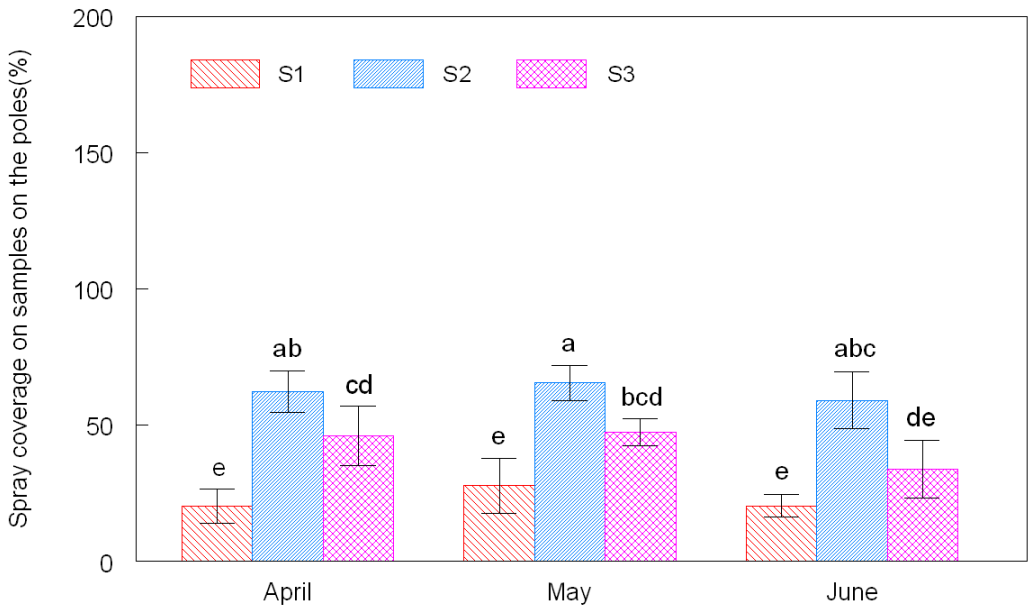

Figure 3.15. Mean spray coverage (%) on water sensitive papers mounted on the poles behind tree canopy for intelligent sprayer with automatic control (S1), intelligent sprayer without automatic control (S2) and conventional air blast sprayer (S3). Standard deviations are represented in the error bars. Means marked with different lower case letters are significantly different ($p < 0.05$).

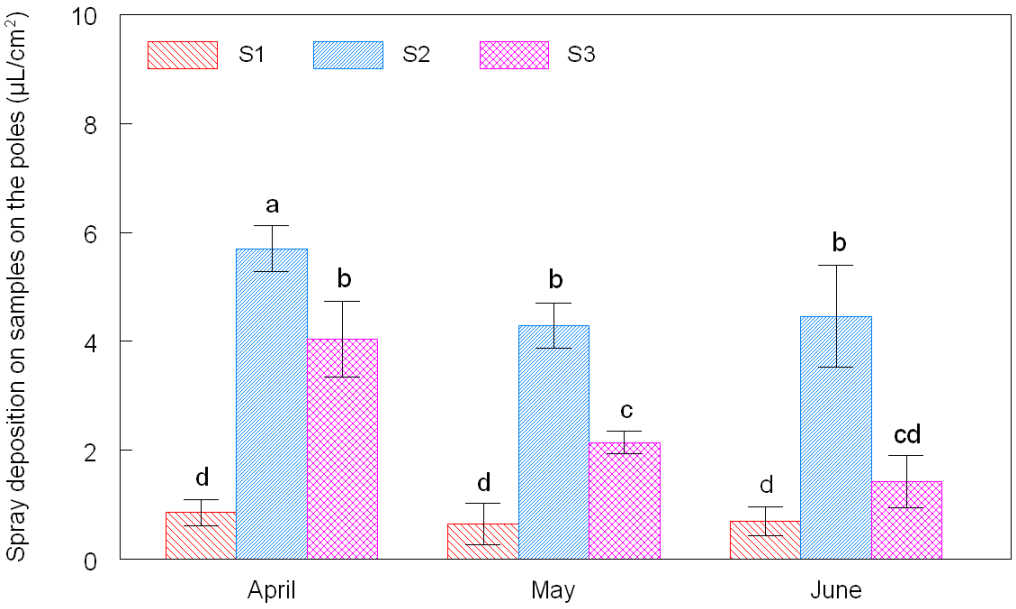

Figure 3.16. Mean spray deposition (µL/cm^2) on the nylon screens mounted on the poles behind tree canopy for intelligent sprayer with automatic control (S1), intelligent sprayer without automatic control (S2) and conventional air blast sprayer (S3). Standard deviations are represented in the error bars. Means marked with different lower case letters are significantly different ($p < 0.05$).

3.6.4 The transition of spray deposition between two trees

To document the transition of spray deposition from one tree canopy to another, three long strips of water sensitive papers were used to collect spray deposits between two trees. The strips were mounted horizontally on three narrow wood bars at three different heights (0.4, 0.9 and 2.0 m above the ground). The three bars were supported by three vertical poles installed behind and between two trees. Each strip of water sensitive papers was formed with four 26mm×508mm water sensitive papers connected together. In this test, part of each strip at both sides was behind part of two tree canopies, and the middle part of the strip was behind the tree gap. The detailed setup of poles and the mounting of long water sensitive paper strips were described in section 2.6.

Figures 3.17 to 3.19 show the coverage results on the long water sensitive paper strips between two trees for the test conducted in April, May and June, respectively. In each figure there are nine rows of long water sensitive paper strips. Each row represents the actual row that was sprayed. Nine rows were grouped into three sets of three rows, and each set was sprayed by one of the three sprayers S1, S2 and S3. The top set of three rows was sprayed with S1, the middle set was sprayed with S2, and the bottom set was sprayed with S3. Within each set, the first and the third rows were placed at heights of 2 m and 0.4 m, where the tree gaps were very large; the second row was placed at 0.9 m height, where the tree gap was narrow.

Figures 3.17 to 3.19 illustrate that S1 had the lowest sprays through tree gaps among all the three sprayer treatments. This result was evidenced by the observation of images shown in Figure 3.17. Obviously, S2 and S3 delivered considerably higher

amount of sprays on three long strips of water sensitive papers at three different heights than S1, even behind trees.

In Figure 3.18 which shows the result from the May test when trees had half foliage, the three rows of long water sensitive paper strips for S2 and S3 had less coverage than there were in April test. This is because there were more leaves on the trees in May and they blocked more spray liquid than the trees in April. Contrarily, the three rows of long water sensitive paper sprayed by S1 had more coverage than those were sprayed in April. This is because S1 automatically increased spray volume as a result of denser canopies in May.

Figure 3.19 shows the result from the June test when trees had fully grown canopies. The very dense foliage at the edge of trees blocked considerable amount of sprays from reaching the long strips of water sensitive papers from S2 and S3. The yellow areas with very few blue dots on the two ends of the strips show that these areas were shadowed by very dense canopies. For S1, the increase of spray coverage on long strips across the wide gap at 0.4 and 2.0 m heights was not visible while this increase was visible at the 0.96 m height where the gap was narrow. This is because there were a few small outward branches triggering nozzles to spray with higher flow rate than in the earlier tests. Also, there were not many leaves on the edge of the trees to intercept spray deposits, so an excessive portion of the sprays reached the water sensitive paper strips.

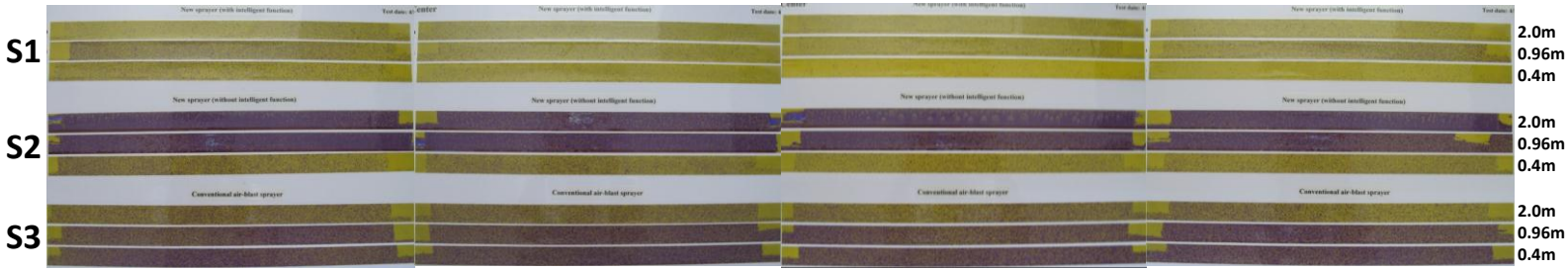

Figure 3.17. Spray deposits on long water sensitive paper strips placed between two trees for the test on April 12. Three rows of paper strips at top set were placed at 2.0 m (high), 0.96 m (middle) and 0.4 m (low) heights above the ground, sprayed by intelligent sprayer with automatic control (S1); three rows of strips at middle set were placed at high, middle and low heights, sprayed by intelligent sprayer without automatic control (S2); and three rows of paper strips at bottom set were placed at high, middle and low heights, sprayed by conventional air blast sprayer (S3).

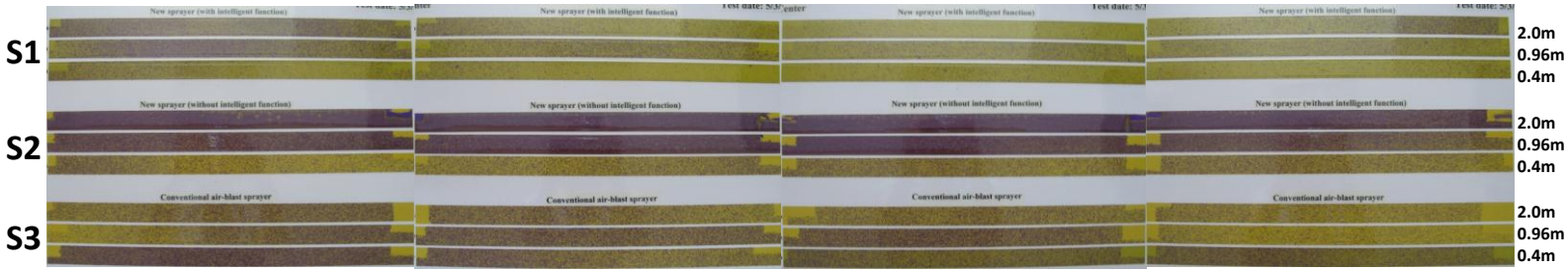

Figure 3.18. Spray deposits on long water sensitive paper strips placed between two trees for the test on May 3. Three rows of paper strips at top set were placed at 2.0 m (high), 0.96 m (middle) and 0.4 m (low) heights above the ground, sprayed by intelligent sprayer with automatic control (S1); three rows of strips at middle set were placed at high, middle and low heights, sprayed by intelligent sprayer without automatic control (S2); and three rows of paper strips at bottom set were placed at high, middle and low heights, sprayed by conventional air blast sprayer (S3).

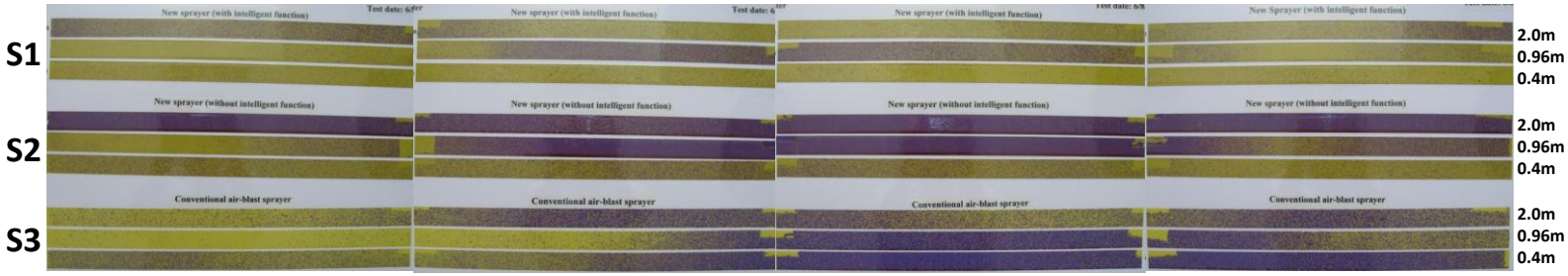

Figure 3.19. Spray deposits on long water sensitive paper strips placed between two trees for the test on June 8. Three rows of paper strips at top set were placed at 2.0 m (high), 0.96 m (middle) and 0.4 m (low) heights above the ground, sprayed by intelligent sprayer with automatic control (S1); three rows of strips at middle set were placed at high, middle and low heights, sprayed by intelligent sprayer without automatic control (S2); and three rows of paper strips at bottom set were placed at high, middle and low heights, sprayed by conventional air blast sprayer (S3).

3.6.5 Downwind spray drift

Tests were conducted to measure airborne drift from spray treatments only during 2nd and 3rd tests conducted in May and June, respectively. Nylon screens were placed 54cm apart at six heights on poles located downwind 5, 15 and 35 m downwind from the centerline of the trees sprayed.

Results for airborne drift from experiments conducted in May are presented in Figure 3.20. Targets on poles 15 and 35 m downwind had extremely low amount of drift deposits. The drift data from the pole nearest to the sprayer (5 m away) showed that among the sprayers tested, sprayer S1 (intelligent sprayer with automatic control) produced the least amount of drift, while S2, the same sprayer without the intelligent function turned to produce the highest amount of airborne drift. The differences are statistically significant. The major reason for S2 to produce the most of amount of drift was that all the nozzles on S2 discharge droplets in a horizontal trajectory, allowing a high volume of spray material moving downwind at a height not much different from the height of the poles. Thus more droplets are likely candidates to be captured by the samplers. Such result corresponds to the result shown in section 3.6.2, where S3 had the most spray lost on the ground, due to its radial spray pattern. In May, significant less drift was created from S1 than S2 and S3. This is because the spray rate of S1 was automatically reduced to match the canopy and thus less liquid was produced to go beyond tree canopy.

Results from the experiments conducted in June shows that there is no significant difference in the airborne drift created from three sprayers and at all three downwind

locations, except that S2 created significantly more drift at 5 m downwind. This indicates that with automatic control S1 is able to reduce airborne drift significantly.

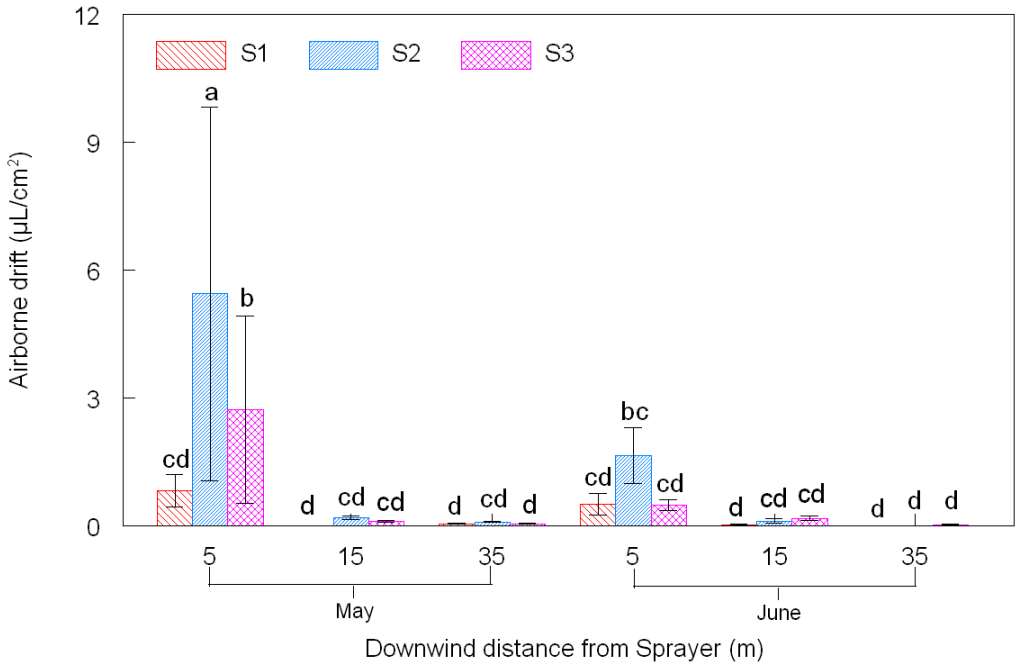

Figure 3.20. Airborne drift (µL/cm^2) on the nylon screens mounted on the poles 5, 15 and 35 m downwind from the centerline of the test row, when using the intelligent sprayer with automatic control (S1), intelligent sprayer without automatic control (S2) and conventional air blast sprayer (S3). Standard deviations are represented with error bars. Means marked with different lower case letters are significantly different ($p < 0.05$).

3.7 Sprayer outdoor tests with container trees

Four container trees (placed 2 m apart from tree center to tree center) were used to determine the intelligent sprayer performance on very dense and thick canopies. The four trees were the same ones used in the indoor spray rate test described in section 3.4. All the four trees had fully grown and very dense canopies. The spray constant used in this test was 0.05.

Among all the water sensitive papers sprayed by the intelligent sprayer with automatic control at 3.2 km/h travel speed, 67% of them had coverage greater than 15% which is considered sufficient coverage. In addition to the coverage data, droplet density data were also calculated. This is especially meaningful for those samples with coverage values lower than 15%. It was found that 87% of the water sensitive papers either had coverage greater than 15% or have droplet density greater than 70 deposits/cm^2 (recommended droplet density for fungicides by Syngenta Crop Protection AG located at CH-4002 Basel, Switzerland), and 94% of the total water sensitive papers either had coverage greater than 15% or had droplet density greater than 30 deposits/cm^2 (recommended droplet density for insecticides by Syngenta Crop Protection AG located at CH-4002 Basel, Switzerland).

For the test conducted at 6.44 km/h, 55% of the water sensitive papers had coverage greater than 15%, 72% of the water sensitive papers either had coverage greater than 15% or had droplet density greater than 70 deposits/cm^2, and 85% of the total water sensitive papers either had coverage greater than 15% or had droplet density greater than 30 deposits/cm^2.

Figures 3.21 to 3.28 show the mean percentage of coverage on the water sensitive papers mounted on different positions inside tree canopies sprayed by the intelligent sprayer with automatic control. Figures 3.21, 3.23, 3.25 and 3.27 show the coverage data when the sprayer was operated at a travel speed of 3.2 km/h, while Figures 3.22, 3.24, 3.26 and 3.28 show the coverage data for travel speed of 6.4 km/h. Comparing the results for the same tree between lower and higher speeds illustrates that the coverage at lower speed was higher.

Data presented on Figures 3.21 to 3.28 also indicates that at both ground speeds there was uniform spray distribution along vertical direction. However, uniformity of horizontal spray distribution (both along the spray direction and travel speed direction) was not good, especially for the positions that were far away from the nozzles. This means that the sprayer was not able to provide conditions that are conducive to penetration of droplets into inner parts of the canopy. This was very likely the result of the sprayer being operated at a relatively low air velocity and low air volume, which is not strong enough to open the canopy sufficiently.

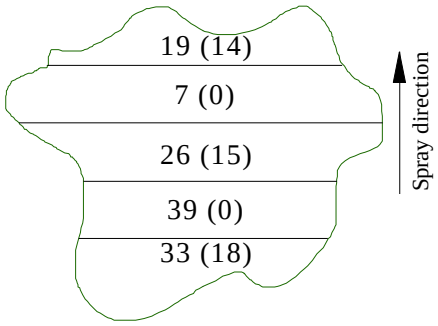

(a) Coverage along spray direction – top view

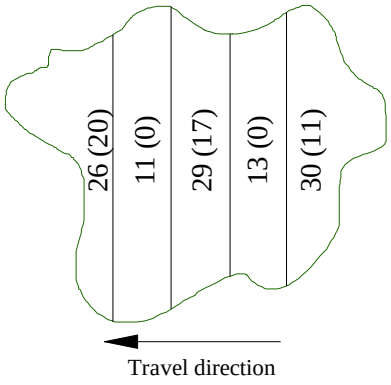

(b) Coverage along ground speed direction – top view

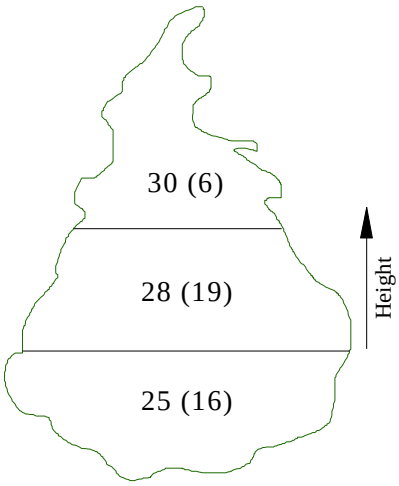

(c) Coverage along tree height – side view

Figure 3.21. Spray coverage (%) and its standard deviation (in parenthesis) at different locations inside the canopy of tree 1 for the intelligent sprayer at 3.22 km/h travel speed. (Data were divided and grouped from three directions: spray direction, ground speed direction and vertical direction.)

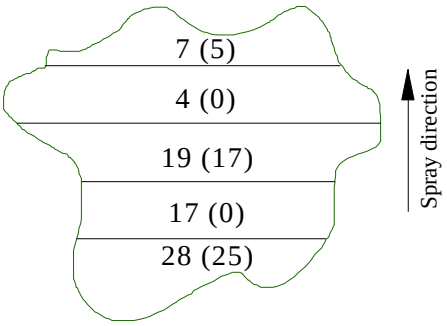

(a) Coverage along spray direction – top view

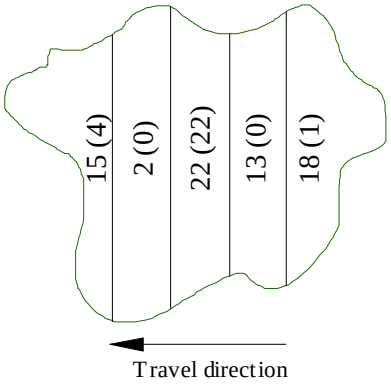

(b) Coverage along ground speed direction – top view

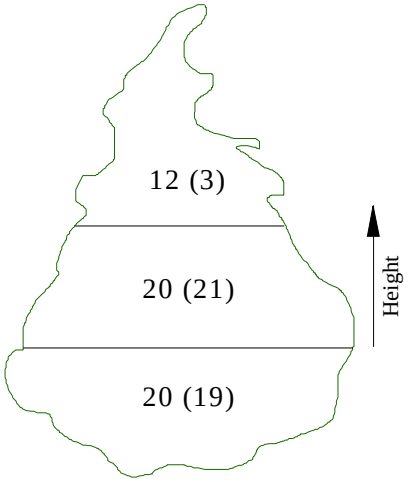

(c) Coverage along tree height – side view

Figure 3.22. Spray coverage (%) and its standard deviation (in parenthesis) at different locations inside the canopy of tree 1 for the intelligent sprayer at 6.44 km/h travel speed. (Data were divided and grouped from three directions: spray direction, ground speed direction and vertical direction.)

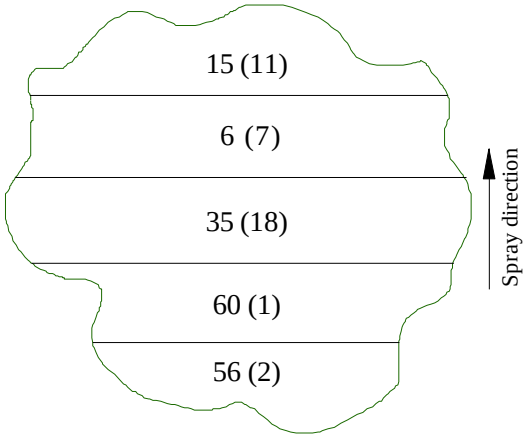

(a) Coverage along spray direction – top view

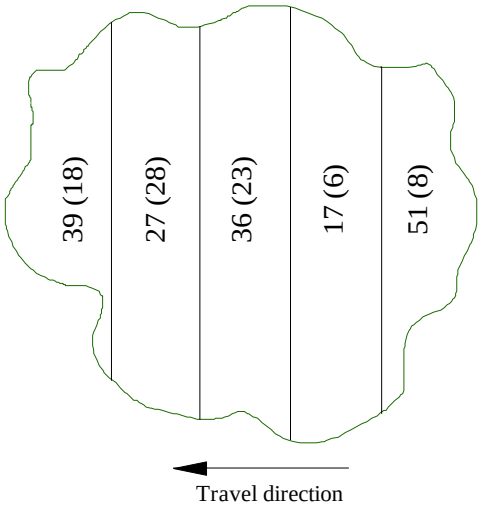

(b) Coverage along ground speed direction – top view

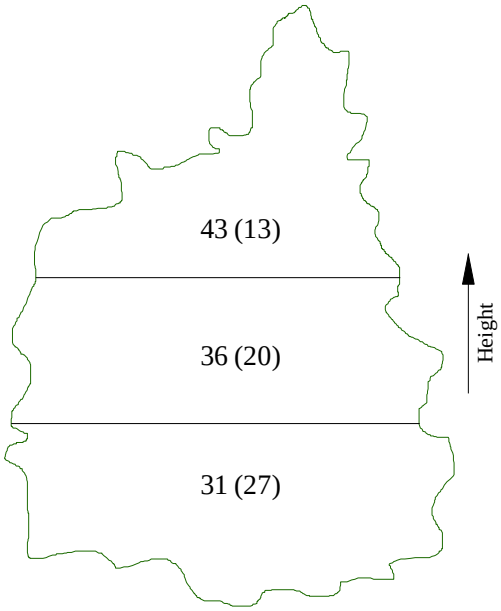

(c) Coverage along tree height – side view

Figure 3.23. Spray coverage (%) and its standard deviation (in parenthesis) at different locations inside the canopy of tree 2 for the intelligent sprayer at 3.22 km/h travel speed. (Data were divided and grouped from three directions: spray direction, ground speed direction and vertical direction.)

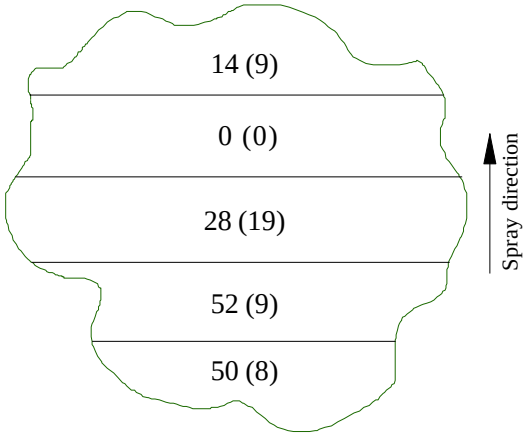

(a) Coverage along spray direction – top view

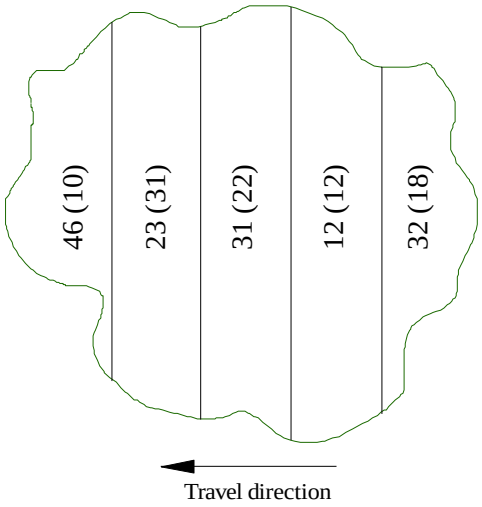

(b) Coverage along ground speed direction – top view

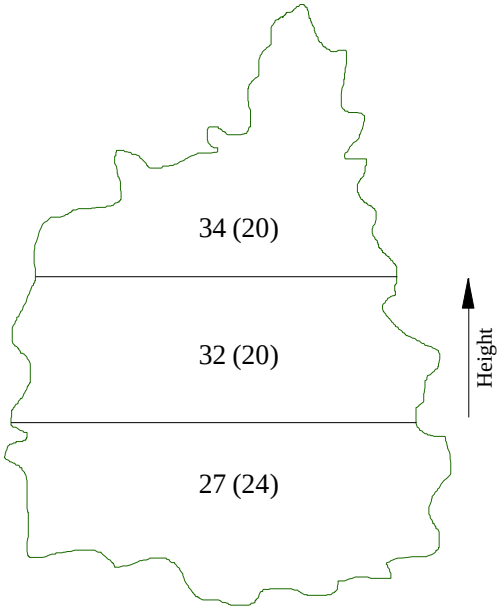

(c) Coverage along tree height – side view

Figure 3.24. Spray coverage (%) and its standard deviation (in parenthesis) at different locations inside the canopy of tree 2 for the intelligent sprayer at 6.44 km/h travel speed. (Data were divided and grouped from three directions: spray direction, ground speed direction and vertical direction.)

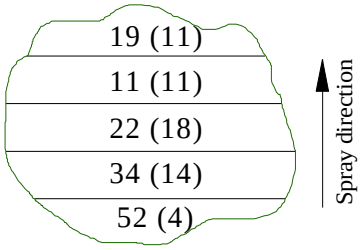

(a) Coverage along spray direction – top view

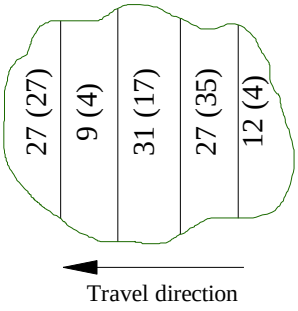

(b) Coverage along ground speed direction – top view

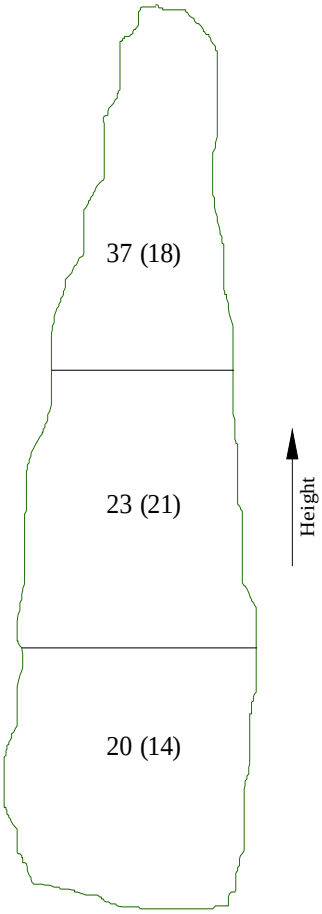

(c) Coverage along tree height – side view

Figure 3.25. Spray coverage (%) and its standard deviation (in parenthesis) at different locations inside the canopy of tree 3 for the intelligent sprayer at 3.22 km/h travel speed. (Data were divided and grouped from three directions: spray direction, ground speed direction and vertical direction.)

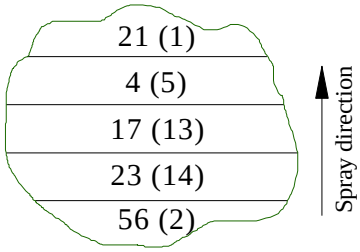

(a) Coverage along spray direction – top view

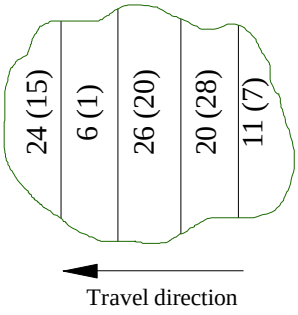

(b) Coverage along ground speed direction – top view

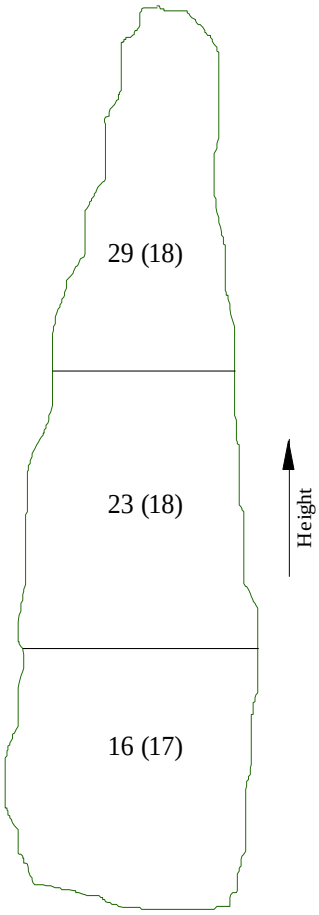

(c) Coverage along tree height – side view

Figure 3.26. Spray coverage (%) and its standard deviation (in parenthesis) at different locations inside the canopy of tree 3 for the intelligent sprayer at 6.44 km/h travel speed. (Data were divided and grouped from three directions: spray direction, ground speed direction and vertical direction.)

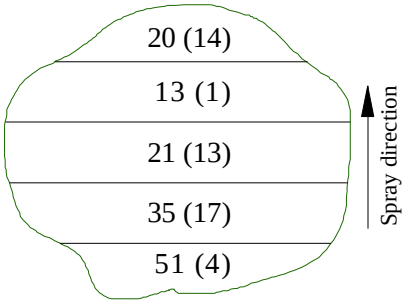

(a) Coverage along spray direction – top view

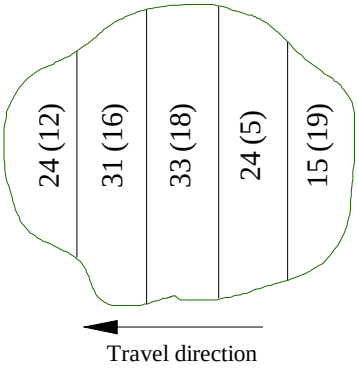

(b) Coverage along ground speed direction – top view

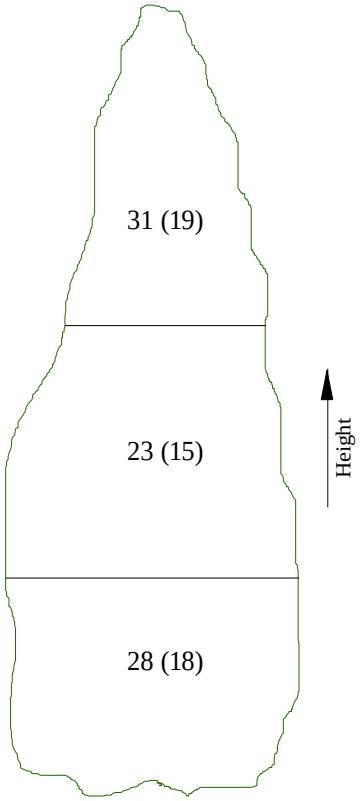

(c) Coverage along tree height – side view

Figure 3.27. Spray coverage (%) and its standard deviation (in parenthesis) at different locations inside the canopy of tree 4 for the intelligent sprayer at 3.22 km/h travel speed. (Data were divided and grouped from three directions: spray direction, ground speed direction and vertical direction.)

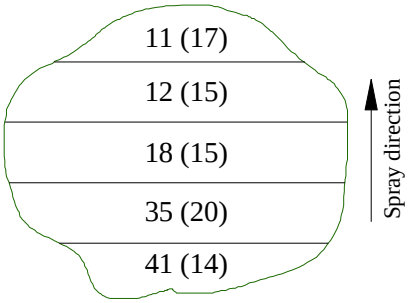

(a) Coverage along spray direction – top view

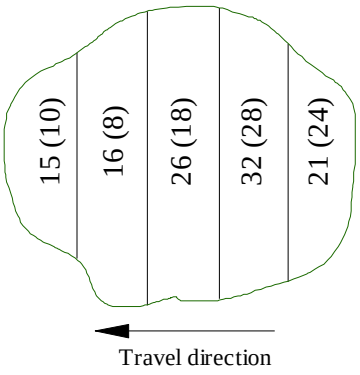

(b) Coverage along ground speed direction – top view

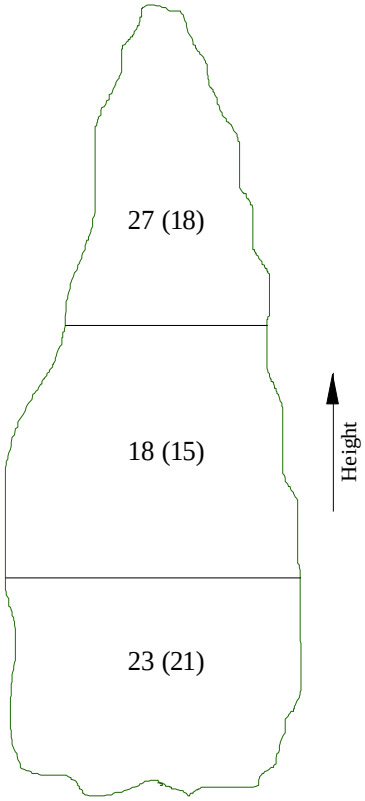

(c) Coverage along tree height – side view

Figure 3.28. Spray coverage (%) and its standard deviation (in parenthesis) at different locations inside the canopy of tree 4 for the intelligent sprayer at 6.44 km/h travel speed. (Data were divided and grouped from three directions: spray direction, ground speed direction and vertical direction.)

3.8 Liquid savings

3.8.1 Field tests

One of the major design goals of the intelligent sprayer equipped with the intelligent system was to reduce consumption of spray liquid. Figure 3.29 summarizes the tests conducted in April, May and June. The intelligent sprayer with automatic control had reduction in liquid consumption by 73%, 70% and 58% compared to the same sprayer without intelligent function, and by 66%, 63% and 47% compared to the conventional air blast sprayer respectively.

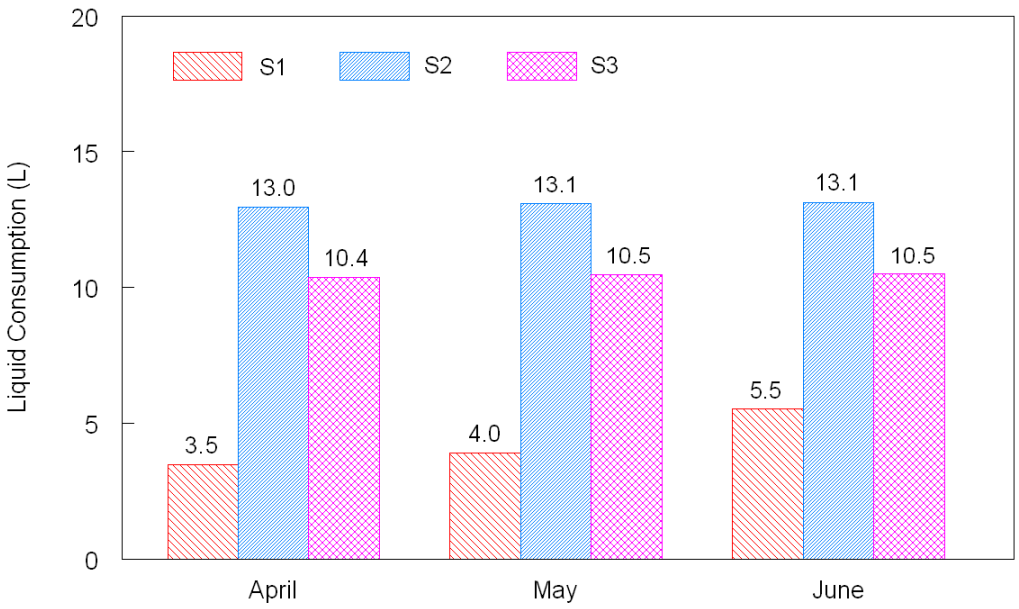

Figure 3.29. Liquid consumption of intelligent sprayer with automatic control (S1), intelligent sprayer without automatic control (S2) and conventional air blast sprayer (S3) for spraying a row of 21 trees in an apple orchard in April, May and June.

These findings demonstrated that the intelligent sprayer system made substantial savings in spray mixture consumption compared to the other two sprayers tested, although the savings decreased as the canopy size and foliage density increased. As shown in Figure 3.29, even at the mature stage when there was full foliage on trees in the orchard (June test), the intelligent sprayer with automatic control still had a 50%

reduction in spray mixture consumption compared to the conventional air assisted sprayer.

3.8.2 Container tree test

Savings in spray mixture consumption were also evaluated for the four trees grown in containers, in the spray test described in section 3.7 (tree measurements were shown in Table 3.1). During the test, the four trees were placed 2 m apart from tree center to center, which was a relatively close spacing for trees with their fully grown canopies.

As shown in Figure 3.30, intelligent sprayer with automatic control had spray consumption savings of 51% and 38% for the four container trees at travel speed of 3.22 km/h and 6.44 km/h, respectively, compared to intelligent sprayer without automatic control.

The main reason for the decrease in the percent savings when the travel speed was increased to 6.44 km/h is that the intelligent sprayer without automatic control could not adjust the application rate according to the travel speed. That is, the nozzle flow rate was the same for the two tests with the sprayer without the intelligent function travelling at both speeds. As the travel speed doubles, the application rate decreased by half. However, when its intelligent function was turned on, the intelligent sprayer was able to adjust the application rate automatically to compensate the speed difference since the travel speed was included in the spray output model.

The decrease in spray consumption of intelligent sprayer with automatic control at a higher travel speed was a result of the decrease of sensor resolution along the travel

direction (from 0.23 m to 0.46 m per slice of data in one refresh period for the solenoid valves, as the speed doubles). This could be improved by replacing the solenoid valves with those that could be operated at a higher frequency and thus a faster system refresh rate could be used in the computing algorithm to increase the resolution along the travel speed direction.

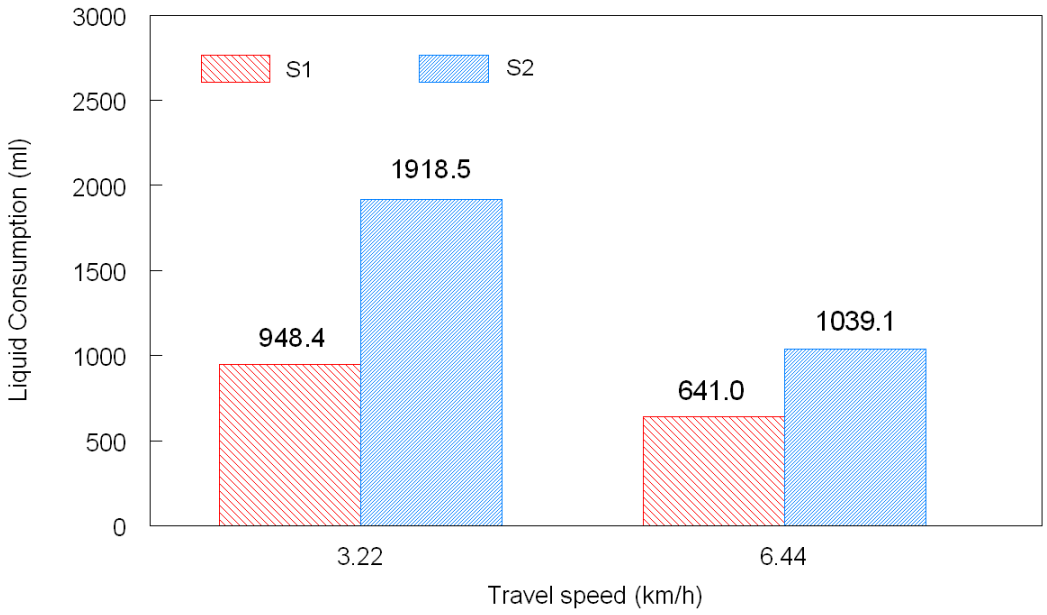

Figure 3.30. Comparison of spray mixture consumptions between intelligent sprayer with automatic control (S1) and intelligent sprayer without automatic control (S2) for spraying four container trees with dense canopies at travel speeds of 3.22 km/h and 6.44 km/h.

Chapter 4: Conclusions and Recommendations

4.1 Conclusions

The intelligent sprayer prototype with intelligent functions for nurseries and orchards developed in this research has several advantages over conventional chemical application systems. By using laser sensing and variable rate control technologies to adjust the amount of spray output based on the need of target canopies, it can not only reduce chemical cost for the growers, but also reduce the risk of potential environmental contamination due to a significant reduction in the chemicals that miss the targets. Other advantages of the intelligent sprayer prototype are that:

1) It implements real-time tree shape and foliage density measurement information into the real-time spray control. It achieves fully automatic variable-rate spray tasks, without human involvement during spray applications.
2) It automatically detects tree row center, which eliminates the requirement to measure and input distance from tractor to the tree center by the operator. When the tractor makes a turn to spray a new row of trees, the tree center will be updated as the tractor goes down the row.
3) It has versatility to treat many varieties of tree crops with different heights and shapes by turning on and off appropriate nozzles, and by adjusting flow rate of nozzles based on canopy size and density. This is especially useful in nurseries where a variety of tree crops are commonly planted together in the same field.

4) The intelligent algorithm inside the control component can handle a wide variety of foliage canopy density changes, and the electro-mechanical controllers are fast enough to activate the sprayer to achieve desired coverage regardless of foliage canopy variations.

However, the limitation of the current intelligent sprayer prototype is that the air velocity is not strong enough to carry spray droplets inside large and dense nursery canopies such as *Tsuga Canadensis.*

A high speed laser scanner was used to acquire data on the geometry, density characteristics and occurrence of the canopy on-the-go. The laser was able to scan the target crops and transfer the measurement data to a laptop computer for further processing. For the laser scanning sensor used and its operation mode chosen in this study, the tree structure measurement had resolution of 1.4 cm vertically and 2.3 cm horizontally.

A fast algorithm was developed to calculate tree canopy characteristic parameters using the data from the laser sensor. The algorithm could also automatically detect the ground surface, and the tree row centerline to assist in the calculations of tree width, height, volume and foliage density. Indoor tests with artificial targets were conducted to validate the algorithm used for calculation of canopy density. Results showed that the calculated density values were very close to the actual densities. The relationship between the calculated and actual densities was linear with correlation coefficients (R^2) ranging from 0.98 to 0.99.

A flow rate control unit was designed with Pulse Width Modulation (PWM) signals to adjust the spray output of nozzles in accordance with the detected tree canopy density in a real-time manner. An experiment station was built to calibrate the nozzle flow rates and to validate the accuracy of hardware and software used for the variable rate controller. During the experiments, pressure fluctuations were observed when operating solenoid valves at 10 Hz frequency and were minimized by a back pressure bypass device added to the spraying system.

A mathematic model was developed to calculate the optimal spray rate for each of 20 individual nozzles based on the concept that spray volume equals the effective canopy volume multiplied by a recommended spray constant. Laboratory tests were conducted to validate the effectiveness of the spray model as well as the performance of the data processing algorithm. Results showed that the spray model was effective in generating an optimal amount of spray that can ensure adequate spray coverage on targets.

A commercially available vineyard sprayer base was used for the development of the intelligent sprayer prototype. The laser sensor and flow rate controller circuits for sensing trees and controlling variable rate were implemented into the sprayer prototype. Four five-port air assisted nozzles with one 8002 XR flat fan nozzle in each port were assembled and mounted on each side of the Intelligent sprayer. Air velocity from each port was measured when the axial fan on the sprayer was running at the high speed mode. The sizes of droplets discharged from the nozzles at different modulation rate of the PWM control signals were also measured at the same air velocity as it was at the port. System response time was determined with a high speed camera system. The latency

between when laser “sees” the target and when the nozzle starts spraying liquid was measured to be approximately 0.119 seconds which includes the time for the software to complete the calculation, and for the electronic, hydraulic and mechanical components to respond in accordance with the computation results.

Field tests were conducted on apple trees in an orchard at three growth stages of tree canopy to compare the spray performances of three sprayers: intelligent sprayer with automatic control, intelligent sprayer without automatic control, and conventional air blast sprayer. Results from the field tests highlighted following important conclusions:

1) Unlike the intelligent sprayer without automatic control and the conventional air blast sprayer, intelligent sprayer with automatic control did not provide excessive sprays on the tree canopies.
2) Intelligent sprayer with automatic control was able to spray the tree canopies with relatively uniform coverage throughout the tree at different growth stages. However, the spray uniformity from the other two sprayers was not as good as that produced by the intelligent sprayer.
3) Unlike the other two sprayers which generally showed significantly lower spray coverage when spraying trees with denser canopies, the spray coverage achieved by the intelligent sprayer varied very little with the foliage density.
4) Intelligent sprayer with automatic control had the least spray loss to the ground, while the conventional air blast spray had the most. This result not only proves that intelligent sprayer with automatic control is able to shut off the nozzles when there is no canopy to spray, but also supports the assumption that the intelligent sprayer

prototype equipped with intelligently-controlled five-port nozzles has a better spray trajectory control than the conventional air blast sprayer.

5) Intelligent sprayer with automatic control had the lowest spray loss through tree gaps and beyond tree canopies than the other two sprayers.

6) Intelligent sprayer with automatic control had the least airborne drift than the other two sprayers.

7) In addition to the advantages listed above, field experiments demonstrated that the intelligent sprayer with automatic control could reduce spray volume by 47% to 73% compared to the other two sprayers and still provide adequate coverage and deposition.

To evaluate the spray coverage achieved from the intelligent sprayer with automatic control when spraying dense canopies such as evergreen trees found in nurseries, spray tests were conducted in four container trees with much denser canopies than the apple trees used in field tests explained above. Results from tests with four dense container-grown nursery trees showed that the uniformity of the spray coverage from the intelligent sprayer was not stable along the horizontal directions (both travel direction and spray direction). The primary reason for this ineffectiveness was that the air velocity and volume from the sprayer was not strong enough to open the dense canopy and help spray droplets penetrate into inner parts of the canopy. Therefore, an improved air-delivery subsystem with more powerful air output is needed for the intelligent sprayer prototype to treat very dense and thick canopies.

4.2 Unique contributions of this study to the intelligent sprayer development

As the evidence from the literature review presented in Chapter 1, in recent years some other researchers also have conducted research with objectives somewhat similar to the objectives of the study described in this dissertation. Although the ultimate goal of all of these studies was to design intelligent sprayers to apply pesticides at optimum rates, the Intelligent Sprayer described in this dissertation has following unique features that set it apart from the other sprayers designed with similar objectives in mind.

1. A commercially available sprayer base was fitted with a high precision laser sensor to determine tree canopy characteristics and occurrence in real time. Others have relied on ultrasonic sensor to acquire canopy occurrence only. The intelligent sprayer described here is able to acquire much more information on canopy structures in a real-time manner with higher accuracy than other sprayers.
2. Working with a rich set of real-time data from the high speed laser sensor, intelligent algorithms were designed and developed to capture the tree canopy characteristics and occurrence to manipulate spray outputs. Compared to the algorithms used by others, the algorithms presented in this study 1) are able to precisely sketch the tree canopy characteristics for a specific section covered by one individual nozzle; 2) do not require original data from laser sensor to be saved and thus reduce overhead in data collection; and 3) they do not require any offline data processing on other computer software such as Matlab (MathWorks Co. Natick, MA), which is often used in similar research.

3. The intelligent sprayer prototype can detect the foliage density in addition to canopy height, width, volume and occurrence, and can adjust flow rate of each nozzle according to the canopy structure measurements and complete the spray decision management on-the-go.
4. It is the first sprayer of its kind that is able to automatically identify the ground surface, the tree row center and tree spacing. No prior orchard or nursery measurement data is required for the application and no human involvement is needed to run the system. The operator only needs to turn on the sprayer with intelligent functions selected and drive the tractor.
5. The intelligent sprayer prototype is the first sprayer system that has the capability to divide a whole tree canopy into many small sections and each section is sprayed with variable rate by an individual nozzle based on the sectional canopy structure measurements. It is the first orchard and nursery sprayer that uses specially designed five-port air assisted nozzles which have better trajectory control than other nozzles.
6. It is also the first sprayer of its kind that employs a back pressure bypass mechanism to limit the pressure fluctuation caused by the modulation of solenoid valves at 10 Hz frequency.

4.3 Recommendations for future study

The main goal of this study was to design and develop software and hardware for an intelligent sprayer that can control variable-rate spray outputs through the nozzles based on availability of a target in sight, and density level of the canopy sprayed. This has been accomplished to a large degree. However, there is still some ineffectiveness associated with the operation of this sprayer that can be addressed by future studies. Following are some of the areas where further research is needed:

1. The height of tree section treated by each nozzle was assumed to be equal to simplify the parameters used in the system. However, in the future research, the height covered by each nozzle (with their specific orientation) should be calibrated and compared with what is done in this study to determine if the sprayer performance can be improved by using the calibrated height treated by each nozzle.
2. Currently the sprayer only has one laser scanner to control one side of the nozzles on the sprayer. It is necessary to investigate spraying from two sides of the sprayer when traveling in the same path by using either a laser scanner with wider field of view or two laser scanners mounted on the sprayer .
3. Currently the intelligent sprayer does not have a speed sensor to measure the travel speed in real time; speed information is manually entered in the computer before the sprayer is operated. Real time speed measurement should be included in the system to improve the accuracy of matching the flow rate to the target regardless of variations in travel speed.

4. A direct injection system should be added to the intelligent sprayer to reduce the possibility of leftover pesticide and water mixture in the tank after the field is sprayed. This will further protect the environment by eliminating the improper practice of dumping leftover spray mixture somewhere in the field after completion of spraying.
5. A GPS and management control logic should be added in the intelligent sprayer. By doing so, the orchard or nursery manager can select pesticide type for a specific field location and GPS will verify that no spraying will take place unless the sprayer is in the right location. This will ensure that chemicals will only be applied to their designated plots.
6. Currently centerlines of all five-port nozzles are oriented horizontally. The current design can be improved so that an optimal orientation can be determined for each nozzle for specific tasks or preferences, such as to spray trees mostly from top down, or bottom up.
7. An air controller should be added to the intelligent sprayer to adjust the air velocity and air volume based on the volume and density of the tree canopy to achieve adequate and uniform spray coverage on targets.
8. The spray model should incorporate with more parameters including weather data, environment information and user preferences for better management of the fate of pesticides applied. This can be achieved by automatic adjustment of the spray rate and air velocity of the sprayer based on environmental conditions such as temperature, wind speed and direction, and proximity of the area to water resources

and other sensitive areas to avoid their contamination and risk to safety and health of nearby people and animals.

References

Al-Gaadi, K. A., Ayers, P. D. (1999). Integrating GIS and GPS into a spatially variable rate herbicide application system. *Applied Engineering in Agriculture, 15*(4), 255-262.

Anonymous. (2000). In National Research Council (Ed.), *The future role of pesticides in US agriculture* National Academy Press, Washington.

Balsari, P., Doruchowski, G., Marucco, P., Tamagnone M., Van de Zande, J. (2007). The development of a crop identification system (CIS) able to adjust spray application to target characteristics. *SuProFruit 2007, 9th Workshop on Spray Application Techniques in Fruit Growing,* Alnarp, Sweden. 17-18.

Bode, L. E. (2008). Agricultural chemical application technology: A remarkable past and an amazing future. *Transactions of the ASABE, 51*(2), 391-395.

Brown, R.B., Steckler, J.P.G.A. (1995). Prescription maps for spatially variable herbicide application in no-till corn. *Transactions of the ASAE, 38*(6), 1659-1666.

Deveau, J. (2009). *Six elements of effective spraying in orchards and vineyards.* Ministry of Agriculture, Food and Rural Affairs, Ontario.

Doruchowski, G., Jedrachowicz, T., Holownicki, R., Godyn, A., Swlechowski, W., Balsari, P., ... Wenneker, M. (2007). Environmentally dependent application system (EDAS) for adjusting the spray application parameters according to the environmental circumstances in orchards - ISAFRUIT project. *SuProFruit 2007, 9th Workshop on Spray Application Techniques in Fruit Growing,* Alnarp, Sweden. 15-16.

Doruchowski, G. (2000). Environmentally friendly spray techniques for tree crops. *Crop Protection, 19*(8-10), 617-622.

Escola, A., Camp, F., Solanelles, F., Planas, S, Rosell, J. R. (2003). Tree crop proportional spraying according to the vegetation volume. first results. *Proceedings of the 7th Workshop on Spray Application Techniques in Fruit Growing, Cuneo, Italy,* 43-49.

Fox, R. D., Derksen, R.C., Zhu, H., Brazee, R.D., Svensson, S.A. (2008). A history of air-blast sprayer development and future prospects. *Transactions of the ASABE, 51*(2), 405-410.

Gil, E., Escola, A., Rosell, J. R., Planas, S., Val, L. (2007). Variable rate application of plant protection products in vineyard using ultrasonic sensors. *Crop Protection, 26*(8), 1287-1297.

Giles, D.K., Delwiche, M.J., Dodd, R.B. (1987). Control of orchard spraying based on electronic sensing of target characteristics. *Transactions of the ASAE, 30*(6), 1624-1630.

Giles, D. K., Delwiche, M.J., Dodd, R.B. (1988). Electronic measurement of tree canopy volume. *Transactions of the ASAE, 31*(1), 264-272.

Giles, D. K., Delwiche, M. J., Dodd, R. B. (1989). Sprayer control by sensing orchard crop characteristics: Orchard architecture and spray liquid savings. *Journal of Agricultural Engineering Research, 43*(4), 271-289.

Han, S., Hendrickson, L. L., Ni, B., Zhang, Q. (2001). Modification and testing of a commercial sprayer with PWM solenoids for precision spraying. *Applied Engineering in Agriculture, 17*(5), 591-594.

Hanks, J. E., Beck, J. L. (1998). Sensor-controlled hooded sprayer for row crops. *Weed Technology, 12*(2), 308-314.

Harris, M.J., Erickson, K., Johnson, J., Morehart, M., Strickland, R., Covey, T., … Dubman, R. *2009 agricultural income and finance outlook / AIS-88 / december 2009.* http://usda.mannlib.cornell.edu/usda/ers/AIS//2000s/2009/AIS-12-22-2009.pdf

Jenkins, E., Hines, R. (2003). Chapter 4: Spraying fruit. *Fruit crop pest management. A guide for commercial applicators category 1C.* Michigan St. Univ. 124pp.

Jerardo, A. (2007). *Floriculture and nursery crops yearbook/FLO-2007/September 2007.* http://www.ers.usda.gov/Publications/Flo/2007/09Sep/FLO2007.pdf

Knutson, R.D., Hall, C.R., Smith, E.G., Contner, S.D., Miller, J.W. (1997). Pesticide-free production a 'disaster'. *Commercial Grower, 52*, 8-10.

Lee, K. H., Ehsani, R. (2008). A laser scanner based measurement system for quantification of citrus tree geometric characteristics. *ASABE Paper no. 083980,* St. Joseph, Mich.: ASABE.

Llorens, J., Gil, E., Llop, J.,Escola, A. (2010). Variable rate dosing in precision viticulture: Use of electronic devices to improve application efficiency. *Crop Protection, 29*, 239-248.

Mooney, D. F., Larson, J. A., Roberts, R. K. English, B. C. (2009).*When does variable rate technology for agricultural sprayers pay? A case study for cotton production in tennessee.* http://economics.ag.utk.edu/publications/precisionag/313_Mooney.pdf

Oerke, E. C. (2006). Crop losses to pests. *The Journal of Agricultural Science, 144*(1), 31.

Oerke, E. C., Dehne, H.W. (2004). Safeguarding production--losses in major crops and the role of crop protection. *Crop Protection, 23*(4), 275-285.

Oerke, E. C., Dehne, H.W., Schonbeck, F., Weber, A. (1994). *Crop production and crop protection: Estimated losses in major food and cash crops.* Amsterdam: Elsevier Science.

Paice, M. E. R., Miller, P. C. H., Bodle, J. D. (1995). An experimental sprayer for the spatially selective application of herbicides. *Journal of Agricultural Engineering Research, 60*(2), 107-116.

Palacin, J., Palleja, T., Tresanchez, M., Teixido, M., Sanz, R., Llorens, J.,...Rosell, J. R. (2008). Difficulties on tree volume measurement from a ground laser scanner. *Instrumentation and Measurement Technology Conference Proceedings, Victoria, Vancouver Island, Canada, ,* 1997-2002.

Palacin, J., Palleja, T., Tresanch, M., Sanz, R., Llorens, J., Ribes-Dasi, M.,... Rosell, J. R. (2007). Real-time tree-foliage surface estimation using a ground laser scanner. *Ieee Transactions on Instrumentation and Measurement, 56*(4), 1377-1383.

Reichard, D. L., Ladd, T. L. (1981). An automatic intermittent sprayer. *Transactions of the ASABE.24 (4),* 893-896

Rosell, J.R., Sanz, R., Llorens, J., Arno, J., Escola, A., Ribes-Dasi, M.,...Palacin, J. (2009a). A tractor-mounted scanning LIDAR for the non-destructive measurement of vegetative volume and surface area of tree-row plantations: A comparison with conventional destructive measurements. *Biosystems Engineering, 102*(2), 128-134.

Rosell, J. R., Llorens, J., Sanz, R., Arno, J., Ribes-Dasi, M., Masip, J.,... Palacin, J. (2009b). Obtaining the three-dimensional structure of tree orchards from remote 2D terrestrial LIDAR scanning. *Agricultural and Forest Meteorology, 149*(9), 1505-1515.

Salyani, M., Wei, J. (2005).Effect of travel speed on characterizing citrus canopy structure with a laser scanner. *Precision Agriculture'05. Papers Presented at the 5th European Conference on Precision Agriculture, Uppsala, Sweden,* 185-192.

Solanelles, F., Escola, A., Planas, S., Rosell, J., Camp, F., Gracia, F. (2006). An electronic control system for pesticide application proportional to the canopy width of tree crops. *Biosystems Engineering, 95*(4), 473-481.

Thorp, K. R., Tian, L. (2004). Performance study of variable-rate herbicide applications based on remote sensing imagery. *Biosystems Engineering, 88*(1), 35-47.

Tian, L., Reid, J.F., Hummel, J.W. (1999). Development of a precision sprayer for site-specific weed management. *Transactions of the ASAE, 42*(4), 893-900.

Tian, L. (2002). Development of a sensor-based precision herbicide application system. *Computers and Electronics in Agriculture, 36*(2-3), 133-149.

Van de Zande, J.C., Wenneker, M., Meuleman, J., Achten, V., Balsari, P., Doruchowski, G. (2007).Development of a crop health sensor (CHS) to minimise spray

applications in apple. *SuProFruit 2007, 9th Workshop on Spray Application Techniques in Fruit Growing*, Alnarp, Sweden. 13-14.

Wei, J., Salyani, M. (2004). Development of a laser scanner for measuring tree canopy characteristics: Phase 1. prototype development. *Transactions of the ASAE, 47*(6), 2101-2107.

Wei, J., Salyani, M. (2005). Development of a laser scanner for measuring tree canopy characteristics: Phase 2. foliage density measurement. *Transactions of the ASAE, 48*(4), 1595-1601.

Zhu, H., Derksen, R.C., Guler, H., Krause, C.R., Ozkan, H.E. (2006). Foliar deposition and off-target loss with different spray techniques in nursery applications. *Transactions of the ASABE, 49*(2), 325-334.

Zhu, H. (2006). A specially designed air-assisted sprayer to improve spray penetration and air jet velocity distribution inside dense nursery crops. *Transactions of the ASABE, 49*(5), 1285-1294.

Appendix A

Block diagram for Data Acquisition program using LMS 291 Laser Scanner (LabVIEW)

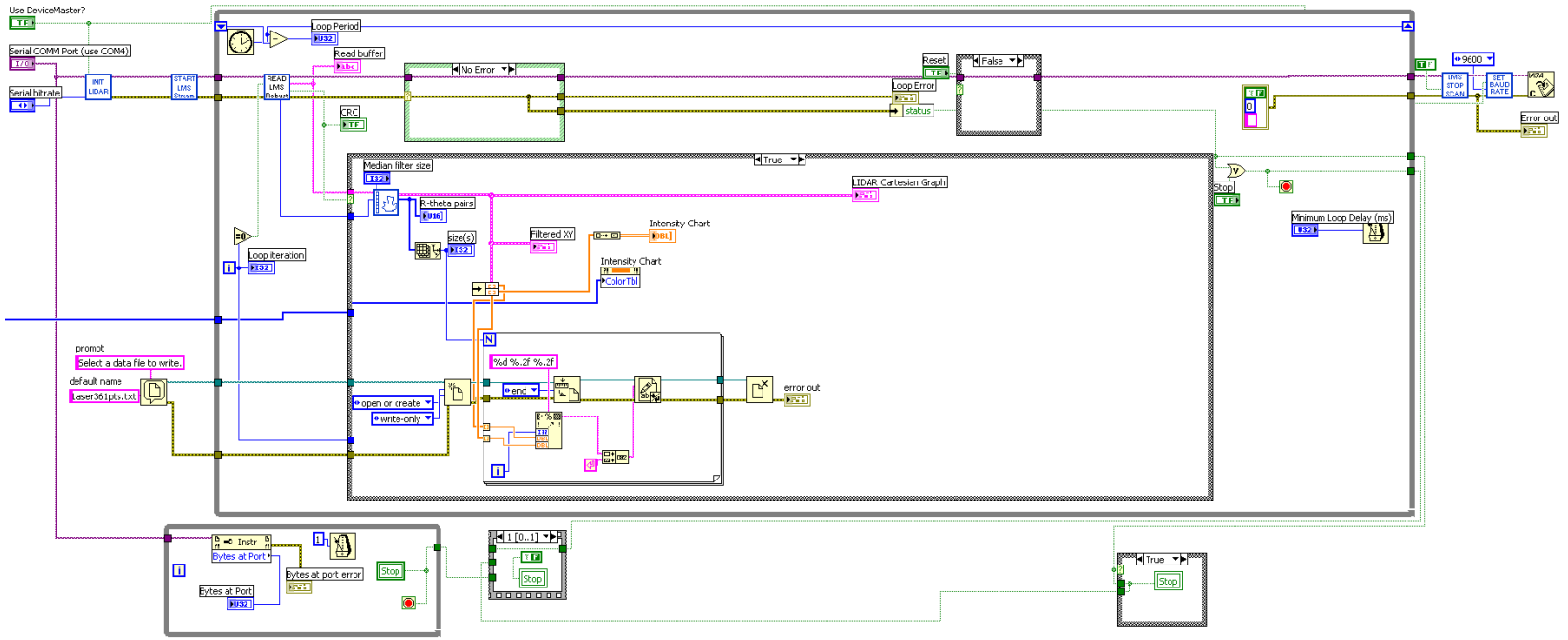
Use DeviceMaster?
Serial COMM Port (use COM4)
Serial bitrate
INIT LIDAR
START LMS Stream
READ LMS Robust
Loop Period
Read buffer
CRC
No Error
Reset
Loop Error
status
False
9600
LMS STOP SCAN
SET BAUD RATE
Error out
Median Filter size
True
LIDAR Cartesian Graph
R-theta pairs
size(s)
Filtered XY
Intensity Chart
Intensity Chart
ColorTbl
Loop iteration
Stop
Minimum Loop Delay (ms)
prompt
Select a data file to write.
default name
Laser361pts.txt
%d %.2f %.2f
end
open or create
write-only
error out
Instr
Bytes at Port
Bytes at port error
Stop
Bytes at Port
1 [0..1]
Stop
True
Stop

Appendix B

Schematic of switching circuit for controlling 10 channels of low power PWM signals

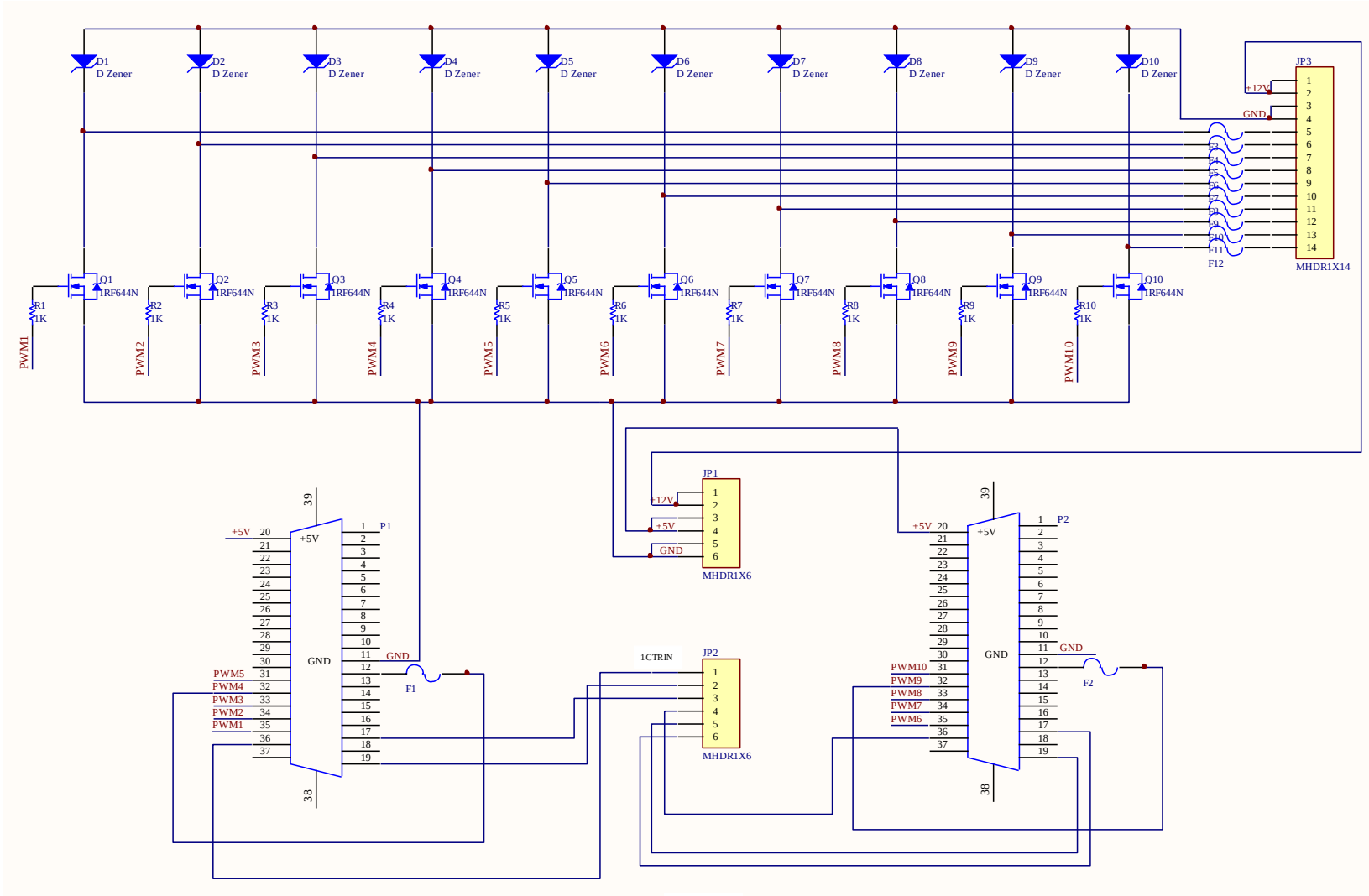
D1 D Zener
D2 D Zener
D3 D Zener
D4 D Zener
D5 D Zener
D6 D Zener
D7 D Zener
D8 D Zener
D9 D Zener
D10 D Zener
JP3
+12V
GND
MHDR1X14
F12
Q1 IRF644N
Q2 IRF644N
Q3 IRF644N
Q4 IRF644N
Q5 IRF644N
Q6 IRF644N
Q7 IRF644N
Q8 IRF644N
Q9 IRF644N
Q10 IRF644N
R1 1K
R2 1K
R3 1K
R4 1K
R5 1K
R6 1K
R7 1K
R8 1K
R9 1K
R10 1K
PWM1
PWM2
PWM3
PWM4
PWM5
PWM6
PWM7
PWM8
PWM9
PWM10
JP1
+12V
+5V
GND
MHDR1X6
P1
+5V
GND
F1
JP2
1CTRIN
MHDR1X6
P2
+5V
GND
F2

Appendix C

Block diagram for generating 10 channels of independent PWM signals with specified 10 duty cycle values (LabVIEW)

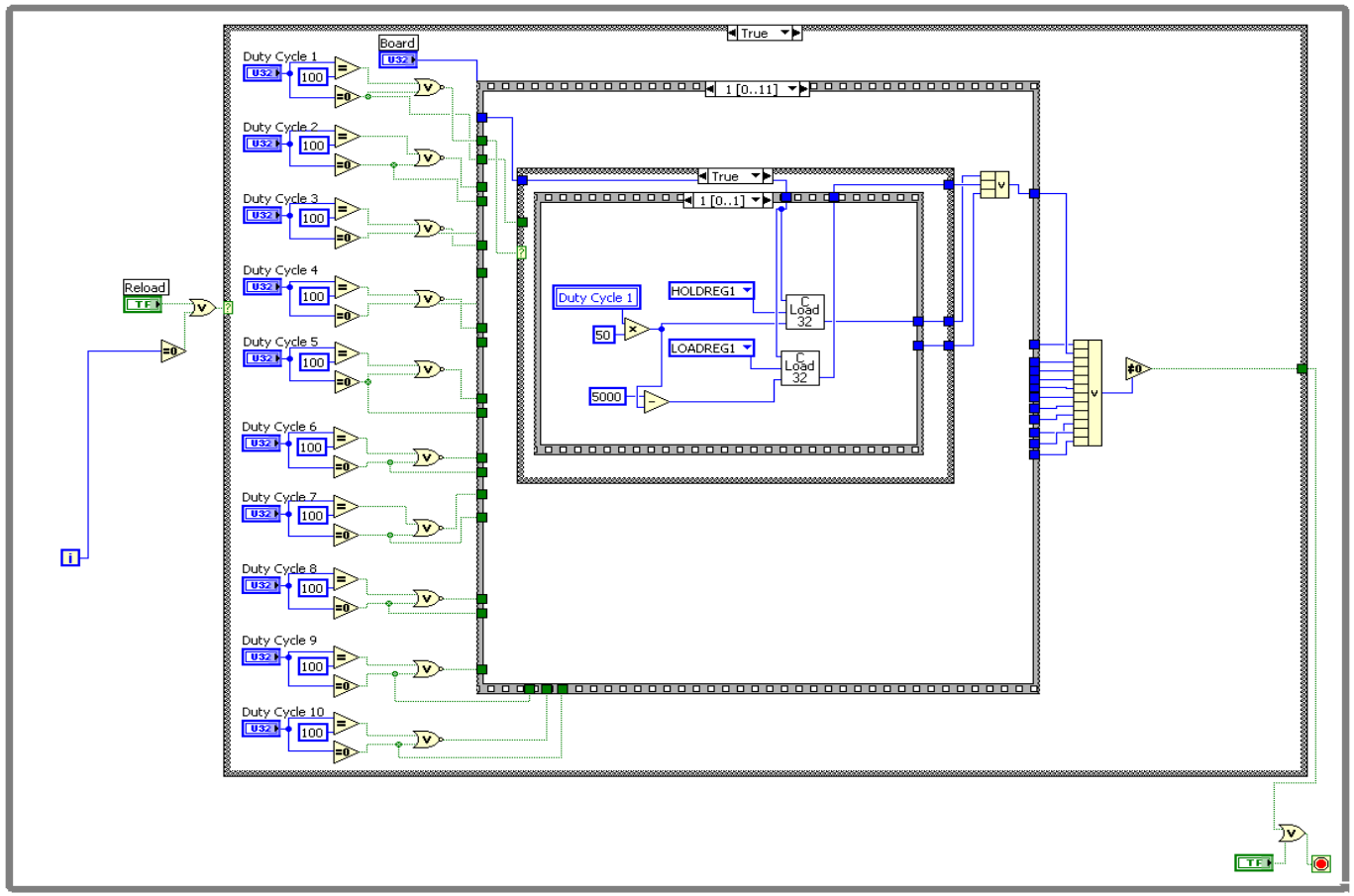
True
Board
U32
Duty Cycle 1
Duty Cycle 2
Duty Cycle 3
Duty Cycle 4
Duty Cycle 5
Duty Cycle 6
Duty Cycle 7
Duty Cycle 8
Duty Cycle 9
Duty Cycle 10
100
=0
1 [0..11]
True
1 [0..1]
Reload
TF
i
HOLDREG1
LOADREG1
C
Load
32
50
5000
≠0

Appendix D

Block diagram for New Spray controller program (LabVIEW)

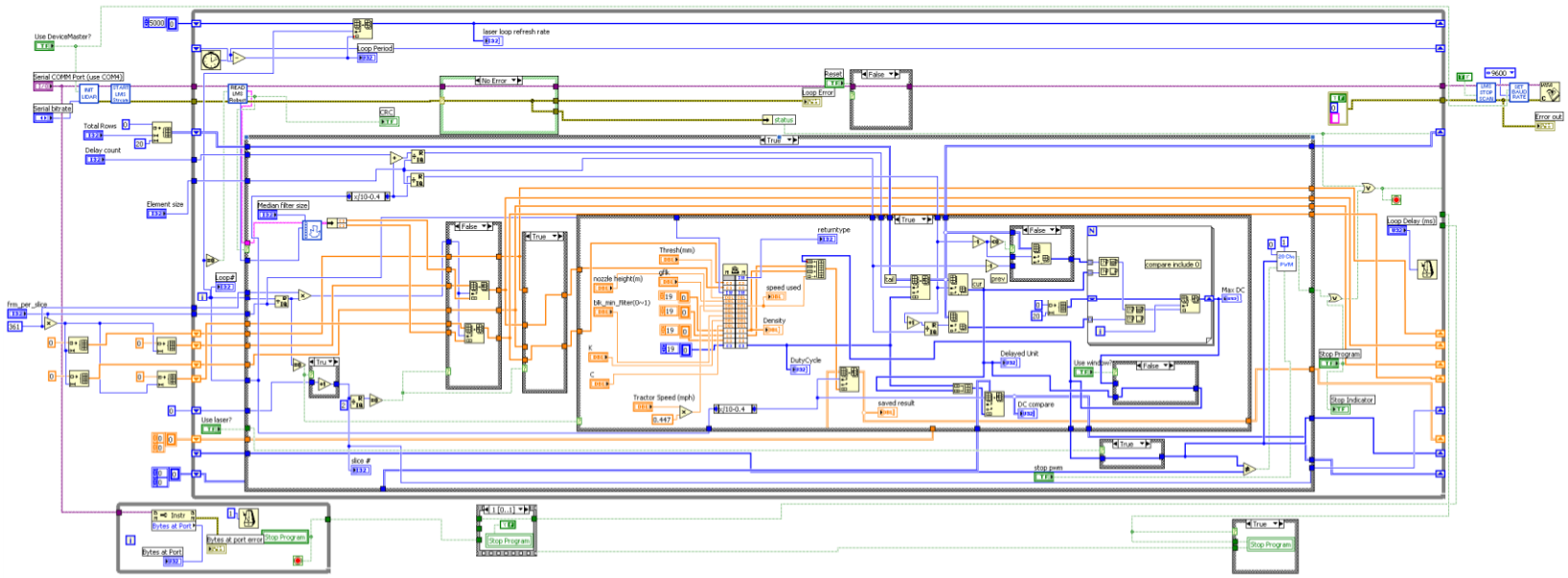
Use DeviceMaster?
Serial COMM Port (use COM4)
Serial bitrate
Total Rows
Delay count
Element size
Median filter size
frm_per_slice
Use laser?
slice #
laser loop refresh rate
Loop Period
No Error
Loop Error
Reset
False
True
status
Thresh(mm)
nozzle height(m)
blk_min_filter(0->1)
K
C
Tractor Speed (mph)
0.447
returntype
speed used
Density
DutyCycle
saved result
Delayed Unit
DC compare
compare include 0
Max DC
Use window
Loop Delay (ms)
Stop Program
Stop Indicator
stop pwm
Bytes at Port
Bytes at port error
Error out

Appendix E

Canopy size and density calculation algorithms source code (C++)

E.1DLL(Dynamic-link library) interface

```
#include "stdafx.h"
#include "alg1.h"
#include "param.h"
#include "queue.h"

#ifdef _MANAGED
#pragma managed(push, off)
#endif

extern "C" __declspec(dllexport)  int Alg1_Calc_Density
( double *data, double *x_data, intnum_frame, double thresh, double gflk, double speed,
doubleblk_x_width,doubleblk_min_filter,doubleK,double C,
double density[], double width[], double height[],unsigned intDutycycle[] );

BOOL APIENTRY DllMain( HMODULE hModule,   DWORD  ul_reason_for_call,
                LPVOID lpReserved
{
return TRUE;
}

/*******************
Input:
        double  data[]
        double  x_data[]
        num_frame:   how many frames in a slice
        thresh:   max possible valid distance from an object to sensor
        gflk:  ground fluctuation
        speed:  motion speed of sensor
        pipe_array: a 2-d array, store DC values from consecutive slices,
                        used as a pipeline for delay timing (20int*element#)
        delay_unit: delay this many slices' worth of time, # of slices from head to tail
        elem_cnt:   how many slices in the array, the max # of slices for storage
```

```
Output:
        density[]: density of canopy in block[i]
        width[]:   max width of canopy in that block[i]
        height[]:  height covered in that block
        dutycycle[]:  nozzle duty-cycle for that block
**********/
int Alg1_Calc_Density( double *data, double *x_data,
                intnum_frame,
                double thresh,
                doublegflk,
                double speed,
                doubleblk_x_width,
                doubleblk_min_filter,
                double K,
                double C,
                double density[], double width[], double height[],unsigned intDutycycle[]
)
{
        static  long count = 0;
        intchannel_num=20;
        intdata_per_frm = 361;
        if( count==0 ){
                init_param(1.50, blk_x_width, 20, 2, &alg1_param);
                set_param(&alg1_param );
        }
        count++;
        Calc_Density(data, x_data,  num_frame, data_per_frm, thresh, gflk,
                blk_min_filter,          density, width, height);
        int i;
        for (i=0; i<channel_num; i++)
        {
                if( density[i] < 0.000001 )
                {
                        Dutycycle[i] = 0;
                }
                else
                {
                        Dutycycle[i] = (int)(K * width[i] * speed * density[i] + C);
                }
                if(Dutycycle[i] > 100 )          Dutycycle[i] = 100;
        }
        return 0;
}
```

```
#ifdef _MANAGED
#pragma managed(pop)
#endif
```

E.2 Compute the parameters for a chosen working mode

```
#ifndef __PARAM_H__
#define __PARAM_H__

#define MAX_BLK    20
#define MAX_DATA_PER_BLK     32
typedefstructs_CalcParam
{
        double d;
        double h;
        int       blk_num;
        intang_res;
        intstart_pos;
        intnum_pts;
        intpts_unit[MAX_BLK];
        doublepts_width[MAX_BLK][MAX_DATA_PER_BLK];

}CalcParam_t;
void    init_param(double d, double h, intnum_h, intang_res, CalcParam_t* param ) ;
#endif


#include "stdafx.h"
#include "string.h"
#include "math.h"
#include <stdio.h>
#include "param.h"

void    init_param(double d, double h, intnum_h, intang_res, CalcParam_t* param )
{
        double pi = 3.14159265;
        doublestart_ang, ang2;
        int       i,j, k;
        inttotal_pts;
        double degree;
        doubleang_inc;
        intpts_per_degree;
        memset(param, 0, sizeof(CalcParam_t) );

        start_ang = atan(d/(h*num_h/2));
        degree = start_ang * 180/pi;
```

```
if(ang_res == 1 ){
        total_pts = 181;
        pts_per_degree = 1;
        i = (int)(degree * 1);
        ang_inc = pi/180;
}
else if(ang_res == 2){
        total_pts = 361;
        pts_per_degree = 2;
        i = (int)(degree*2);
        ang_inc = pi/180/2;
}
else if( ang_res == 3){
        total_pts = 401;
        pts_per_degree = 4;
        i = (int) ((degree - 40) * 4);
        ang_inc = pi/180/4;
}
else{
        printf("Error: unknown angular-resolution %d\n", ang_res);
        return;
}

if( i<0 )  i = 0;
param->start_pos = i;
param->num_pts = (total_pts- i*2);
param->d = d;
param->h = h;
param->blk_num = num_h;
param->ang_res = ang_res;

intlast_pt = i;
for(i=1; i<num_h/2; i++)
{
        ang2 = atan( d / ((num_h/2-i)*h) );

        if(ang_res == 3 ) {
                j = ( (ang2*180/pi) - 40) * 4;
        }
        else{
                j = (ang2 * 180/pi) * pts_per_degree;
        }

        param->pts_unit[i-1] = j - last_pt;
```

```
            last_pt = j;
        }
        param->pts_unit[i-1] = total_pts/2 - last_pt;

        for(i=num_h/2; i<num_h; i++ )
        {
            param->pts_unit[i] = param->pts_unit[num_h-1-i];
        }

        double tmp[401];
        doublelast_ang = start_ang;
        doublelast_x  = h*num_h/2  * 1000;
        doublecurrent_x;
        doublecurrent_ang = last_ang;

        for(i=1; i<= param->num_pts/2; i++)
        {
            current_ang += ang_inc;
            current_x = 1000 * d * cos(current_ang)/sin(current_ang);

            last_x = current_x;
        }
        tmp[i-1] = tmp[i-2];
        for(i=param->num_pts/2;  i<param->num_pts; i++)
        {
            tmp[i] = tmp[ param->num_pts - 1 - i ];
        }

        j = 0;
        for(i=0; i<num_h; i++ )
        {
            for(k=0; k<param->pts_unit[i]; k++, j++)
                param->pts_width[i][k] = tmp[j];

            if( i == num_h/2-1 )
                j++;
        }
}
```

E.3 Algorithm to calculate canopy width and foliage density

```
#include "stdafx.h"
#include "string.h"
#include "math.h"
#include <stdio.h>
#include "alg1.h"
#include "param.h"


#define FRAME_PER_SLICE 50
#define DATA_PER_FRAME          401

static double  glb_slice_data[FRAME_PER_SLICE][DATA_PER_FRAME];
static double  glb_x_data[FRAME_PER_SLICE][DATA_PER_FRAME];

staticintglb_data_per_frame = 361;
staticintglb_trunk_len;
staticintglb_blk_per_frm = 20;

double  glb_gnd_fluc;
intglb_centermode;

typedefstructwidth_s
{
        intidx;
        double  width;
}width_t;


CalcParam_t   alg1_param;
CalcParam_t *cur_param;

#define  CENT_WIND_SIZE  5

width_tglb_cent_width[CENT_WIND_SIZE];
intglb_cent_width_cnt  = 0;

doublecenter_width = -1;

void    set_param(CalcParam_t* param)
{
        cur_param = param;
```

```
}

voidinternal_quickSort(double a[], int lo, int hi)
{
int i=lo, j=hi, h;
double x=a[(lo+hi)/2];

do
   {
while (a[i]<x) i++;
while (a[j]>x) j--;
if (i<=j)
       {
          h=a[i]; a[i]=a[j]; a[j]=h;
i++; j--;
       }
   } while (i<=j);

if (lo<j) internal_quickSort(a, lo, j);
if (i<hi) internal_quickSort(a, i, hi);
}


void    quick_sort(double* data, intnum)
{
        internal_quickSort(data, 0, num-1);
}


double get_min_dist( double* data, intnum, double percent )
{
        int n, i = 0;
        double min = 0;

        while( i<num )
        {
                if( data[i] > 0.01 )
                        break;
                i++;
        }

        n = num - i;
        if( n > 0 )
        {
```

```
                min = data[i + (int)(n*percent)];
        }

        return min;
}


doubleget_average(double* data, intnum)
{
        double sum = 0;
        int n, i = 0;

        while( i<num )
        {
                if( data[i] > 0.01 )
                        break;
                i++;
        }


        n=0;
        for(; i<num; i++)
        {
                sum += data[i];
                n++;
        }

        return sum/n;
}

voidTruncate_Data(double *data, double *x_data, intnum_frame, double thresh)
{
        intflen = glb_data_per_frame;

        int i, j, k;
        intstart_pos;

        start_pos = cur_param->start_pos;
        glb_trunk_len = 0;
        for(i=0; i<glb_blk_per_frm; i++ )
        {
                glb_trunk_len += cur_param->pts_unit[i];
        }
```

```
        doublegnd_high;

        for(i=0; i<num_frame; i++)
        {
                k = i*flen + start_pos;
                gnd_high = *(x_data+i*flen);

                memcpy(glb_slice_data[i], data+k, glb_trunk_len*sizeof(double));
                memcpy(glb_x_data[i], x_data+k, glb_trunk_len*sizeof(double));

                for(j=0; j<glb_trunk_len; j++ )
                {
                        if(fabs( *(x_data+k+j)-gnd_high )<= glb_gnd_fluc )
                        {
                                glb_slice_data[i][j] = 0;
                        }
                        else if( glb_slice_data[i][j] >= thresh )
                        {
                                glb_slice_data[i][j] = 0;
                        }
                        else if(glb_slice_data[i][j] < 0 )
                        {
                                glb_slice_data[i][j] = 0;
                        }
                }
        }
}

doubleGet_Row_Center(intnum_frame, intflen)
{
        staticwidth_ttop_distance[64];
        memset((void*)top_distance, 0, 64*sizeof(width_t));

        int i, j;

        if(glb_cent_width_cnt == 0 )
        {
                memset(glb_cent_width, 0, CENT_WIND_SIZE*sizeof(width_t) );
        }

        for(i=0; i<num_frame; i++)
        {
                for(j=flen-1; j>=0; j--)
                {
```

```
                    if(glb_slice_data[i][j] > 0 )
                    {
                        top_distance[i].idx = j;
                        top_distance[i].width = glb_slice_data[i][j];
                        break;
                    }
                }
            }


            double max = -1;
            inttop_idx = -1;
            for(i=0; i<num_frame; i++)
            {
                if(top_distance[i].idx>top_idx )
                {
                    top_idx = top_distance[i].idx;
                    max = top_distance[i].width;
                }
                else if( top_distance[i].idx == top_idx )
                {
                    if(top_distance[i].width > max )
                    {
                        top_idx = top_distance[i].idx;
                        max = top_distance[i].width;
                    }
                }
            }


            i = glb_cent_width_cnt%CENT_WIND_SIZE;

            glb_cent_width[i].idx = top_idx;
            glb_cent_width[i].width = max;
            glb_cent_width_cnt++;

            max = -1;
            for(i=0; i<CENT_WIND_SIZE; i++)
            {
                if(glb_cent_width[i].width > max )
                    max = glb_cent_width[i].width;
            }
            return max;
}
```

```
void  Calculate(intnum_frame, intnon_zero_row_thresh, double* x_data,
                doubleblk_min_filter,
                double density[], double width[], double height[])
{
        static   double sortdata[1024];
        int              sort_len = 0;


        int i, j, k,t;
        int row, col;
        intnon_zero_rows, tmp;

        intx_start = 0;
        intx_end = 0;
        doublex_len;
        doubleblk_x_len=0;

        doublemin_dist;
        doublevol, max_vol;
        int bottom = 0;

        doublemax_dist = Get_Row_Center(num_frame, glb_trunk_len);

        for( i=0; i<glb_blk_per_frm; i++ )
        {
                density[i] = width[i] = 0;
                height[i] = cur_param->h;
        }

        if(max_dist< 10 )
        {
                return;
        }

        col = 0;
        for(k=0; k<glb_blk_per_frm; col+= cur_param->pts_unit[k], k++ )
        {
                min_dist = 1000000;
                vol = 0;
                bottom = 0;

                sort_len = 0;
                non_zero_rows=0;
                for(i=0; i<num_frame; i++)
```

```
{
        tmp=0;
        for(j=col; j<col+cur_param->pts_unit[k]; j++)
        {
                if(glb_slice_data[i][j] >max_dist)
                {
                        glb_slice_data[i][j] = 0;
                }
                else if( glb_slice_data[i][j] > 0.05 )
                        tmp++;
        }

        memcpy(sortdata+sort_len, &glb_slice_data[i][col],
                                cur_param->pts_unit[k]*sizeof(double) );
        sort_len += cur_param->pts_unit[k];

        if(tmp>non_zero_row_thresh )
                non_zero_rows++;
        else
                continue;

        for(j=col; j<col+cur_param->pts_unit[k]; j++)
        {
                if(glb_slice_data[i][j] <= 0 || glb_slice_data[i][j]>max_dist
)
                {
                        continue;
                }
                if(glb_slice_data[i][j] <min_dist )
                {
                        min_dist = glb_slice_data[i][j];
                }

                bottom++;
                vol += (max_dist - glb_slice_data[i][j]) *
                        cur_param->pts_width[k][t];
        }
}
if(vol< 1 || (max_dist<min_dist) )
{
        continue;
}

blk_x_len = 0;
```

```
                for(i=0; i<cur_param->pts_unit[k]; i++)

                if (non_zero_rows>0)
                {
                        quick_sort(sortdata, sort_len );
                        min_dist = get_min_dist(sortdata, sort_len, blk_min_filter);

                        max_vol = (max_dist - min_dist) * non_zero_rows * blk_x_len;
                        if(max_vol<vol )
                                max_vol = vol - 1.0;

                        density[k] = vol / max_vol;
                        width[k] = (max_dist - min_dist)/1000;
                        height[k] = cur_param->h;
                }
        }
}


intCalc_Density( double *data, double *x_data,
                intnum_frame, intdata_per_frm, double thresh,  double  gflk,
                doubleblk_min_filter,
                double density[], double width[], double height[])
{
        intnon_zero_thr = 2;
        glb_gnd_fluc=gflk;

        Truncate_Data(data, x_data, num_frame, thresh);

        Calculate(num_frame, non_zero_thr, x_data,
                blk_min_filter,
                density, width, height);

        int i;
        double t;
        doublemax_density = -1;

        for (i=0;i<glb_blk_per_frm/2;i++)
        {
                t = density[glb_blk_per_frm-1-i];
                density[glb_blk_per_frm-1-i] = density[i];
                density[i] = t;

                t = width[glb_blk_per_frm-1-i];
```

```
        width[glb_blk_per_frm-1-i] = width[i];
        width[i] = t;

        t = height[glb_blk_per_frm-1-i];
        height[glb_blk_per_frm-1-i] = height[i];
        height[i] = t;
}

return 0;}
```